MEDJ

Volume: 39 Issue: 2 June 2024

MEDENIYET MEDICAL JOURNAL

THE OFFICAL JOURNAL OF ISTANBUL MEDENIYET UNIVERSITY FACULTY OF MEDICINE

Formerly Göztepe Tıp Dergisi

ISSN 2149-2042
E-ISSN 2149-4606

www.medeniyetmedicaljournal.org

ISSN 2149-2042
E-ISSN 2149-4606

MEDENIYET MEDICAL JOURNAL

Formerly Göztepe Tıp Dergisi

Year 2024
Volume 39
Issue 2

www.medeniyetmedicaljournal.org

Administrative Office
Istanbul Medeniyet University Dumlupınar Mahallesi, D-100 Karayolu No:98, 34000 Kadıköy, İstanbul, Türkiye

Publication type: Periodical

Finance: Istanbul Medeniyet University Scientific Research Fund

Publisher
Galenos Publishing House
Address: Molla Gürani Mah. Kaçamak Sk. No: 21/1 34093 İstanbul, Türkiye
Phone: +90 (530) 177 30 97
E-mail: info@galenos.com.tr/yayin@galenos.com.tr
Web: www.galenos.com.tr

Printing at:
Son Sürat Daktilo Dijital Baskı San. Tic. Ltd. Şti.
Gayrettepe Mah. Yıldızposta Cad. Evren Sitesi A Blok No: 32 D: 1-3 34349 Beşiktaş/İstanbul
Phone: +90 212 288 45 75

Printing Date: June 2024

International scientific journal published quarterly.

Medeniyet Medical Journal is the official journal of Istanbul Medeniyet University

It is published four times a year (March, June, September, December).

MEDJ is an open Access, free and peer-reviewed journal

PubMed Abbreviation: Medeni Med J

"Please refer to the journal's webpage (**https://medeniyetmedicaljournal.org/jvis.aspx**) for "Publication Policy", "Instructions to Authors" and "Aims and Scope".

The Medeniyet Medical Journal and/or its editors are members of ICMJE, COPE, WAME, CSE and EASE, and follow their recommendations.

The Medeniyet Medical Journal is indexed in **Emerging Sources Citation Index (Web of Science), PubMed/MEDLINE, PubMed Central, Scopus, EBSCO Academic Search Complete, i-Journals, J-Gate, Türk Medline, Türkiye Atıf Dizini** and **TÜBİTAK ULAKBİM TR Index**.

The journal is printed on an acid-free paper and published electronically.

Owner: İSTANBUL MEDENİYET UNİVERSİTY FACULTY OF MEDİCİNE

Responsible Manager: M. Tayyar KALCIOGLU

www.medeniyetmedicaljournal.org

International Advisory Board

MEDJ

International Advisory Board

Contents

Original Articles

Review

MEDJ

Contents

Case Reports

Letters to the Editor

Contents

DOI: 10.4274/MMJ.galenos.2024.15853
Medeni Med J 2024;39:74-84

Original Article

Impact of Long COVID on Lung Function in Children

Uzun Süreli COVID'in Çocuklarda Akciğer Fonksiyonlarına Etkisi

Zeynep Reyhan ONAY[1], Sinem CAN OKSAY[1], Deniz MAVI TORTOP[1], Gulay BILGIN[1], Yetkin AYHAN[1], Ferit DURANKUS[2], Saniye GIRIT[1]

[1]Istanbul Medeniyet University Faculty of Medicine, Department of Pediatric Pulmonology, Istanbul, Türkiye
[2]Istanbul Medeniyet University Faculty of Medicine, Department of Pediatrics, Istanbul, Türkiye

ABSTRACT

Objective: While the coronavirus disease-2019 (COVID-19) pandemic has generally resulted in milder illness among children than adults, persistent respiratory symptoms have been increasingly reported in this population.

Methods: We conducted a prospective, single-center cohort study focusing on children experiencing prolonged respiratory symptoms after contracting COVID-19. Spirometry, 6- minute walk tests (6MWTs), and tests of lung volume, the diffusing capacity of the lungs for carbon monoxide (DLCO), and fractional exhaled nitric oxide (FeNO) were performed on COVID-19 survivors at least 4 weeks after infection and a group of healthy control subjects.

Results: Fifty-five children with long-term COVID and 55 healthy control subjects were recruited. The weight, height, and body mass index Z-scores were similar in the groups. Within a median duration of 85 days (minimum-maximum: 35-194) following COVID-19 infection, a restrictive pattern was observed to be more common in the study group (p=0.021). In children with long COVID, 6MWT distances, DLCO Z-scores, and the predicted values of spirometry and lung volume tests were found to be significantly lower but in the normal range. The average predicted values for DLCO, FeNO, and 6MWT were similar in the two groups.

Conclusions: Prolonged respiratory symptoms often persist long after COVID-19 infection, necessitating comprehensive evaluation of affected children. Close monitoring, including spirometry and lung volume assessments, is crucial for children with abnormalities in lung imaging. However, FeNO measurements were found to be ineffective in monitoring long COVID.

Keywords: Children, diffusing capacity, fractional exhaled nitric oxide, long COVID, 6-minute walk test

ÖZ

Amaç: Koronavirüs hastalığı-2019 (COVID-19) pandemisinin başlangıcından bu yana, çocuklarda hastalığın seyrinin yetişkinlerdeki kadar şiddetli olmadığı gözlemlenmiştir. Bununla birlikte, uzun vadeli solunum semptomları görülebilmektedir.

Yöntemler: Çalışmamız prospektif, tek merkezli kohort çalışması olarak tasarlandı. Spirometri, 6 dakika yürüme testi (6DYT), akciğer hacim ölçümleri, karbon monoksit için akciğerlerin difüzyon kapasitesi (DLCO) ve fraksiyonel nitrik oksit (FeNO) testleri, COVID-19 enfeksiyonu geçiren ve solunumsal semptomları en az dört haftadır devam eden çocuklar ile aynı sayıda sağlıklı kontrol grubuna uygulandı.

Bulgular: COVID-19 sonrası solunum semptomları devam eden 55 çocuk çalışma grubu olarak, herhangi bir akciğer hastalığı bulunmayan 55 çocuk ise kontrol grubu olarak çalışmaya dahil edildi. Ağırlık, boy ve vücut kitle indeksi Z-skorları gruplar arasında benzerdi. COVID-19 enfeksiyonunu takiben ortanca 85 günde (minimum-maksimum: 35-194 gün) restriktif solunum paternini çalışma grubunda daha fazla olduğu gözlendi (p=0,021). Uzun süreli COVID'e sahip çocuklarda, 6DYT mesafeleri, DLCO Z-skorları ve spirometri ile akciğer hacmi testlerinin tahmin edilen değerleri daha düşük bulundu, ancak ortalama değerler normal referans aralığındaydı. DLCO, FeNO ve 6DYT için ortalama tahmin edilen değerler iki grup arasında benzerdi.

Sonuçlar: COVID-19 enfeksiyonu sonrasında ısrarcı solunumsal semptomları devam eden çocukların solunum fonksiyon testleri ile detaylı değerlendirilmesi gerekir. Akciğer görüntülemesinde anormallikleri olan çocuklar, özellikle spirometri ve akciğer hacim ölçümleri ile ayrıntılı değerlendirilmelidir. FeNO ölçümlerinin uzun süreli COVID izleminde anlamlı olmadığı bulunmuştur.

Anahtar kelimeler: Çocuklar, difüzyon kapasitesi, fraksiyonel solunan nitrik oksit, uzun süreli COVID, 6 dakika yürüme testi

INTRODUCTION

The coronavirus disease-2019 (COVID-19) pandemic, caused by the novel coronavirus severe acute respiratory syndrome coronavirus-2 (SARS-CoV-2), has been associated with significant morbidity and mortality. The prolonged process of the pandemic has brought with it many questions about long-term sequelae in patients and studies that seek answers to these questions. It has been strongly suggested that there are "long-term symptoms," as evidenced by adult studies[1]. Although the definition of long COVID is constantly changing, most studies define

Address for Correspondence: S. Girit, Istanbul Medeniyet University Faculty of Medicine, Department of Pediatric Pulmonology, Istanbul, Türkiye
E-mail: saniyegirit@gmail.com **ORCID ID:** orcid.org/0000-0001-7556-6568

Received: 18 January 2024
Accepted: 25 April 2024
Online First: 21 May 2024

Cite as: Onay ZR, Can Oksay S, Mavi Tortop D, Bilgin G, Ayhan Y, Durankus F, Girit S. Impact of Long COVID on Lung Function in Children. Medeni Med J Medeni Med J 2024;39:74-84

it as the persistence of symptoms or development of sequelae more than 3 or 4 weeks after the onset of acute symptoms of COVID-19[2].

A study from Australia reported that 8% of children aged 0-19 years, most with a mild history of COVID-19, had persistent symptoms 3-6 months after acute onset[2]. A cross-sectional study of 129 children in Italy noted that 42.6% had at least one persistent symptom after more than 60 days[3]. Reductions in spirometry values and the diffusing capacity of the lungs for carbon monoxide (DLCO) are the most frequently reported disorders in adults, but pediatric data on this issue are insufficient[4-6].

We aimed to investigate whether respiratory complaints impact pulmonary function test (PFT) findings in children with long-term COVID. Because pre-infection PFT values in this population are unknown, we excluded children with lung diseases and compared post-COVID individuals with healthy controls. In addition, we determined whether clinical and radiological findings from the acute period of COVID-19 affected the PFT results of post-COVID individuals. For this purpose, detailed PFTs [spirometry and tests of lung volume, DLCO, and fractional exhaled nitric oxide (FeNO)] and exercise capacity tests [the 6-minute walk test (6MWT), modified Borg dyspnea scale, and fatigue scale] were performed on children with long COVID and healthy controls.

MATERIALS and METHODS

Study Design and Participants

This investigation was designed as an analytical, non-randomly controlled, prospective cohort study at a university hospital in Istanbul, Türkiye. The subjects were referred to a pediatric pulmonology clinic between January and July 2021 to evaluate persistent respiratory symptoms manifesting 6 weeks or more after acute SARS-CoV-2 infection. The inclusion criteria consisted of a history of positive SARS-CoV-2 RNA testing and, subsequently, the presence of persistent respiratory symptoms, such as cough, dyspnea, and chest pain, for 6 weeks. The medical data of the COVID-19-positive patients were obtained from the National Electronic Medical Record System (NEMRS)[7], which was also used to extract clinical data on demographics, comorbidities, SARS-CoV-2 polymerase chain reaction (PCR) test results, chest imaging [thorax computed tomography (CT) and chest X-rays], specific COVID-19 treatments, and hospitalization (if necessary).

All participants yielded negative results on SARS-CoV-2 PCR tests at our center. FeNO tests and then spirometry, lung volume, and DLCO measurements were performed. After the participants rested for 1 h, 6MWTs were initiated.

"Long COVID" was defined as the persistence of respiratory symptoms for at least 4 weeks after the completion of the acute infection period (two weeks). The time span from symptom onset to admission (the day PFTs were performed) was also recorded in days. Based on clinical data collected during the acute phase of the original COVID-19 infection, each participant's disease severity was classified in accordance with the World Health Organization criteria as asymptomatic, mild, moderate, severe, and critical infection[8].

Healthy children of approximately the same age who had no history of lung disease and applied to a general pediatric outpatient clinic for any reason were classified as the control group. None of the participants in the control group or their families had a history of COVID-19, which was confirmed by NEMRS data. The exclusion criteria ruled out participants with chronic lung diseases (including asthma and allergic rhinitis), smokers, and those who did not want to participate (Figure 1).

Demographic and Clinical Data

We recorded the age, gender, weight, height, and body mass index (BMI) Z-scores, oxygen saturation at room air, and comorbidities of each individual in both groups. We classified the comorbidities into organ-specific diseases (obesity; pulmonary, cardiac, connective tissue, metabolic, and endocrinological diseases; and hematologic diseases in patients predisposed to thromboembolism).

Chest X-rays and thorax CTs taken during the acute period were evaluated by the same pediatric pulmonologist. The quantitative radiological scoring system was used to define idiopathic pulmonary fibrosis due to SARS infection. This test, used in previous years, evaluates signs including ground glass opacities, consolidation, reticulosis, bronchiectasis, honeycombing, parenchymal bands, fibrosis, and air trapping. The five lobes in the lungs are scored between 0 and 5 according to the density of the lung area involved; a total score of 0 is considered normal, while <5% involvement for each lobe yields 1 point, 5-25% yields 2 points, 25-49% yields 3 points, 50-75% yields 4 points, and >75% involvement is scored as 5 points. The scores calculated for each segment and the total score were calculated from 0 to 25[9-12].

Pulmonary Function Tests

All PFT measurements were performed in the pulmonary function laboratory of a pediatric pulmonology department according to the guidelines

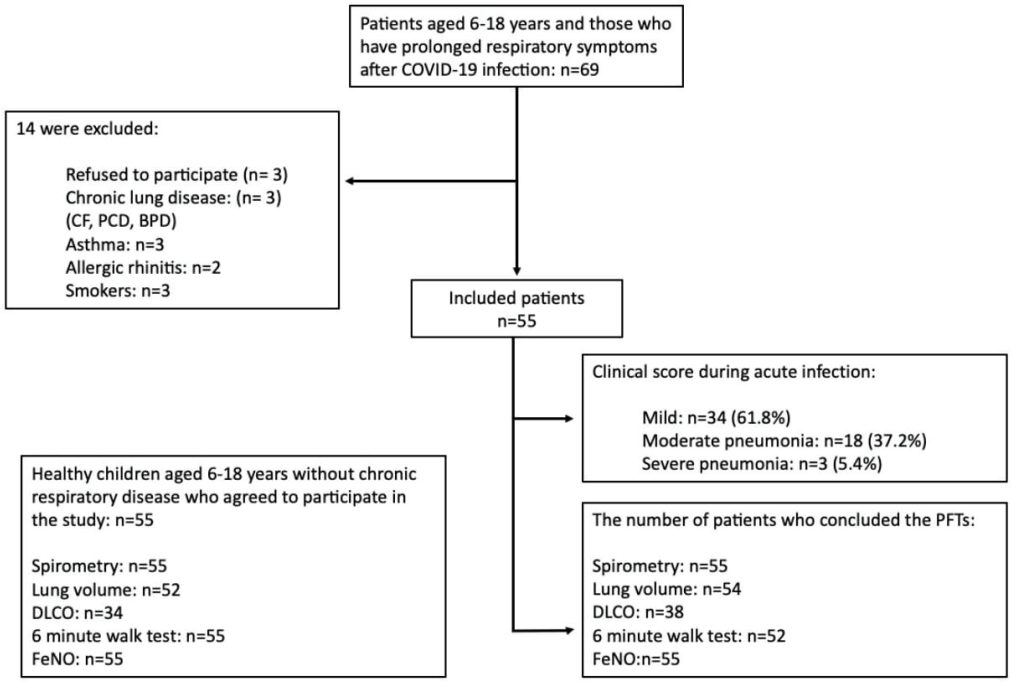

Figure 1. The participate diagram of the study.

COVID-19: Coronavirus disease-2019, CF: Cystic fibrosis, PCD: Primary ciliary dyskinesia, BPD: Bronchopulmonary dyskinesia, FeNO: fractional exhaled nitric oxide, PFT: Pulmonary function test, DLCO: Diffusing capacity for carbon monoxide

of the American Thoracic Society (ATS) and European Respiratory Society (ERS) by a single qualified pulmonary function technologist[13]. During the measurements, the PFT technologist performed control measures against COVID-19. The flowmeter calibration was performed daily using a 3 L syringe. Forced expiratory maneuvers were performed on all participants while they sat comfortably in a chair.

Spirometry, Lung Volume and Pulmonary Diffusion Capacity

Pulmonary flow, lung volume, and diffusing capacity were evaluated using the Minibox+ (PulmOne Advanced Medical Devices, Ra'ananna, Israel) following the ATS/ERS guidelines[13]. Each subject underwent three accepted maneuvers for spirometry; the highest values were recorded and used in subsequent analyses. The DLCO single-breath technique was adjusted for each participant's hemoglobin concentration. The following parameters were measured: forced expiratory volume in the first second (FEV_1), forced vital capacity (FVC), forced expiratory flows at 25% and 75% of FVC (FEF_{25-75}), FEV_1/FVC, total lung capacity (TLC), residual volume (RV), RV/TLC, VC, and functional residual capacity (FRC). All spirometry measurements were expressed as percentages of predicted normal values, which were calculated automatically based on age, sex, height, and ethnicity[14]. The spirometry and plethysmography values and DLCO Z-scores of the measurements were calculated using the Global Lung Function Initiative Calculator according to age, gender, and height[15]. The criteria for classifying lung function abnormalities were based on the current ERS guidelines: starting from the FEV_1/FVC ratio, we determined whether an obstruction existed by checking whether the ratio was lower than the lower limits of normal (LLN, Z-score <-1.64). If an obstruction was present, the FVC was assessed to determine whether there was simply an obstruction or whether there might have been a restrictive pattern. TLC measurement was used to define the restriction. If the FEV_1/FVC ratio was normal, it was determined that there was no obstruction, and the FVC was evaluated again. If the FVC was normal, spirometry was considered normal; however, if the FVC was below the LLN, the TLC measurement was evaluated, and a possible restriction was considered. If the DLCO value was above the LLN in patients with a restrictive pattern, restriction by the chest wall or musculoskeletal system was considered. However, if the DLCO value was below the LLN, it was considered that there might be parenchymal damage (Figure 2)[16].

Fractional Exhaled Nitric Oxide

Airway inflammation was measured noninvasively and quantitatively using the NObreathe® FeNO analyzer. This process was performed according to the ATS/ERS recommendations[17].

Six-Minute Walk Test and Borg Scale

The 6MWT was performed by the same pulmonary functional technologist in accordance with the ATS guidelines[18]. The modified Borg dyspnea and fatigue scale was administered to the participants, who were requested to assess their respective conditions by responding to the following questions: "Please indicate the degree of your shortness of breath using this scale" and "Please indicate the degree of your fatigue using this scale." The participants were instructed to select a number on a scale ranging from 0 (representing no symptoms) to 10 (representing extremely severe symptoms)[18].

The 6MWT percentage values were determined by calculating the percentage of the distance walked as the ideal walking distance[19] [The ideal 6MWT distance equation for men is 1140 – (5.61 x BMI) – (6.94 x age); the equation for women is 1017 – (6.24 x BMI) – (5.83 x age)].

Ethical Committee Approval and Informed Consent

This study adhered to the revised Declaration of Helsinki and received approval from the Clinical Research Ethics Committee of Istanbul Medeniyet University Goztepe Training and Research Hospital on January 27, 2021 (decision no: 2021/0068). Both participants and their parents provided informed consent before participation.

Statistical Analysis

The statistical analysis was performed using the Number Cruncher Statistical System (NCSS) 2007 software (Kaysville, Utah, USA). Descriptive statistics, including mean, standard deviation, median, frequency, ratio, minimum (min), and maximum (max), were employed to analyze the study data. Normal distribution of quantitative data was assessed via the Shapiro-Wilk test and graphical methods. Two-group comparisons of normally distributed quantitative data were conducted using Student's t-test, whereas non-normally distributed data were analyzed using the Mann-Whitney U-test. Qualitative data were compared using Pearson's chi-square test, Fisher's exact test, and Fisher-Freeman-Halton test. For group comparisons involving three

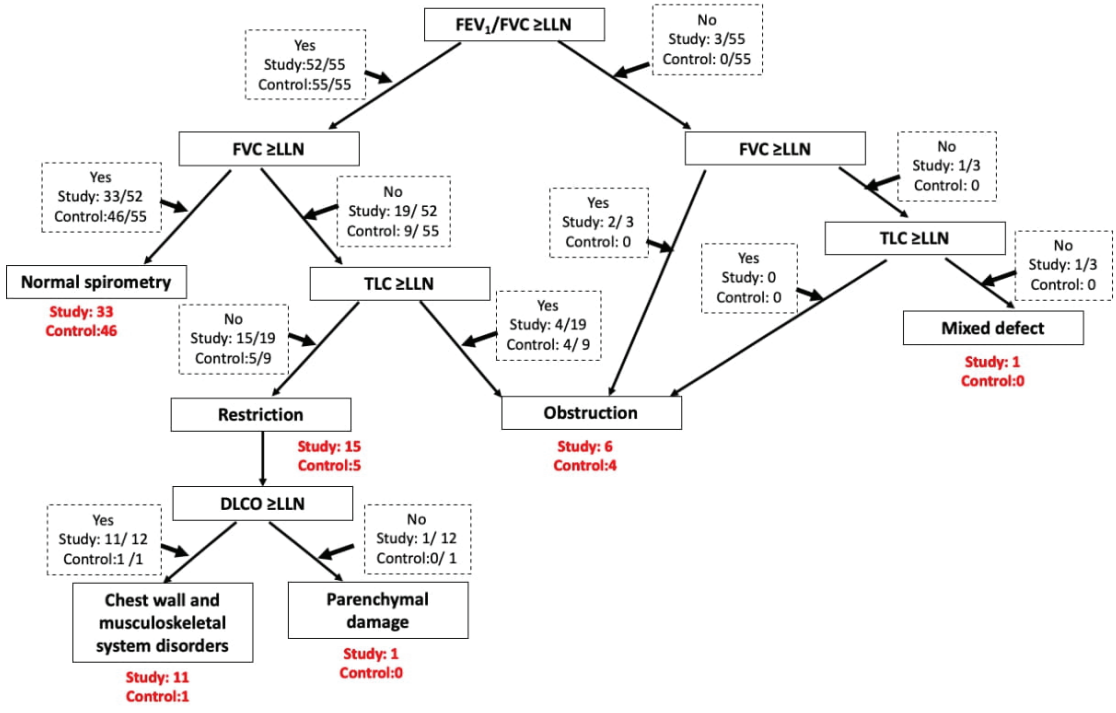

Figure 2. Pulmonary function test evaluation of the participants in both study and control groups.

FEV_1/FVC: The ratio of forced expiratory volume in the first second (FEV_1) to forced vital capacity (FVC), LLN: Lower limits of normal (Z-score <-1.64), FVC: Forced vital capacity, TLC: Total lung capacity, DLCO: Diffusing capacity of lungs for carbon monoxide

or more groups with non-normal distribution, the Kruskal-Wallis test was employed, followed by pairwise comparisons using the Bonferroni-Dunn test. Spearman's correlation analysis was used to assess the relationships between variables. The significance level was set at $p<0.05$.

RESULTS

General Characteristics of the Participants

Fifty-five of the 69 children with long COVID and 55 healthy controls participated in the study. Fourteen patients were excluded from the study group (three patients refused to participate, three had chronic lung disease, three had asthma, two had allergic rhinitis, and three were smokers). Figure 1 presents the participants' characteristics and results of the spirometry, lung volume, DLCO, 6MWT, and FeNO tests.

The mean age of the study group was 14.71±3.03 years (min: 7.1, max: 18.6), and that of the control group was 12.5±2.9 years (min: 6.8, max: 17.5) (p=0.001). Thirty-one patients (56.4%) in the study group and 27 patients (49.1%) in the control group were female (p=0.445). The weight, height, and BMI Z-scores were similar between the two groups (p=1.000 in all groups). In total, 14 of the 55 (25.5%) patients in the study group had comorbidities: one had experienced a total pulmonary venous return abnormality (that was operated upon), two had obesity, two had hematologic issues (Evans syndrome and polycythemia), two had connective tissue diseases (familial Mediterranean fever), and five had endocrine and metabolic system diseases (hypothyroidism, type IV glycogen storage disease, isovaleric acidemia, hypophosphatemic ricketss, and growth hormone deficiency). Three patients in the control group were obese.

Characteristics Associated with Acute COVID-19 Infection and Long COVID

In the study group, most of the participants (61.8%) had mild infections, approximately one-third (37.2%) had moderate pneumonia, and only 5.4% had severe pneumonia. More than one-third of the participants had a history of hospitalization, with an average stay of 10.11±4.48 days. When the treatments of 18 hospitalized patients were reviewed, it was observed that the most frequently used treatment options were favipiravir and antibiotics. Most patients had undergone more than one treatment method. Twenty-one of the patients showed consolidation on chest X-rays during acute infection, and all underwent thoracic CT. Seventeen participants had pulmonary involvement on thoracic CT, and the median CT score was 6.23. The average number of days from the onset of acute infection to admission to our clinic was 88.62±30.84. The clinical findings of the participants in the study group during the acute COVID-19 infection period are presented in Table 1.

In the acute phase of COVID-19 infection, the most common symptoms were cough (63.6%) and fever (50.9%). Other symptoms were fatigue (40%), myalgia (38.2%), headache (32.7%), chest pain (25.5%), dyspnea (23.6%), runny nose (18.2%), nausea and vomiting (14.5%), and sore throat (10.9%). The most common long COVID

Table 1. Clinical findings of the participants in the study group at the time of acute COVID-19 infection.

Study group	Data
Severity of disease, n (%)	55 (100)
Mild infection	34 (61.8)
Moderate pneumonia	18 (32.7)
Severe pneumonia	3 (5.4)
Number of hospitalized patients, n (%)	18 (32.7)
Hospitalization days, mean ± SD	10.11±4.48
Treatments administered during hospitalization among 18 patients, n (%)	
Favipiravir	13 (72.2)
Antibiotics	10 (55.6)
Anticoagulants	5 (27.8)
Oral steroids	5 (27.8)
IVIG	3 (16.7)
Hydroxychloroquine	2 (11.1)
Azithromycin	2 (11.1)
Follow-up without treatment	1 (5.6)
PICU admission, n (%)	2 (3.6)
Supportive treatment, n (%)	
Oxygen	3 (5.5)
HFNC	1 (1.8)
Consolidation on chest X-ray, n (%)	21 (38.2)
Number of patients who underwent thorax CT, n (%)	21 (38.2)
Number of patients with normal thorax CT findings, n (%)	4 (19)
Number of patients with abnormal thorax CT findings, n (%)	17 (81)
Thorax CT score, median (min-max) (n=17)	6.23 (1-14)
Number of days to PFT date after COVID-19 infection, median (min-max)	85 (35-194)

COVID-19: Coronavirus disease-2019, SD: Standard deviation, IVIG: Intravenous immunoglobulin, PICU: Pediatric intensive care unit, HFNC: High flow nasal cannula, CT: Computed tomography, PFT: Pulmonary function test, min-max: Minimum-maximum

symptoms when our study began were cough (52.7%), dyspnea (32.7%), and chest pain (14.5%).

Pulmonary Function Tests

There were significant differences between the study and control groups in FEV_1, FVC, and FEF_{25-75} percentages and Z-scores; average FEV_1/FVC and z-scores; TLC, RV, and FRC percentages and Z-scores; RV/TLC ratios and Z-scores; and VC Z-scores. The values were higher in the control group. No differences were detected in the average DLCO or FeNO values across the two groups, whereas the DLCO Z-scores were significantly lower in the study group (p=0.007). There was no difference between the two groups in exercise test results and modified Borg scale scores (Table 2).

The spirometry results of the children participating in our study were classified as normal, restrictive, obstructive, or mixed based on the ERS recommendations[16], as shown in Figure 3. In total, 33 children in the study group (60%) and 46 (83.6%) in the control group had normal spirometry results. Fifteen patients (27.2%) in the study group and five (9.1%) in the control group had restrictive PFTs. Thirteen out of 20 children with restrictive PFTs had DLCO data; one had a DLCO value below the LLN, whereas the other 12 had DLCO values above the LLN.

Table 2. Spirometry, lung volume, DLCO, FeNO, and exercise test results of the two groups.

Pulmonary function test		Study group	Control group	p-value
FEV_1	% predicted, mean ± SD	87.20±12.92	100.26±10.92	**0.001**[a]
	Z-score, Q2 (Q1-Q3)	-0.92 (-1.46-0.04)	0.37 (-0.59-1.38)	**0.001**[b]
FVC	% predicted, mean ± SD	84.98±13.80	91.09±12.04	**0.015**[a]
	Z-score, Q2 (Q1-Q3)	-1.17 (-1.91-0.03)	-0.31 (-1.30-1.18)	**0.001**[b]
FEV_1/FVC	Mean ± SD	101.93±9.17	110.02±6.27	**0.001**[a]
	Z-score, Q2 (Q1-Q3)	0.70 (-0.04-1.30)	1.50 (0.66-2.55)	**0.001**[b]
FEF_{25-75}	% predicted, mean ± SD	89.73±20.36	114.35±23.22	**0.001**[a]
	Z-score, Q2 (Q1-Q3)	-0.12 (-1.03-0.31)	0.75 (-0.31-1.23)	**0.001**[b]
TLC	% predicted, mean ± SD	82.02±16.89	90.40±19.06	**0.019**[a]
	Z-score, Q2 (Q1-Q3)	-2.99 (-3.96- -1.21)	1.16 (-1.17-3.04)	**0.001**[b]
RV	% predicted, mean ± SD	53.46±49.00	74.33±43.29	**0.003**[a]
	Z-score, Q2 (Q1-Q3)	-1.72 (-2.73-0.16)	-0.28 (-1.0-0.87)	**0.001**[b]
RV/TLC	mean ± SD	59.04±45.08	78.75±33.38	**0.012**[a]
	Z-score, Q2 (Q1-Q3)	-1.0 (-2.19-0.49)	-0.35 (-0.95-0.34)	**0.001**[b]
VC	% predicted, mean ± SD	86.78±11.51	91.04±15.39	0.109[a]
	Z-score, Q2 (Q1-Q3)	-2.94 (-3.88- -1.01)	0.47 (-1.57-4.22)	**0.001**[b]
FRC	% predicted, mean ± SD	70.95±42.06	93. 45±43.17	**0.022**[a]
	Z-score, Q2 (Q1-Q3)	-2.30 (-4.48- -1.20)	0.06 (-1.20-2.75)	**0.001**[b]
DLCO	%, mean ± SD	97.13±18.40	103.76±14.87	0.099[a]
	Z-score, Q2 (Q1-Q3)	-0.48 (-1.33-0.20)	0.23 (-0.66-0.89)	**0.007**[b]
FeNO	ppb, mean ± SD	9.58±6.75	7.55±5.79	0.070[b]
sPO_2	%, mean ± SD	98.13±0.82	98.00±0.94	0.340[b]
6MWT	meter, mean ± SD	568.69±107.47	588.51±44.20	**0.013**[b]
	%, mean ± SD	66.45±12.70	67.31±7.25	0.183[b]
Borg dyspnea score	Median (min-max)	0.5 (0-5)	0 (0-6)	0.258[b]
Borg fatigue score	Median (min-max)	0.5 (0-5)	0.5 (0-5)	0.691[b]

[a]Student's t-test, [b]Mann-Whitney U test. FEV_1: Forced expiratory volume in the first second, Q1: First-quarter value, Q2: Median, Q3: Third-quarter value, FVC: Forced vital capacity, FEF_{25-75}: Forced expiratory flows at 25 and 75% of FVC, TLC: Total lung capacity, RV: Reserve volume, VC: Vital capacity, FRC: Functional residual capacity, DLCO: Diffusing capacity of lungs for carbon monoxide, FeNO: Fractional exhaled nitric oxide, PPB: Parts per billion, sPO_2: Peripheral oxygen saturation, 6MWT: 6-minute-walk test, SD: Standard deviation, min-max: Minimum-maximum

Comparing the PFT results in two groups, a restrictive pattern was observed significantly more often in the study group (p=0.021). While six patients in the study group had low DLCO values (four had mild and two had moderate diffusing impairments), none of the participants in the control group had low DLCO results (p=0.015). When the six patients in the study group whose DLCO Z-scores were found to be below the LLN were examined, it was detected that two of them presented as normal, two suffered obstruction, one suffered restriction, and one had mixed PFT findings.

The FEV_1, FVC, TLC, and VC values of the group with consolidation on chest X-rays were found to be significantly lower than those of the group without consolidation (p=0.018, p=0.044, p=0.035, p=0.014, and p=0.018, respectively) (Table 3). No significant correlation was found between CT scores and spirometric values, but a negative correlation was found with TLC (p=0.026, r=-0.497), RV (p=0.027, r=-0.495), RV/TLC (p=0.021, r=-0.513), and FRC (p=0.002, r=-0.707) values (Table 4). No significant differences were found between clinical scores (mild and moderate/severe) and PFT values. Furthermore, no statistically significant relationship was found between clinical scores and FeNO levels (p=0.083).

No significant difference was found between the current symptoms (cough, chest pain, and dyspnea) of the COVID-19 survivors and their spirometry and plethysmography values. A significant difference was found between current symptoms and DLCO and

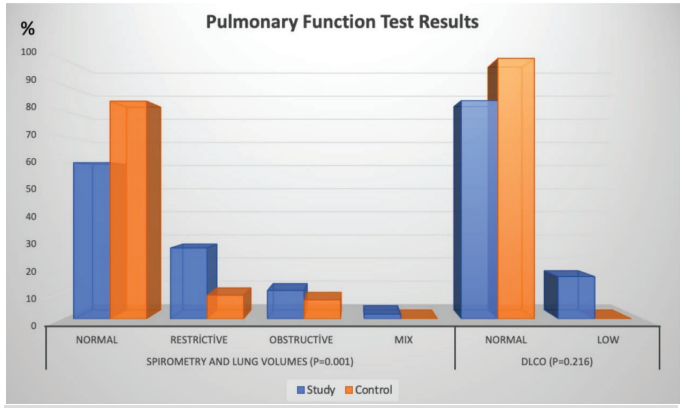

Figure 3. The comparisons of pulmonary function test results between study and control groups.

Table 3. Relationships between PFTs, presence of consolidation on chest X-rays, severity of disease, and long COVID symptoms among children with long COVID.

	Presence of consolidation on chest X-ray		Severity of disease			Current symptoms			
	Yes n=21	p	Mild n=34	Moderate-severe n=21	p[b]	Cough	Chest pain	Dyspnea	p[c]
FEV_1, %, mean ± SD	82.0±14.3	**0.018**[a]	88.6±10.7	81.8±19.2	0.467	89.2±13.2	87.9±11.1	83.7±13.1	0.322
FVC, %, mean ± SD	80.2±15.1	**0.044**[a]	86.2±12.2	80.1±18.7	0.377	85.6±14.1	85.0±12.6	84.0±14.5	0.801
FEV_1/FVC, mean ± SD	102.2±10.8	0.869[a]	102.3±9.1	100.6±9.6	0.577	103.0±9.3	103.5±3.6	99.5±10.4	0.471
TLC, %, mean ± SD	86.1±20.1	0.182[a]	82.4±17.7	80.7±13.2	0.982	79.0±13.9	90.4±17.4	83.2±20.2	0.280
RV, %, mean ± SD	67.8±59.9	0.162[b]	55.8±52.3	43.3±30.6	0.902	46.7±46.3	69.0±52.2	57.0±52.5	0.353
FeNO, ppb, mean ± SD	11.6±7.9	0.086[b]	8.5±5.2	13.7±10.3	0.083	8.9±6.1	9.0±4.6	10.9±8.5	0.812
DLCO, %, mean ± SD	96.5±18.6	0.874[a]	96.0±17.9	100.7±20.2	0.259	106.9±17.5	92.3±13.2	86.6±15.1	**0.008**
6MWT, %, mean ± SD	70.3±15.9	0.240[b]	64.8±11.6	74.2±15.3	0.100	62.1±9.9	78.7±16.0	68.9±12.3	**0.018**

[a]Student's t-test, [b]Mann-Whitney U test, [c]Kruskal-Wallis test. FEV_1: Forced expiratory volume in the first second, FVC: Forced vital capacity, FEF_{25-75}: Forced expiratory flow at 25% and 75% of FVC, TLC: Total lung capacity, RV: Reserve volume, DLCO: Diffusing capacity of lungs for carbon monoxide, FeNO: Fractional exhaled nitric oxide, PPR: Parts per billion, 6MWT: 6-minute-walk test, SD: Standard deviation, COVID: Coronavirus disease, PFT: Pulmonary function test

6MWT percentages (p=0.008 and p=0.018, respectively). DLCO values were found to be lower in the group with dyspnea (p=0.008), and 6MWT percentages were found to be lower in the group with cough symptoms (p=0.018) (Table 3).

DISCUSSION

In our study, 16.2% of patients with long COVID had diffusion impairments and 27.2% had restrictive respiratory disorders. We found that clinical scores in the acute period did not affect long-term PFTs. Decreases in lung volume and expiratory flow were observed in patients with consolidation on chest X-rays and high thorax CT scores. The DLCO values of patients with dyspnea were found to be lower than those of individuals with coughing and chest pain. Exercise capacity was found to be the lowest in those with cough symptoms.

At the end of the first year of the pandemic, the National Institute for Health and Care Excellence published a rapid guideline for managing long-term COVID[20]. In children, long COVID was first reported in the literature in November 2020 by Ludvigsson[21] when the long-term symptoms of five pediatric patients were noticed. The first study to examine the pulmonary manifestations of long COVID in children was conducted by Bottino et al.[5] In this study, forced spirometry, DLCO, and lung ultrasound results were examined, and it was emphasized that pulmonary sequelae did not develop in the children in the follow-up.

Table 4. Correlations between CT scores and pulmonary function test values.

	CT score*	
	p	**r**
FEV_1, %	0.285	-0.245
FVC, %	0.098	-0.371
FEV_1/FVC	0.964	-0.011
FEF_{25-75}, %	0.795	-0.06
TLC, %	**0.026**	-0.497
RV, %	**0.027**	-0.495
VC, %	0.940	0.018
FRC, %	**0.002**	-0.707
FeNO, ppb	0.679	0.096
DLCO, %	0.302	-0.297
6MWT, meter	0.640	-0.108
6MWT, %	0.591	-0.124
Borg dyspnea score	0.895	0.031
Borg fatigue score	0.739	-0.077

*Based on the lung involvement of the disease, CT scores were assigned from 0-25. As the CT score increases, lung involvement increases. FEV_1: Forced expiratory volume in the first second, FVC: Forced vital capacity, FEF_{25-75}: Forced expiratory flows at 25% and 75% of FVC, TLC: Total lung capacity, RV: Reserve volume, VC: Vital capacity, FRC: functional residual capacity, DLCO: Diffusing capacity of the lungs for carbon monoxide, FeNO: Fractional exhaled nitric oxide, PPB: Parts per billion, 6MWT: 6-minute-walk test, r: Spearman's correlation coefficient, CT: Computed tomography

COVID-19 appears to harm the lungs the most, causing a variety of pathophysiological events in parts of the alveolar structure, including the alveolar epithelium, hyaline membrane, capillary, and alveolar septum[22,23]. It may impede gas diffusion due to damage to the alveolar epithelium and endothelial cells and eventually lead to restrictive respiratory conditions. In addition, secondary fibroproliferation, starting from the terminal bronchioles accompanying this pathway mentioned in the first sentence, may also cause airway obstruction and create obstructive respiratory conditions[23]. In Salem et al.[1], reductions were found in TLC, FVC, FEV_1, and DLCO on the long-term PFTs of adult COVID-19 survivors. Half of the COVID-19 survivors they studied suffered from restrictive lung impairment, and more than one-third of the patients had diffusion impairments[1]. Bottini et al.[5] prospectively investigated 16 children with asymptomatic or mild infections for at least 1 month after COVID-19 infection and found that none of the participants had any abnormalities on spirometry, DLCO, airway resistance, and lung ultrasonography tests. Öztürk et al.[6] retrospectively evaluated 50 children with and without respiratory symptoms using PFTs 3 months after acute infection. They found that the spirometry values were similar in children with and without respiratory symptoms and were all within the normal range. However, diffusion impairment was found to be significantly more common in children with severe COVID-19 infections than in those with mild infections[6]. In our study, it was found that expiratory flow and lung volume were lower in children with long COVID; 10.9% had obstructive, 27.2% had restrictive, and 1.8% had mixed respiratory patterns, whereas 16.2% had diffusion impairments. We found that DLCO Z-scores were slightly impaired in children with long COVID. Nevertheless, it should be noted that although the spirometry results and DLCO Z-scores of the healthy children were lower than those of the afflicted children, the latter's mean values were within the normal range. Because there was no long-term radiological evaluation of the COVID-19 survivors, we cannot offer sufficient commentary on this subject. In our study, contrary to that of Öztürk et al.[6], no significant relationship was found between diffusion impairment and clinical scores. This may be because most of the patients had mild to moderate infections in the acute phase of COVID-19. In the existing literature, the extent to

which a DLCO decrease is expressed in symptoms is not yet clear. Histopathologically speaking, alveolocapillary membrane involvement, impaired gas exchange, and inadequate oxygenation can lead to dyspnea during exercise, as assessed by DLCO measurement[23]. In addition, functional loss of respiratory muscle due to overuse because of symptoms such as cough and dyspnea may also cause restrictive lung disease[24]. In this study, parenchymal damage was identified due to decreased DLCO in only one participant, who had restrictive PFT results; because the DLCO values were above the LLN in the other 12 patients, it was thought that there might be a restriction for a reason other than the lungs. In cases where the DLCO is normal and the patient suffers from dyspnea, other systemic conditions that may cause symptoms in patients should be investigated.

In follow-up studies on long-term COVID, the 6MWT and modified Borg scale are commonly used to evaluate functional capacity in adults. In one study conducted with 29 children who had protracted respiratory findings, 9 who completed the 6MWT walked 66.7% of the predicted distance (4). In a study conducted by Cortes-Telles et al.[25], both Borg fatigue and dyspnea scores were significantly higher among adults with both dyspnea and fatigue observed 30-90 days after acute COVID-19 infection. In our study, the 6MWT percentage and Borg scale values were similar in the patients and healthy controls, whereas the 6MWT distances were lower in the study group. For interpreting the 6MWT results in children, the use of estimated percentages based on age, BMI, and gender is crucial, and using similar estimated percentages is more valuable than using different 6MWT distances in both groups. In some studies, the low exercise capacity of patients with long COVID may be an effect of muscle weakness due to COVID-19 infection[26,27]. In our study, based on persistent complaints, it was observed that the 6MWT percentages of patients afflicted by coughing were lower than those of patients with chest pain and dyspnea. Even if the respiratory parameters of children with long COVID are within normal limits, they should be closely monitored in terms of exercise capacity.

Fractionally exhaled NO is mostly used for diagnosing asthma exacerbations in clinical practice[28]. Although prolonged inflammation may persist in long COVID, most studies have shown that FeNO measurement is not a useful method for detecting it[29,30]. However, FeNO has been accepted as a useful biomarker for assessing airway inflammation and oxidative stress in the lungs[29]. Lior et al.[28] found that lower levels of FeNO were associated with more severe disease, and Cameli et al.[31] reported increased FeNO values in post-COVID patients, which supports its correlation with pulmonary inflammation. Betancor et al.[30] found FeNO levels to be within the normal range during the acute phase of COVID-19, with some increase during the recovery phase. Although there is no consensus on FeNO measurement in adult studies, we did not find FeNO particularly useful in the long-term follow-up of COVID-19 in children.

Some adult studies have attempted to identify the relationship between the long-term effects of COVID-19 and demographic, clinical, and laboratory findings upon diagnosis[1]. In our study, we observed decreases in both the expiratory flows of patients with consolidation on chest X-rays and the lung volumes of patients with consolidation on thorax CT. We believe that it is important to follow up on children exhibiting consolidation on chest X-rays and thorax CT to detect other long-term symptoms using spirometry and lung volume tests. We also found that their clinical scores did not affect the long-term PFTs of children with long COVID. Diffusion impairment was more common in children with dyspnea than in those with other symptoms. Moreover, children with cough had lower functional capacity than children with other symptoms. It is important to monitor children with dyspnea carefully for DLCO and to follow-up on children with persistent coughing through 6MWTs after COVID-19.

To the best of our knowledge, in the limited body of literature on PFTs in long COVID during childhood, our study is the first to have recruited a healthy control group. It also used the highest number of children in the evaluation of PFTs. Moreover, the modified Borg dyspnea and fatigue scale was used for the first time to evaluate the long-term effects of COVID-19 on children's functional capacity. However, our study had some limitations. Although the mean age of the healthy children in the control group (who were selected randomly) was different from that of the study group, their heights, weights, and BMI Z-scores were similar. We believe that this limitation can be accepted because their body proportions were similar. In addition, there was no comparison of thorax imaging between the acute phase and the long-term follow-up stage. Despite these limitations, we believe that our data, along with the comparison with healthy control subjects, provide enlightening insights into the long-term monitoring of COVID-19 patients.

CONCLUSION

In conclusion, it is important to follow-up long COVID symptoms in children. In particular, in children with long COVID and respiratory complaints, expiratory flow and lung volume may decrease, and restrictive patterns may

be obvious. Where COVID symptoms such as cough, dyspnea, or chest pain emerge, spirometry and DLCO results may provide valuable insights into assessing functional capacity and determining potential chronic lung damage. There is a need for future studies in which longer-term PFTs are conducted to determine the duration of respiratory disorders.

Ethics

Ethics Committee Approval: This study was approved by the Clinical Research Ethics Committee of Istanbul Medeniyet University Goztepe Training and Research Hospital on January 27, 2021, with the decision number 2021/0068.

Informed Consent: Both participants and their parents provided informed consent before participation.

Author Contributions

Surgical and Medical Practices: Z.R.O., S.C.O., D.M.T., G.B., Y.A., F.D., S.G., Concept: Z.R.O., S.G., Design: Z.R.O., S.G., Data Collection and/or Processing: Z.R.O., S.C.O., D.M.T., G.B., Y.A., F.D., S.G., Analysis and/or Interpretation: Z.R.O., S.C.O., D.M.T., G.B., Y.A., F.D., S.G., Literature Search: Z.R.O., S.C.O., D.M.T., G.B., Y.A., F.D., S.G., Writing: Z.R.O., S.G.

Conflict of Interest: The authors have no conflict of interest to declare.

Financial Disclosure: The authors declared that this study has received no financial support.

REFERENCES

1. Salem AM, Al Khathlan N, Alharbi AF, et al. The Long-Term Impact of COVID-19 Pneumonia on the Pulmonary Function of Survivors. Int J Gen Med. 2021;14:3271-80.
2. Zimmermann P, Pittet LF, Curtis N. How Common is Long COVID in Children and Adolescents? Pediatr Infect Dis J. 2021;40:e482-7.
3. Buonsenso D, Munblit D, De Rose C, et al. Preliminary evidence on long COVID in children. Acta Paediatr. 2021;110:2208-11.
4. Leftin Dobkin SC, Collaco JM, McGrath-Morrow SA. Protracted respiratory findings in children post-SARS-CoV-2 infection. Pediatr Pulmonol. 2021;56:3682-7.
5. Bottino I, Patria MF, Milani GP, et al. Can Asymptomatic or Non-Severe SARS-CoV-2 Infection Cause Medium-Term Pulmonary Sequelae in Children? Front Pediatr. 2021;9:621019.
6. Öztürk GK, Beken B, Doğan S, Akar HH. Pulmonary function tests in the follow-up of children with COVID-19. Eur J Pediatr. 2022;181:2839-47.
7. Ministry of Health, Republic of Turkey. E-Nabız Personal Health System. Available from: https://enabiz.gov.tr/.
8. World Health Organization. Clinical management of COVID-19: living guideline, 13 January 2023. Available from: https://www.who.int/publications/i/item/WHO-2019-nCoV-clinical-2023.1 (Accessed on May 19, 2023).
9. Wasilewski PG, Mruk B, Mazur S, Półtorak-Szymczak G, Sklinda K, Walecki J. COVID-19 severity scoring systems in radiological imaging - a review. Pol J Radiol. 2020;85:e361-8.
10. Li K, Wu J, Wu F, et al. The Clinical and Chest CT Features Associated With Severe and Critical COVID-19 Pneumonia. Invest Radiol. 2020;55:327-31.
11. Chang YC, Yu CJ, Chang SC, et al. Pulmonary sequelae in convalescent patients after severe acute respiratory syndrome: evaluation with thin-section CT. Radiology. 2005;236:1067-75.
12. Dai H, Zhang X, Xia J, et al. High-resolution Chest CT Features and Clinical Characteristics of Patients Infected with COVID-19 in Jiangsu, China. Int J Infect Dis. 2020;95:106-12.
13. Graham BL, Steenbruggen I, Miller MR, et al. Standardization of Spirometry 2019 Update. An Official American Thoracic Society and European Respiratory Society Technical Statement. Am J Respir Crit Care Med. 2019;200:e70-88.
14. Hankinson JL, Odencrantz JR, Fedan KB. Spirometric reference values from a sample of the general U.S. population. Am J Respir Crit Care Med. 1999;159:179-87.
15. Global Lung Function Initiative. Calculators for spirometry, TLCO and lung volume. Available from: http://gli-calculator.ersnet.org/index.html (Accessed on September 10, 2021).
16. Stanojevic S, Kaminsky DA, Miller MR, et al. ERS/ATS technical standard on interpretive strategies for routine lung function tests. Eur Respir J. 2022;60:2101499.
17. Dweik RA, Boggs PB, Erzurum SC, et al. An official ATS clinical practice guideline: interpretation of exhaled nitric oxide levels (FENO) for clinical applications. Am J Respir Crit Care Med. 2011;184:602-15.
18. ATS Committee on Proficiency Standards for Clinical Pulmonary Function Laboratories. ATS statement: guidelines for the six-minute walk test. Am J Respir Crit Care Med. 2002;166:111-7.
19. Enright PL, Sherrill DL. Reference equations for the six-minute walk in healthy adults. Am J Respir Crit Care Med. 1998;158:1384-7.
20. COVID-19 rapid guideline: managing the long-term effects of COVID-19. London: National Institute for Health and Care Excellence, (NICE); 2020 Dec 18.
21. Ludvigsson JF. Case report and systematic review suggest that children may experience similar long-term effects to adults after clinical COVID-19. Acta Paediatr. 2021;110:914-21.
22. Antoniou KM, Vasarmidi E, Russell AM, et al. European Respiratory Society statement on long COVID follow-up. Eur Respir J. 2022;60:2102174.
23. Torres-Castro R, Vasconcello-Castillo L, Alsina-Restoy X, et al. Respiratory function in patients post-infection by COVID-19: a systematic review and meta-analysis. Pulmonology. 2021;27:328-37.
24. Swarnakar R, Jenifa S, Wadhwa S. Musculoskeletal complications in long COVID-19: A systematic review. World J Virol. 2022;11:485-95.
25. Cortés-Telles A, López-Romero S, Figueroa-Hurtado E, et al. Pulmonary function and functional capacity in COVID-19 survivors with persistent dyspnoea. Respir Physiol Neurobiol. 2021;288:103644.
26. Zampogna E, Ambrosino N, Saderi L, et al. Time course of exercise capacity in patients recovering from COVID-19-associated pneumonia. J Bras Pneumol. 2021;47:e20210076.
27. Silva CC, Bichara CNC, Carneiro FRO, et al. Muscle dysfunction in the long coronavirus disease 2019 syndrome: Pathogenesis and clinical approach. Rev Med Virol. 2022;32:e2355.

28. Lior Y, Yatzkan N, Brami I, et al. Fractional exhaled Nitric Oxide (FeNO) level as a predictor of COVID-19 disease severity. Nitric Oxide. 2022;124:68-73.

29. Maniscalco M, Ambrosino P, Poto R, et al. Can FeNO be a biomarker in the post-COVID-19 patients monitoring? Respir Med. 2022;193:106745.

30. Betancor D, Valverde-Mongue M, Gomez-Lopez A, et al. Evaluation of Fractional Exhaled Nitric Oxide During SARS-CoV-2 Infection. J Investig Allergol Clin Immunol. 2022;32:301-3.

31. Cameli P, Bargagli E, Bergantini L, et al. Alveolar Nitric Oxide as a Biomarker of COVID-19 Lung Sequelae: A Pivotal Study. Antioxidants (Basel). 2021;10:1350.

DOI: 10.4274/MMJ.galenos.2024.45578
Medeni Med J 2024;39:85-90

Original Article

Characteristics of Posterior Ethmoidal Artery and Its Relationship with Anterior Ethmoidal Artery and Skull Base on CT Scan

BT Taramasında Posterior Etmoidal Arterin Özellikleri ve Anterior Etmoidal Arter ve Kafa Tabanı ile İlişkisi

Thuy Chung TRAN PHAN[1], Kiet Vuong DANG[2]

[1]Vietnam National University Faculty of Medicine, Department of Otolaryngology, Ho Chi Minh City, Vietnam
[2]Pham Ngoc Thach University of Medicine, Ho Chi Minh City, Vietnam

ABSTRACT

Objective: Investigation of the anterior and posterior ethmoidal arteries on computed tomography (CT) scans of the sinuses before and during surgery is important, especially for inexperienced surgeons. The aim of this study was to examine the anatomical characteristics of the posterior ethmoid artery in Vietnamese and the distance from the posterior ethmoid artery to the anterior ethmoid artery and the skull base on CT scan.

Methods: A cross-sectional study was conducted involving patients aged ≥18 years who underwent CT scan imaging at the Ear, Nose and Throat Hospital of Ho Chi Minh City from February 2023 to July 2023.

Results: There were 100 patients in this study, of whom 51% (51/100) were female and 49% (49/100) were male. Patient ages ranged from 20 to 84 years. Their average age was 40.92±14.65 years. The distance on CT scan between the posterior and anterior ethmoidal arteries was 13.98±1.95 mm (9.3 to 18.6 mm). This distance in males was significantly higher than female (p=0.001). However, there is no difference in this distance between the left and right side (p=0.67). The distance between the posterior ethmoid artery and skull base ranged from 0 to 5.4 mm. The average distance between the posterior ethmoidal artery and skull base on CT scan was 0.95±0.94 mm. The diameter of the posterior ethmoid artery was 0.57-0.91 mm. The average diameter of the posterior ethmoidal artery on CT scan was 0.76±0.09 mm.

Conclusion: The characteristics of the posterior ethmoid artery should be considered when examining the CT scan. Distance from the posterior ethmoid This study provides useful information on the characteristics of the posterior ethmoid artery on CT scans, which can be applied in endoscopic sinus surgery and skull base surgery.

Keywords: Posterior ethmoid artery, anterior ethmoid artery, skull base on CT scan

ÖZ

Amaç: Ameliyat öncesinde ve sırasında sinüslerin bilgisayarlı tomografi (BT) taramalarında anterior ve posterior etmoidal arterlerin incelenmesi, özellikle deneyimsiz cerrahlar için önemlidir. Bu çalışmanın amacı Vietnamlılarda posterior etmoid arterin anatomik özelliklerini ve BT taramasında posterior etmoid arterin anterior etmoid artere ve kafa tabanına olan mesafesini incelemektir.

Yöntemler: Şubat 2023 ile Temmuz 2023 tarihleri arasında Ho Chi Minh City Kulak, Burun ve Boğaz Hastanesi'nde BT taraması yapılan ≥18 yaşındaki hastaları içeren kesitsel bir çalışma yürütülmüştür.

Bulgular: Bu çalışmada %51'i (51/100) kadın ve %49'u (49/100) erkek olmak üzere 100 hasta yer aldı. Hastaların yaşları 20 ile 84 arasında değişmekteydi. Ortalama yaş 40,92±14,65 yıl idi. BT taramasında posterior ve anterior etmoidal arterler arasındaki mesafe 13,98±1,95 mm (9,3 ile 18,6 mm) idi. Erkeklerde bu mesafe kadınlara göre anlamlı derecede yüksekti (p=0,001). Ancak sağ ve sol taraf arasında bu mesafe açısından fark yoktu (p=0,67). Posterior etmoid arter ile kafa tabanı arasındaki mesafe 0 ile 5,4 mm arasında değişmekteydi. BT taramasında posterior etmoidal arter ile kafa tabanı arasındaki ortalama mesafe 0,95±0,94 mm idi. Posterior etmoid arterin çapı 0,57-0,91 mm idi. BT taramasında posterior etmoidal arterin ortalama çapı 0,76±0,09 mm idi.

Sonuçlar: BT taraması incelenirken posterior etmoid arterin özellikleri göz önünde bulundurulmalıdır. Bu çalışma, BT taramalarında posterior etmoid arterin özellikleri hakkında endoskopik sinüs cerrahisi ve kafa tabanı cerrahisinde uygulanabilecek yararlı bilgiler sağlamaktadır.

Anahtar kelimeler: Posterior etmoid arter, anterior etmoid arter, BT taramasında kafa tabanı

Address for Correspondence: T. C. Tran Phan, Vietnam National University Faculty of Medicine, Department of Otolaryngology, Ho Chi Minh City, Vietnam
E-mail: drthuytranent@gmail.com **ORCID ID:** orcid.org/0009-0002-1154-2262

Received: 26 March 2024
Accepted: 27 April 2024
Online First: 29 May 2024

Cite as: Tran Phan TC, Dang KV. Characteristics of Posterior Ethmoidal Artery and Its Relationship with Anterior Ethmoidal Artery and Skull Base on CT Scan. Medeni Med J 2024;39:85-90

INTRODUCTION

The anterior ethmoidal arteries (AEA) and posterior ethmoidal arteries (PEA) are branches of the ophthalmic artery, originating from the internal carotid artery. The ethmoidal artery is one of the main blood supplies to the ethmoidal cells and nasal septum[1]. The AEA is an important anatomical landmark to which surgeons should pay special attention to avoid damage during endoscopic sinus surgery[2]. According to many authors, the AEA is more susceptible to injury than the PEA during endoscopic sinus surgery[3,4]. Consequently, prior research has primarily concentrated on the front ethmoidal artery, whereas there is a scarcity of publications regarding the PEA[5].

Since skull base surgery has become increasingly popular and developed, surgeons have begun to pay more attention to the PEA. Cauterization of the ethmoidal arteries to limit bleeding is necessary and almost mandatory during surgery on anterior skull base masses, such as olfactory tumors[6]. Hence, it is crucial to perform a comprehensive examination of the anterior and PEAs on computed tomography (CT) scans before and during surgery, particularly for new surgeons. This study aimed to analyze the anatomical features of the Vietnamese PEA, the length from the PEAs to the AEAs, and the skull base, as observed using CT scans.

MATERIALS and METHODS

Subjects

A cross-sectional investigation was conducted on patients aged ≥18 years who underwent CT imaging at the Ear, Nose and Throat Hospital of Ho Chi Minh City from February 2023 to July 2023. We excluded patients who had injuries to the ethmoidal sinuses or skull base causing deformation of the skull, congenital craniofacial abnormalities, ethmoidal sinusitis, which obscured anatomical structures and landmarks that needed to be investigated, and patients with unidentified AEA on CT scan. The necessary sample size for this investigation was 186 CT scans, which was similar to the sample sizes used in previous studies that specifically examined the ethmoidal arteries. This study was approved by the Department of Otorhinolaryngology of Pham Ngoc Thach University of Medicine and the Medical Ethics Council of Pham Ngoc Thach University of Medicine and Ho Chi Minh City Ear, Nose and Throat Hospital (29/GCN-BVTMH, no. 226/QĐ-TĐHYPNT, date: 19.01.2023). This study obtained fully informed consent from all patients.

CT Scan

The CT scanner used was the Somatom Emotion 32-slice version, which was manufactured by Siemens Healthineers AG in Forchheim, Germany. The images obtained were thin-sliced (0.625 mm). The gap between each slice was 0.6 mm. The data were processed using a three-dimensional Digital Imaging and Communications in Medicine (DICOM) viewer, namely the OsiriX Lite version 12.0 developed by Pixmeo SARL in Geneva, Switzerland. The examinations were conducted using three-dimensional photographs as the basis.

The AEA was recognized as the initial transverse canal observed on coronal slices when viewed from the front to the back. The PEA was observed as the initial transverse channel on coronal slices when viewed from the posterior to anterior direction. The location of the anterior and PEAs was then confirmed on the sagittal plane. The length from the posterior to AEAs was determined as the distance from the PEA to the AEA on sagittal CT. The length across the PEA and the skull floor was measured by determining the length of the vertical section from the skull base to the PEA on the sagittal CT scan. The PEA's diameter was determined as the length of the longest horizontal line crossing the PEA (anteroposterior diameter) on the sagittal CT scan.

Statistical Analysis

We used the Kolmogorov-Smirnov and Shapiro-Wilk tests to verify the normal distribution of the data. Data were normally distributed when $p>0.05$. We used Student's t-test to compare two independent samples. CT scans of the study participants' noses and sinuses were performed in accordance with the treatment protocol of Ho Chi Minh City Ear, Nose and Throat Hospital. Statistical analysis of all data was performed using the SPSS Statistics software version 20.0.0 for Windows (SPSS, Chicago, IL, USA) and MedCalc version 22.009 software (MedCalc Software Ltd, Ostend, Belgium). A two-tailed p-value <0.05 was considered statistically significant.

RESULTS

Characteristics of Patients in the Study

There were 100 patients in this study, of whom 51% (51/100) were female and 49% (49/100) were male. The patients' ages ranged from 20 to 84 years. Their average age was 40.92±14.65 years.

Rate of Identification of Posterior Ethmoidal Artery on CT Scan

There were 200 sinus CT scans, of which the PEA was present in 187 CT scans (93.5%). On CT, the presence of the PEA was unidentified in 13 cases, which accounted for 6.5% of the total. CT successfully identified the PEA

in women at a rate of 96.08% (98 of 102 cases). In men, the prevalence of the PEA on CT scan is 90.82% (89 of 98 cases). The prevalence of the PEA in males and females on CT scan was not statistically different (p=0.136).

The rate of presence of the right PEA on CT scan is 93% (93/100 CT scans). The rate of presence of the left PEA on CT scan was 94% (94/100 CT scans). There was no statistically significant difference in the prevalence of left and right PEAs on CT scan (p=0.776).

Distance Between the Posterior and Anterior Ethmoidal Arteries on CT Scan

The average distance between the posterior and AEAs was 13.98±1.95 mm, with the longest distance was 18.6 mm (Figure 1) and the shortest distance was 9.3 mm (Figure 2).

Difference in Sex

In female patients, the distance between the posterior and AEAs was 9.3-18.5 mm. The average distance between the posterior and AEAs on CT in women was 13.54±1.84 mm. In male patients, the distance between the posterior and AEAs was 9.4-18.6 mm. The average length from the posterior to the AEAs on CT in men was 14.47±1.96 mm. There was a significant difference in this length between the sexes (p=0.001) (Table 1) (Figure 3).

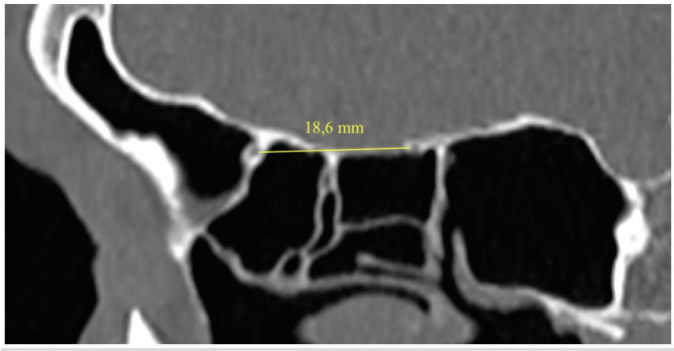

Figure 1. Distance between the posterior ethmoidal artery and anterior ethmoidal artery on CT scan of patient Vo Hoang V. Source: Dang Vuong Kiet, 2023.

CT: Computed tomography

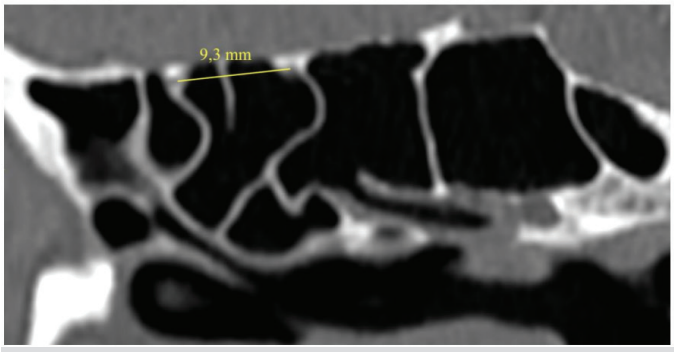

Figure 2. Distance between the posterior ethmoidal artery and anterior ethmoidal artery on CT scan of patient Tran Thi Ngoc H. Source: Dang Vuong Kiet, 2023

CT: Computed tomography

Difference in Sides

The distance between the right PEA and the right AEA was 9.4-18.6 mm. The average distance between the right PEA and the right AEA on CT scan was 13.92±1.98 mm. The distance between the left PEA and the left AEA was 9.3-18.5 mm. The average distance between the left PEA and the left AEA on CT scan was 14.04±1.93 mm. There was no significant difference in the average distance from the PEA to the AEA on CT between the left and right sinuses (p=0.678) (Table 2).

Distance Between the Posterior Ethmoidal Artery and Skull Base on CT

The distance between the PEA and skull base ranged from 0 to 5.4 mm (Figure 4). The average distance between the PEA and skull base on CT scan was 0.95±0.94 mm.

Table 1. Difference in distance PEA-AEA between sexes.

	Distance between PEA and AEA	p*
Male	14.47±1.96 mm	0.001
Female	13.54±1.84 mm	

*Independent sample test

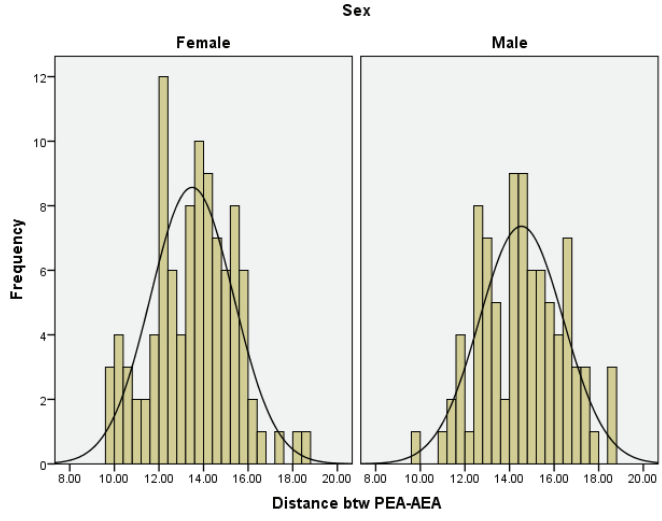

Figure 3. Difference in distance between PEA and AEA between males and females.

Posterior Ethmoidal Artery Diameter on a CT Scan

The diameter of the PEA ranged from 0.57 mm (Figure 5) to 0.91 mm (Figure 6). The average diameter of the PEA on CT scan was 0.76±0.09 mm.

DISCUSSION

Characteristics of Patients in the Study

First, we found that there was no significant difference in the gender ratio (1.04) in our study compared with previous studies[5,7]. However, there was a significant difference in the gender ratio in this study compared with other studies[8,9]. We observed a significant difference in the average age in this study compared with previous studies[5,7,8].

Table 2. Difference in distance PEA-AEA between the left and right sides.

	Distance between PEA and AEA	p*
Left	14.04±1.93 mm	0.678
Right	13.92±1.98 mm	

*Independent sample test

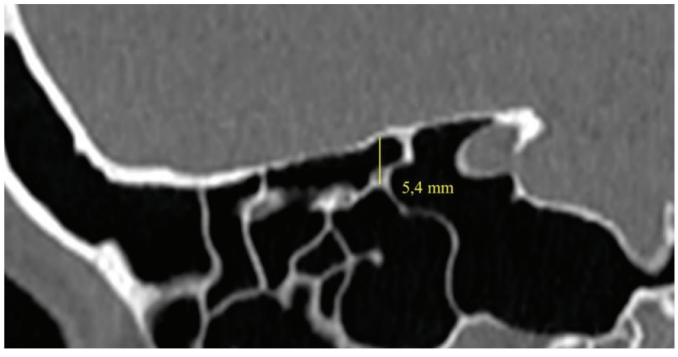

Figure 4. Distance between the posterior ethmoidal artery and skull floor on CT scan of patient Ho Thi T. Source: Dang Vuong Kiet, 2023.

CT: Computed tomography

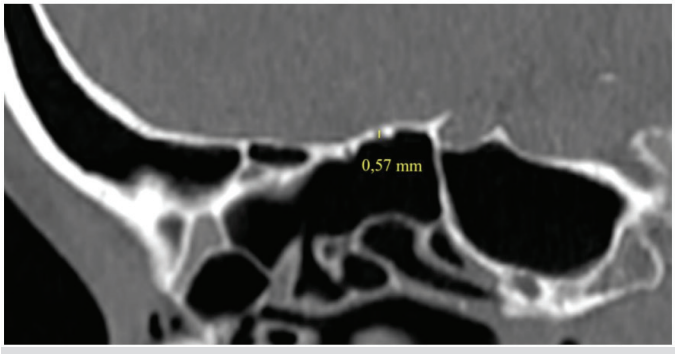

Figure 5. Posterior ethmoidal artery diameter on a CT scan of patient Pham Thi V. Source: Dang Vuong Kiet, 2023.

CT: Computed tomography

Rate of Identification of the Posterior Ethmoidal Artery on CT Scan

We found no significant difference in the rate of presence of the PEA in our study compared with previous studies[7,8,10]. We found a significant difference in the rate of the PEA in our study compared with that in prior studies[5,9]. The reason for this difference may be different research methods, especially the slice thickness of the CT scan and ethnicity.

The identification of the PEA on CT scan varied among the studies from 86% to 100% (Table 3).

The differences might be due to the thickness of the CT scan and ethnicity. As in Yamamoto et al.'s[5] study, this rate was 100% as the study was conducted in Japan using a CT scan with a thickness of 0.5 mm. In Kho et al.'s[9] study and our study, the thickness of CT scan was 0.75 mm and 0.625 mm, respectively.

In addition, according to Cankal et al.[7], the thinner the slide of the CT scan, the higher the rate of identification of the PEA on the CT scan (Table 4).

Distance Between the Ethmoidal Arteries on a CT Scan

The average distance between the posterior and AEAs in males is 14.47±1.96 mm, and the average distance between the posterior and AEAs in females is 13.54±1.84 mm. In our study, there was a statistically significant difference in the average distance between the posterior and AEAs between males and

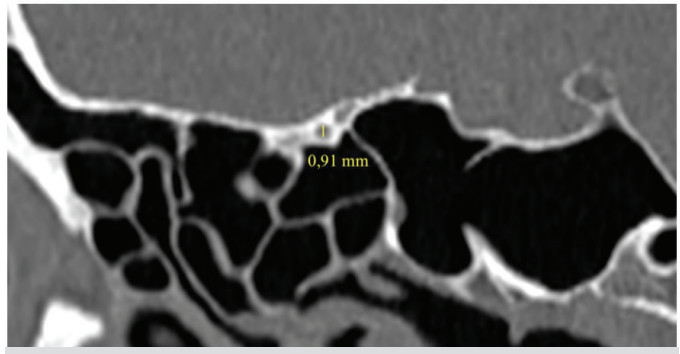

Figure 6. Posterior ethmoidal artery diameter on a CT scan of patient Pham Van T. Source: Dang Vuong Kiet, 2023.

CT: Computed tomography

females (p=0.001). However, there was no significant difference in distance between the ethmoidal arteries between genders in Kho et al.'s[9] study. The studies of Cankal et al.[7] and Vatanasapt et al.[8] did not analyze the difference between genders.

In this investigation, we observed that the mean distance between the posterior and AEAs did not show any significant variations compared with prior studies[7,8]. However, we found that there was a significant difference in the average distance between the posterior and AEAs in this study compared with that in another study[9]. The reason for this difference is probably because there are different significant factors between the two studies (the slice thickness of the CT scan, the rate of presence of the PEA on CT scan, the gender ratio of the study population, and the method of research).

Distance Between Posterior Ethmoidal Artery and Skull Base on CT Scan

In our study, we observed that the mean distance between the PEA and the skull base on CT scan was not significantly different from that in previous studies. However, we did find a significant difference in the average distance between the PEA and the skull base on CT scan when comparing our study with that of study[5]. The reason for this difference is probably because there were significant differences in factors between the two studies (the slice thickness of the CT scan, the prevalence of the PEA on CT scan, the average age of the participants, and the study population). The prevalence of the suspended PEA on CT was 10.16% (19/187 on the sinus side). Accurately identifying the location of the PEA in relation to the skull base on a CT scan prior to surgery, particularly in its mesentery state (Figure 7), is very significant because the PEA in the mesentery is vulnerable to injury during endoscopic sinus surgery. Finally, damage to the ethmoidal artery can result in many severe problems, such as hemorrhage, orbital hematoma, and loss of vision.

Posterior Ethmoidal Artery Diameter on CT

We found that the average diameter of the PEA in our study was similar to that in previous studies. There was a significant difference in the average diameter of the PEA

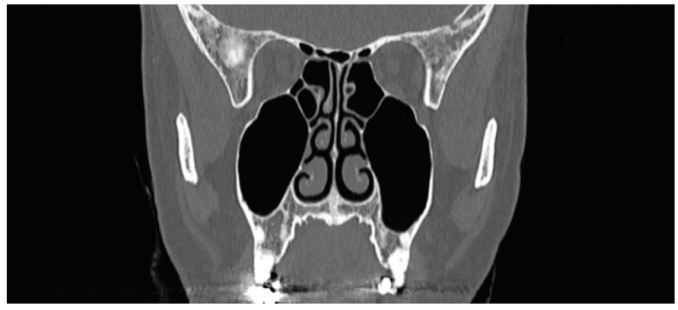

Figure 7. The bilateral posterior ethmoidal arteries are in a hanging form on the CT scan of patient Ho Thi T. Source: Dang Vuong Kiet, 2023.

CT: Computed tomography

Table 3. Identification of the posterior ethmoidal artery on CT scan varied among the research.

Studies	Research's method	Rate of identification	n
Cankal et al.[7] (2004)	CT scan	92%	300
Yamamoto et al.[5] (2018)	CT scan	100%	200
Kho et al.[9] (2019)	CT scan	86%	108
Our study	CT scan	93.5%	200

CT: Computed tomography

Table 4. Thickness of CT scan slides used in the study.

Studies	Thickness of the CT scan slides	Rate of identification
Cankal et al.[7] (2004)	3 mm	56%
	2 mm	72%
	1 mm	92%
Kho et al.[9] (2019)	0.75 mm	86%
Yamamoto et al.[5] (2018)	0.5 mm	100%
Our study	0.625 mm	93.5%

CT: Computed tomography

in our study compared with previous findings[10]. The main reason for this difference is probably due to different research methods and study populations.

There are some limitations to this study. We employed a research methodology to analyze the attributes of the PEA using CT imaging. We did not analyze the attributes of the PEA in cadavers. The study sample size was relatively small. Furthermore, the thickness of the CT scan slice is not optimal (CT scan slice thickness in recent studies was 0.5 mm) to examine the PEA (which is a relatively small anatomical structure) in the most comprehensive way. The sample in our study is not comprehensive enough and is limited to the research group of patients who came for medical examination and had a CT scan of their nose and sinuses at Ho Chi Minh City Ear, Nose and Throat Hospital.

CONCLUSION

We observed that the average distance between the PEA and the anterior ethmoidal on CT scan is 13.98±1.95 mm. The average distance between the PEA and the skull base on CT scan is 0.95±0.94 mm. The average diameter of the PEA on CT scan is 0.76±0.09 mm.

The characteristics of the PEA should be considered when examining CT scans. This study provides useful information on the characteristics of the PEA on CT scan, which can be applied in endoscopic sinus surgery and skull base surgery.

Ethics

Ethics Committee Approval: This study was approved by the Department of Otorhinolaryngology of Pham Ngoc Thach University of Medicine and the Medical Ethics Council of Pham Ngoc Thach University of Medicine and Ho Chi Minh City Ear, Nose and Throat Hospital (29/GCN-BVTMH, no. 226/QĐ-TĐHYPNT, date: 19.01.2023).

Informed Consent: This study obtained fully informed consent from all patients.

Author Contributions

Surgical and Medical Practices: T.C.T.P., K.V.D., Concept: T.C.T.P., K.V.D., Design: T.C.T.P., K.V.D., Data Collection and/or Processing: T.C.T.P., K.V.D., Analysis and/or Interpretation: T.C.T.P., K.V.D., Literature Search: T.C.T.P., K.V.D., Writing: T.C.T.P., K.V.D.

Conflict of Interest: The authors have no conflict of interest to declare.

Financial Disclosure: The authors declared that this study has received no financial support.

REFERENCES

1. Araujo Filho BC, Weber R, Pinheiro Neto CD, Lessa MM, Voegels RL, Butugan O. Endoscopic anatomy of the anterior ethmoidal artery: a cadaveric dissection study. Braz J Otorhinolaryngol. 2006;72:303-8.
2. Lee WC, Ming Ku PK, van Hasselt CA. New guidelines for endoscopic localization of the anterior ethmoidal artery: a cadaveric study. Laryngoscope. 2000;110:1173-8.
3. Joshi AA, Shah KD, Bradoo RA. Radiological correlation between the anterior ethmoidal artery and the supraorbital ethmoid cell. Indian J Otolaryngol Head Neck Surg. 2010;62:299-303.
4. Sah BP, Chettri ST, Gupta M, Shah SP, Poudel D, Manandhar S. Radiological correlation between the anterior ethmoidal artery and the supraorbital ethmoid cell in relation to skull base. A Ad Med Sc. 2018;2:11-5.
5. Yamamoto H, Nomura K, Hidaka H, Katori Y, Yoshida N. Anatomy of the posterior and middle ethmoidal arteries via computed tomography. SAGE Open Med. 2018;6:2050312118772473.
6. Manjila S, Cox EM, Smith GA, et al. Extracranial ligation of ethmoidal arteries before resection of giant olfactory groove or planum sphenoidale meningiomas: 3 illustrative cases with a review of the literature on surgical techniques. Neurosurg Focus. 2013;35:E13.
7. Cankal F, Apaydin N, Acar HI, et al. Evaluation of the anterior and posterior ethmoidal canal by computed tomography. Clin Radiol. 2004;59:1034-40.
8. Vatanasapt P, Thanaviratananich S, Chaisiwamongkol K. Landmark of ethmoid arteries in adult Thai cadavers: application for sinus surgery. J Med Assoc Thai. 2012;95 Suppl 11:S153-6.
9. Kho JPY, Tang IP, Tan KS, Koa AJ, Prepageran N, Rajagopalan R. Radiological Study of the Ethmoidal Arteries in the Nasal Cavity and Its Pertinence to the Endoscopic Surgeon. Indian J Otolaryngol Head Neck Surg. 2019;71:1994-9.
10. Erdogmus S, Govsa F. The anatomic landmarks of ethmoidal arteries for the surgical approaches. J Craniofac Surg. 2006;17:280-5.

DOI: 10.4274/MMJ.galenos.2024.08504
Medeni Med J 2024;39:91-100

Original Article

Relationship Between Motion Sickness Susceptibility and Vestibular Test Results

Hareket Hastalığı Duyarlılığı ve Vestibüler Test Sonuçları Arasındaki İlişki

Ozge GEDİK TOKER[1], Elif KURU[1], Sumeyye OZDEMIR[1], Betul RENCBER[1], Ege TAKAN[1], Serdar ARAZ[1], Meliha BASOZ BEHMEN[1], Nilufer BAL[2], Fadlullah AKSOY[3]

[1]Bezmialem Vakif University Faculty of Health Sciences, Department of Audiology, Istanbul, Türkiye
[2]Marmara University Faculty of Medicine, Department of Audiology, Istanbul, Türkiye
[3]Bezmialem Vakif University Faculty of Medicine, Department of Otorhinolaryngology, Istanbul, Türkiye

ABSTRACT

Objective: There is no test parameter with high sensitivity and specificity for the diagnosis of motion sickness. The aim of this study was to demonstrate a correlation between vestibular function tests and motion sickness. In addition, our secondary aim is to evaluate the sensitivity of the skull vibration-induced nystagmus test (SVINT) in the diagnosis of motion sickness.

Methods: A total of 44 young adults aged 19-25 who had no hearing loss, complaints of dizziness/vertigo, or any diagnosed neurological disease were included. According to the motion sickness susceptibility questionnaire-short form (MSSQ-SF), participants were divided into the motion sickness group (21±1.38 years) and control group (20.5±1.18 years). Mean MSSQ-SF score for the motion sickness group is 78.18±12.2 and for control group 19.09±17.08. Ocular and cervical vestibular evoked myogenic potential tests, SVINT, video head impulse test, and oculomotor tests were performed.

Results: The only significant difference between the groups was in n1-p1 amplitudes in the left ocular vestibular evoked myogenic potential test (p=0.014). None of the other parameters differed between the two groups (p>0.05).

Conclusions: There was no significant relationship between motion sickness susceptibility and the results of any vestibular function test. Performing diagnostic tests for motion sickness in an environment that creates significant sensory conflict may yield different results. This study contributes to the literature in terms of evaluating the vestibular system using a comprehensive test battery and is the first to use the SVINT test in motion sickness.

Keywords: Motion sickness, oculomotor tests, skull vibration induced nystagmus test, vestibular evoked myogenic potentials, video head impulse test

ÖZ

Amaç: Hareket hastalığının tanısı için sensitivite ve spesifitesi yüksek bir test parametresi bulunmamaktadır. Bu çalışmadaki amaç, vestibüler fonksiyon testleri ile hareket hastalığı arasındaki ilişkiyi ortaya koymaktır. Ayrıca, ikincil amacımız kafatası vibrasyonu ile uyarılmış nistagmus testinin (KVUNT) hareket hastalığı tanısındaki duyarlılığını değerlendirmektir.

Yöntemler: Çalışmaya işitme kaybı, dizziness/vertigo şikayeti olmayan ve herhangi bir nörolojik hastalığı bulunmayan, yaşları 19-25 arasında değişen toplam 44 genç yetişkin dahil edildi. Hareket hastalığı duyarlılık ölçeği-kısa formuna (HHDÖ-KF) göre katılımcılar hareket hastalığı grubu (21±1,38 yaş) ve kontrol grubu (20,5±1,18 yaş) olarak ikiye ayrıldı. Ortalama HHDÖ-KF puanı, hareket hastalığı grubu için 78,18±12,2 ve kontrol grubu için 19,09±17,08. Bütün katılımcılar oküler ve servikal vestibüler uyarılmış miyojenik potansiyeller, KVUNT, video baş itme testi ve okülomotor testler ile değerlendirildi.

Bulgular: Gruplar arasındaki tek anlamlı fark sol oküler vestibüler uyarılmış miyojenik potansiyel testinde n1-p1 amplitüdünde gözlenmiştir (p=0,014). Diğer parametrelerin hiçbirinde iki grup arasında farklılık gözlenmemiştir (p>0,05).

Sonuçlar: Hareket hastalığına yatkınlık ile vestibüler fonksiyon test sonuçları arasında anlamlı bir ilişki saptanmamıştır. Önemli duyusal çatışma yaratan bir ortamda hareket hastalığına yönelik tanısal testlerin yapılması farklı sonuçlar doğurabilmektedir. Bu çalışma vestibüler sistemin kapsamlı bir test bataryası ile değerlendirilmesi açısından literatüre katkı sağlamakta olup, KVUNT testinin hareket hastalığında kullanıldığı ilk çalışmadır.

Anahtar kelimeler: Hareket hastalığı, okülomotor testler, kafatası vibrasyonu ile uyarılmış nistagmus, vestibüler uyarılmış miyojenik potansiyeller, video baş itme testi

Address for Correspondence: O. Gedik Toker, Bezmialem Vakif University Faculty of Health Sciences, Department of Audiology, Istanbul, Türkiye
E-mail: ogediktoker@bezmialem.edu.tr **ORCID ID:** orcid.org/0000-0003-1315-9080

Received: 23 February 2024
Accepted: 01 May 2024
Online First: 23 May 2024

Cite as: Gedik Toker O, Kuru E, Ozdemir S, Rencber B, Takan E, Araz S, Basoz Behmen M, Bal N, Aksoy F. Relationship Between Motion Sickness Susceptibility and Vestibular Test Results. Medeni Med J Medeni Med J 2024;39:91-100

INTRODUCTION

Motion sickness is characterized by symptoms of autonomic and physiological discomfort that usually occur while traveling by vehicles such as cars, buses, trains, aircraft, and boats or during other types of movement such as swinging, spinning, and rolling[1,2]. It typically presents with dizziness, unsteadiness, nausea, and sometimes vomiting. Motion sickness can also be caused by perceived motion, such as when watching a moving scene or experiencing virtual reality[3]. Depending on the environment in which it occurs, motion sickness is also called travel sickness, sea sickness, car sickness, space sickness, and simulator sickness/movie sickness/cybersickness[4]. Although the incidence of motion sickness varies depending on the intensity of the stimulus and the individual's sensitivity, its general prevalence has been reported to be 13.4% in the healthy adult population[5]. Motion sickness is more common in the pediatric population. Children aged 6-12 years are highly susceptible to motion sickness, with a peak in susceptibility between 9 and 10 years of age[2]. One study reported the prevalence of motion sickness in school-age children to be 43.4% in cars and 43.2% on buses[6].

Although research on the pathophysiology of motion sickness continues, the most widely accepted theory is the sensory mismatch theory, which describes motion sickness as sensitivity to conflicting information received through the vestibular, visual, and somatosensory systems[7]. Sensory conflict impairs the homeostatic stability of vestibulo-autonomic pathways. Although individuals susceptible to motion sickness have healthy vestibular, visual, or somatosensory structures and associated reflex arcs, motion sickness can be triggered by direct or indirect stimuli due to mismatches in the visual-vestibular-autonomic pathways. Thus, unwanted vestibulo-autonomic responses may occur[8]. However, sensory mismatch theory cannot easily explain motion sickness induced by conditions such as passive low-frequency vertical acceleration. A theory proposed by Bos and Bles[9] suggests that uncertainty in perceived vertical orientation is the specific cause of motion sickness. This theory points to the importance of the otolith organs (saccule and utricle) responsible for linear acceleration and tilt sensation in the pathogenesis of motion sickness[9], which has been supported by observations that motion sickness does not occur in the absence of the motion-sensing vestibular organs of the inner ear[10].

According to the Barany society, motion sickness is diagnosed when the stimulus that causes the disease is physical movement. The presence of two or four attacks is required for a possible diagnosis of motion sickness. In the absence of other disorders affecting vestibular function, susceptibility to motion sickness peaks in adolescence and decreases with age. Defining whether symptoms refer to the age range ≤12 years or >12 years will help to accurately communicate the current situation and identify prognostic variables. Scales used in research are used to show overlap in symptoms. Multiple symptom checklists regarding severity, single-answer severity state questionnaires, and retrospective scales to measure personal sensitivity can be used. The Barany Society recommends that each measure be used according to its specific advantages for the research question or clinical practice[11].

Numerous attempts have been made to identify physiological parameters that predict motion sickness susceptibility. To date, however, no single physiological or functional parameter with high sensitivity and specificity has been identified that would serve as a diagnostic tool for individual susceptibility to motion sickness. Thus, there is no gold standard test for the diagnosis of motion sickness. Some studies have reported the results of the cervical vestibular evoked myogenic potential (cVEMP) test[12], ocular vestibular evoked myogenic potential (oVEMP) test[13], video head impulse test (vHIT)[14], videonystagmography (VNG) caloric testing[15], and posturography[16] in motion sickness. Although some of these studies demonstrated vestibular system involvement[12,14-16], others showed no effect on vestibular test results[5,13,17].

The skull vibration induced nystagmus test (SVINT), which has been frequently used by Dumas et al.[18] in the evaluation of the vestibular system in recent years, is a practical, simple, and well-tolerated test and is a useful method for detecting vestibular asymmetry. Although it is more sensitive in the detection of peripheral vestibular disorders, central disorders can also be affected[18]. Although there are studies on SVINT and various vestibular pathologies in the literature, there is no study showing SVINT findings in individuals with motion sickness sensitivity. This study is the first to use the SVINT test for motion sickness. Using these test methods, we analyzed the peripheral and central vestibular pathways in a holistic approach to the diagnosis of motion sickness.

In most studies, participants were evaluated using one or two test methods[13-15]. This does not allow the evaluation of the different regions of the vestibular system in individuals with motion sickness. Therefore, we aimed to examine the state of vestibular influence in different regions of the vestibular system in the same people with motion sickness, where research continues and various theories are put forward. In addition, our secondary aim

is to evaluate the sensitivity and specificity of the SVINT in the diagnosis of motion sickness and its relationship with other vestibular tests.

MATERIALS and METHODS

The study was conducted in the Audiology Clinic of Bezmialem Vakif University. Approval for the study was obtained from the Non-Interventional Ethics Committee of Bezmialem Vakif University on 08/02/2022 (no: 2022/2). An informed consent form was obtained from the individuals who volunteered to participate in the study, which was conducted in accordance with the ethical principles specified in the Declaration of Helsinki.

A total of 44 young adults aged 19-25 who had normal hearing (pure-tone average ≤20) and normal ear, nose, and throat examination findings, no complaints of dizziness/vertigo, or any diagnosed neurological disease were included. Participants were selected from patients and their relatives who applied to the Hospital Polyclinic of Bezmialem Vakif University. The motion sickness susceptibility questionnaire-short form (MSSQ-SF), recommended by the Barany Society to determine general motion sickness susceptibility, was used to identify participants in the study[11].

The MSSQ-SF, created by Reason and Brand[19] and revised by Golding[20], was administered. The Turkish validity and reliability study for the MSSQ-SF was conducted by Ugur et al.[21]. The Turkish version includes 20 questions in total, 10 about symptoms in childhood (before 12 years of age) and 10 about symptoms in the last 10 years. Total raw and percentile scores were determined according to the provided scoring guide. Participants with a motion sickness susceptibility of 60% or higher (n=22) were included in the motion sickness group (21±1.38 years; 20F, 2M) and those with a motion sickness susceptibility of 40% or lower (n=22) were included in the control group (20.5±1.18 years; 16F, 6M)[22].

Hearing was assessed using pure tone audiometry using a Madsen Astera® 2 audiometer. Air conduction hearing thresholds at octave frequencies of 125-8000 Hz were evaluated using Telephonics® TDH-39 headphones, and bone conduction hearing thresholds at frequencies of 250-4000 Hz were evaluated using a RadioEar™ B71 bone vibrator. Individuals with a pure tone average (for 0.5, 1, 2, and 4 kHz) ≤20 dB HL were included in the study. Individuals with middle ear pathology according to the immunometric evaluation performed using a GSI Tympstar were excluded from the study.

oVEMP and cVEMP tests were performed using an Interacoustics Eclipse EP25 (Middelfart, Denmark). Using inserted earphones, a 500 Hz tone burst stimulus at a 100 dB nHL intensity level, a repetition rate of 5.1 Hz, and 200 sweeps were recorded by double-trace recording. In the cVEMP test, the positive electrode was placed on the upper sternum, the ground electrode on the forehead, and the negative electrodes on the upper third of the right/left sternocleidomastoid muscle (SCM). It was ensured that the participant performed neck flexion and rotation to the contralateral side in a way that would cause the right and left SCM muscles to contract. For effective contraction of the SCM, electromyographic (EMG) activity was maintained between 50 and 200 μV with the EMG feedback system. An example of the cVEMP measurement is shown in Figure 1. In the oVEMP test, the negative electrodes were placed on the right/left inferior oblique muscle, the positive electrode was placed below the negative electrodes, and the ground electrode was placed on the forehead. The participant was asked to look at a fixation point 30°-40° above without moving his/her head throughout the test. An example of the oVEMP measurement is shown in Figure 2. In the oVEMP and cVEMP testing for both ears, p1 and n1 absolute latency; p1-n1 interwave latency; p1-n1 amplitude, and amplitude asymmetry ratio were determined. cVEMP and oVEMP thresholds were screened in all participants to rule out the possible presence of third window syndrome.

SVINT was performed at 100 Hz with a Synapsys® VVIB 3F (Marseilles, France) using VNG goggles with a cover and excluding fixation. The researcher performed the test, preferably standing in front of or behind the patient, holding the vibrator firmly with the dominant hand to ensure reproducibility. The test was performed by sequential stimulation of the two mastoid processes and vertex in three stimulation sequences, each lasting 5-10 seconds (s). In the mastoid application, a vibrator was applied behind the auricle at the level of the external auditory canal. The researcher used his free hand to hold the patient's head in the correct position[23].

Criteria for a positive result in SVINT:

• SVIN starts and stops with stimulation, does not recur after the stimulus is removed, does not change direction, and beats in the same direction after simulation of the left and right mastoid processes (e.g., beats right when the right mastoid process is stimulated and beats right when the left mastoid process is stimulated).

• SVIN should have a slow phase velocity ≥2.5°/s,

• The SVIN should be reproducible and identical or similar in two consecutive tests[23].

Oculomotor tests in the VNG test battery were evaluated with Micromedical VisualEyes™ VNG (Chatham, IL, USA) and VisualEyes™ EyeSeeCam model goggles.

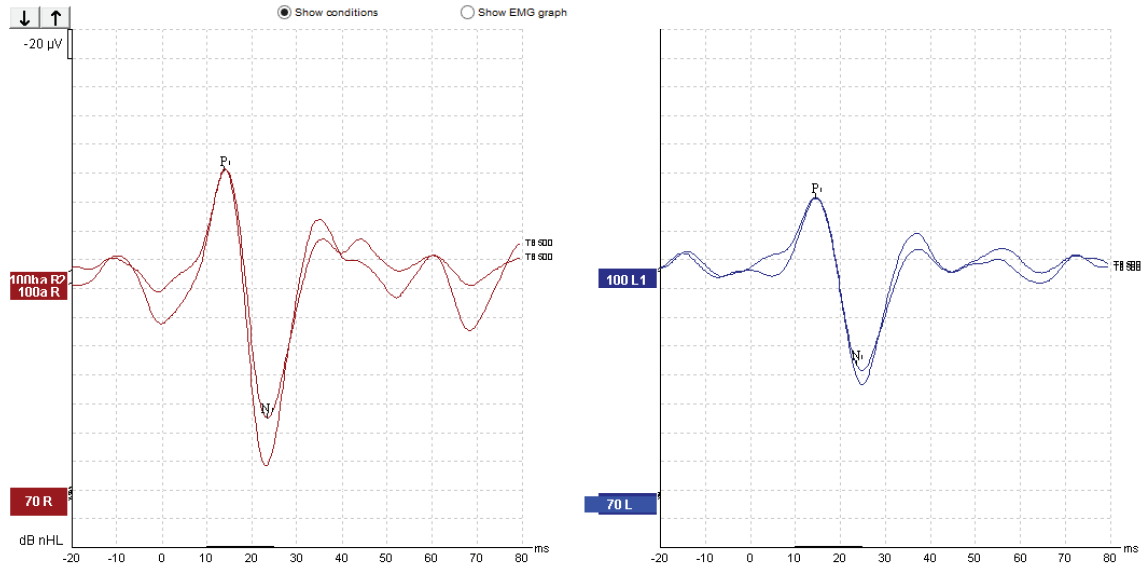

Figure 1. Example of cVEMP measurement.

EMG: Electromyogram, cVEMP: Cervical vestibular evoked myogenic potential

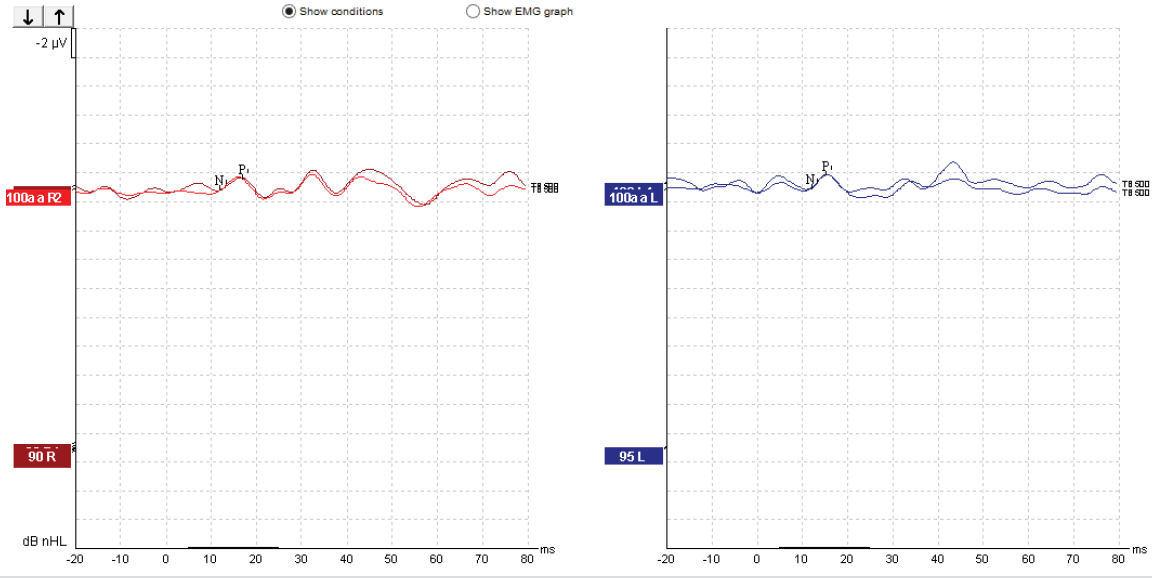

Figure 2. Example of oVEMP measurement.

EMG: Electromyogram, oVEMP: Ocular vestibular evoked myogenic potential

The test was conducted in a dark environment, and the distance between the participant and the light bar was 100-105 cm. The participant was seated directly opposite the light bar, which was adjusted to the eye height. Calibration was performed before the test, and the participants were asked to keep their heads steady and follow the target with their eyes during the test. Gaze, spontaneous nystagmus, smooth pursuit, saccade, and optokinetic tests were evaluated.

In the gaze test, the participants were asked to keep their gaze fixed for 15 s on a visual stimulus 15° below and above in the vertical plane and 20° to the right and left in the horizontal plane. The presence of saccadic oscillation and nystagmus was also checked. In the saccade test, the patient was requested to follow a light randomly moving 7°-24° right and left. Recordings were taken for 30 targets (15 right, 15 left). Accuracy, velocity, and latency were evaluated for both gaze directions. In the smooth

pursuit test, a target that moved at frequencies of 0.1, 0.2, and 0.4 Hz on the horizontal plane was used, and a 10 s recording was taken at each frequency. The gain and asymmetry values of the tested frequencies were evaluated for both viewing directions. In the optokinetic test, the target speed was set as 30°/s to the right and 30°/s to the left while the light bar was in the horizontal position, and the gain values were calculated for both gaze directions. In the spontaneous nystagmus test, the VNG goggles were covered, and the participants were asked to fixate on a fixation light. The fixation light was then removed, and another recording was obtained in the same way. Nystagmus was assessed in the presence and absence of fixation.

vHIT was performed using a Synapsys® vHIT Ulmer II (Marseilles, France). Both horizontal and vertical semicircular canals were evaluated during the test. The participants were asked to fixate on a target point at 0° to evaluate the horizontal semicircular canals. While the participant's head was at 30° flexion, the researcher performed a high-acceleration head impulse with 10-20° excursion applied at a speed of 120-150°/s. Then participants were asked to fixate on target points 20° to the right for the right anterior-left posterior semicircular canals and 20° to the left for the left anterior-right posterior semicircular canals. With the head in these positions, the clinician rotated the head 30°-45° right and left, respectively, and pulsed the head up and down at a velocity of 120°-150°/s. Vestibulo-ocular reflex (VOR) gain and asymmetry values were measured for each semicircular canal.

Statistical Analysis

The descriptive statistics of the evaluated parameters were calculated using IBM SPSS version 22.0. Normality testing of continuous numerical variables was performed using the Shapiro-Wilk test. Variables with normal distribution (bilateral anterior, posterior, and lateral vHIT gains, bilateral saccade velocity and latency, right saccade accuracy, left optokinetic gain, bilateral cVEMP n1 latency, and left cVEMP p1-n1 interpeak latency oVEMP amplitude asymmetry) were compared between the motion sickness and control groups using the independent samples t-test, and those with non-normal distribution (bilateral 0.1, 0.2, and 0.4 Hz smooth pursuit gain, right optokinetic gain, right saccade accuracy, and posterior, anterior, lateral vHIT asymmetry, bilateral cVEMP p1 latency, right cVEMP p1-n1 interpeak latency, bilateral cVEMP p1n1 amplitude, and cVEMP amplitude asymmetry, bilateral oVEMP n1 and p1 latency, bilateral oVEMP n1-p1 amplitude and interpeak latency) were compared using the Mann-Whitney U test. For the categorical variables (SVINT), statistical analysis was performed using the chi-square test. All analyses were performed at a 95% confidence interval, and the significance level was determined as $p<0.05$. G-Power analysis was performed to determine the sample size, and the required sample size was calculated to be 16 per group with α of 0.05 and power of 0.80.

RESULTS

A total of 44 participants, including 22 participants in the control group (16 females, 6 males) and 22 participants in the motion sickness group (20 females, 2 males), participated in the study. The mean age of the study participants was 21±1.38 years (range, 19-25 years) in the control group and 20.5±1.18 years (range, 19-25 years) in the motion sickness group. There was no statistical difference between the motion sickness group and the control group's age ($p=0.124$). Control and MS the mean MSSQ-SF score was 19.09±17.08 (range, 0-40) in the control group and 78.18±12.2 (range, 60-100) in the MS group. The motion sickness group's scores were significantly higher ($p<0.001$). The demographic features of the participants are reviewed in Table 1.

In the cVEMP test, all participants in both groups had p1-n1 responses. In the oVEMP test, no response was obtained from five people in each group. Although the motion sickness group had shorter latency values and larger amplitude values than the control group in both the cVEMP and oVEMP, the only significant difference between the groups was in the n1-p1 amplitudes in the left oVEMP (Table 2).

In the SVINT, positive results were obtained in three participants in the control group (13.6%) and one participant in the motion sickness group (4.5%). Fisher's Exact test showed no association between the motion sickness and control groups ($p=0.607$) for SVINT results. In the oculomotor evaluation, no significant difference was observed between the two groups in saccade, pursuit, or optokinetic tests (Table 3). In both groups, there were no abnormal results in the gaze test. In the spontaneous nystagmus test with fixation, abnormal results (nystagmus and saccadic oscillation) were

Table 1. Demographic features of participants.

Group	Control	Motion sickness
Gender (n)	Female: 16	Female: 20
	Male: 6	Male: 2
Age (mean ± SD)	20.5±1.18	21±1.38
MSSQ-SF (mean ± SD)	19.09±17.08	78.18±12.2

SD: Standard deviation, MSSQ-SF: Motion Sickness Susceptibility Questionnaire–Short Form

Table 2. Intergroup comparison of cVEMP and oVEMP results.

	cVEMP					oVEMP			
	Group	**Mean**	**SD**	**p-value**		**Group**	**Mean**	**SD**	**p-value**
P1 latency-right	Control	17.478	2.501	0.071	N1 latency-right	Control	11.906	1.285	0.560
	MS	16.173	1.484			MS	11.666	1.334	
P1 latency-left	Control	17.677	2.639	0.093	N1 latency-left	Control	12.387	1.430	0.229
	MS	16.280	1.297			MS	11.905	1.155	
N1 latency-right	Control	26.211	2.563	0.237	P1 latency-right	Control	17.186	2.005	0.478
	MS	25.440	2.143			MS	16.840	1.280	
N1 latency-left	Control	26.640	1.900	0.110	P1 latency-left	Control	17.440	1.766	0.723
	MS	25.746	2.183			MS	17.047	1.371	
P1-N1 amplitude-right	Control	117.855	49.900	0.624	N1-P1 amplitude-right	Control	4.912	3.709	0.326
	MS	129.743	60.314			MS	5.866	4.092	
P1-N1 amplitude-left	Control	117.279	44.626	0.660	N1-P1 amplitude-left	Control	4.614	3.549	0.014*
	MS	128.638	63.732			MS	7.287	4.800	
Asymmetry ratio	Control	0.131	0.088	0.264	Asymmetry ratio	Control	0.257	0.159	0.565
	MS	0.176	0.130			MS	0.226	0.206	

*p<0.05. MS: Motion sickness, SD: Standard deviation, cVEMP: Cervical vestibular evoked myogenic potential, oVEMP: Ocular vestibular evoked myogenic potential

Table 3. Intergroup comparison of oculomotor tests results.

		Group	**Mean**	**SD**	**p-value**
Saccade test	Saccade velocity left moving	Control	339.73	21.03	0.468
		MS	334.35	33.21	
	Saccade velocity right moving	Control	278.76	20.50	0.240
		MS	283.85	23.31	
	Saccade latency left moving	Control	214.37	20.14	0.430
		MS	216.44	25.83	
	Saccade latency right moving	Control	217.24	22.46	0.746
		MS	216.90	22.94	
	Saccade accuracy left moving	Control	96.92	3.21	0.199
		MS	92.51	15.59	
	Saccade accuracy right moving	Control	98.99	8.06	0.274
		MS	98.95	5.59	
Optokinetic test	Optokinetic gain right	Control	0.93	0.13	0.397
		MS	0.91	0.12	
	Optokinetic gain left	Control	0.93	0.09	0.184
		MS	0.92	0.11	
Smooth pursuit test	0.1 Hz left	Control	0.97	0.04	0.625
		MS	0.97	0.04	
	0.1 Hz right	Control	0.97	0.04	0.540
		MS	0.96	0.04	
	0.2 Hz left	Control	0.98	0.04	0.818
		MS	0.99	0.02	
	0.2 Hz right	Control	0.98	0.58	0.689
		MS	0.98	0.04	
	0.4 Hz left	Control	0.97	0.54	0.591
		MS	0.98	0.03	
	0.4 Hz right	Control	0.97	0.68	0.054
		MS	0.97	0.03	

MS: Motion sickness, SD: Standard deviation

observed in three participants in the control group and four participants in the motion sickness group, whereas in the spontaneous nystagmus test without fixation, abnormal results were observed in five participants in the control group and four participants in the motion sickness group.

In the vHIT, no significant difference was observed between the groups in bilateral horizontal, posterior, and anterior canal gains or asymmetry values (Table 4). In addition, no covert or overt saccades were observed in either group.

DISCUSSION

In this study, we aimed to evaluate peripheral and central vestibular system function using VNG-oculomotor tests[15]; saccule function using cVEMP[12]; crossed vestibuloocular pathway and utricle function using oVEMP[13]; VOR and six semicircular canal gains using vHIT[14]; and asymmetry in otolith function and vestibular receptors using SVINT[18]. These tests include different stimulation frequency characteristics and evaluate various the vestibular frequency spectrum. To the best of our knowledge, no previous study has examined the relationship between motion sickness susceptibility and a comprehensive range of vestibular function test results. Our study revealed no significant difference in the results of the oculomotor test, vHIT, SVINT, or cVEMP evaluations between young adults with motion sickness and the control group. Only the n1-p1 amplitude in oVEMP testing of the left ear was significantly greater in the motion sickness group.

The widely accepted sensory mismatch theory explains the clinical symptoms of motion sickness. Movement estimation depends on inputs from the visual and somatosensory systems, mainly the vestibular system. Sensory mismatch occurs when these inputs differ from patterns learned from previous experiences, resulting in the development of motion sickness symptoms[24]. Studies have stated that motion sickness is not observed in individuals without peripheral vestibular system function. Therefore, the vestibular system plays a critical role in the development of motion sickness[10]. Maladaptive vestibular system responses to vertical stimuli and asymmetric otolith function between the two labyrinths are possible causes of motion sickness[9]. These findings have led researchers to use vestibular test batteries to evaluate vestibular disorders that may cause motion sickness.

Various studies have used the oVEMP and cVEMP tests to assess otolith function in people with motion sickness, with evaluations made in terms of amplitude, threshold, and asymmetry. In several studies involving cVEMP, evaluation of the saccule (which responds

Table 4. Intergroup comparison of vHIT results.

	Group	Mean	SD	p-value
Right anterior SCC gain	Control	1.029	0.067	0.424
	MS	1.016	0.053	
Left anterior SCC gain	Control	1.018	0.075	0.620
	MS	1.009	0.057	
Anterior SCCs asymmetry	Control	2.533	1.925	0.139
	MS	1.800	1.554	
Right posterior SCC gain	Control	0.997	0.053	0.734
	MS	0.991	0.064	
Left posterior SCC gain	Control	1.003	0.060	0.682
	MS	0.997	0.062	
Posterior SCCs asymmetry	Control	1.733	1.460	0.674
	MS	1.760	1.164	
Right lateral SCC gain	Control	0.997	0.039	0.396
	MS	1.006	0.038	
Left lateral SCC gain	Control	0.991	0.041	0.340
	MS	1.002	0.043	
Lateral SCCs asymmetry	Control	1.466	1.008	0.584
	MS	1.280	1.021	

MS: Motion sickness, SCC: Semicircular canal, SD: Standard deviation, vHIT: Video head impulse test

to vertical acceleration) showed that amplitude and asymmetry were greater in the motion sickness group[12,25,26]. The magnitude of the amplitude values obtained in the motion sickness group is associated with the otolith in the vestibular system and/or its relationship with its neural pathways and hypersensitivity in these pathways/systems[9,26]. The differences in asymmetry obtained in cVEMP responses are based on the theory that the response produced by bilateral otolith organs is asymmetrical and that motion sickness symptoms occur because of the transmission of this asymmetrical response to the central structures. However, numerous studies have reported the absence of any difference in asymmetry[5,15,27–29], amplitude, and latency[5,12,25,27-29] in people with motion sickness on the cVEMP test. Similarly, we observed no difference in latency, amplitude, or asymmetry in the cVEMP results of the motion sickness group. This is consistent with the idea that there may not be a neural influence in the saccule and vestibulocolic reflex pathways in motion sickness that would affect cVEMP test results[12].

Studies have reported that asymmetry, latency, and amplitude differences were not observed in oVEMP tests evaluating utricle function[13,25,28]. We also observed no significant difference in the latency or asymmetry values in the oVEMP tests. Amplitudes were higher in the motion sickness group, but a significant difference was observed only in left n1-p1 amplitude. This result differs from those of a few other studies in the literature[13,25,28]. The differences in cVEMP and oVEMP test results reported in the literature may be due to the differences in the questionnaires used in the studies, the inclusion of people who feel less motion sickness symptoms due to continuous exposure to stimuli such as sea travel[28,29], and the difference in the test methods applied. Based on the differences between studies, VEMP tests lack the specificity to identify the possible otolith organ dysfunction that causes motion sickness.

Unlike other studies in the literature, we applied SVINT to both groups in our study. Because this test has been reported to give a differential result in unilateral vestibular weakness[30], we investigated whether it would support the theory of otolith asymmetry causing motion sickness. However, we observed no significant difference in SVINT, with positive results in 4.5% of the motion sickness group and 13.6% of the control group. Two studies reported that in normal individuals without auditory and vestibular complaints, 20-27% of participants had vibration-evoked nystagmus[31,32]. Additionally, Zamora et al.[32] reported that the number of positive results with repeated SVINT varied in normal individuals, with none of the participants having positive results in all six repetitions. Based on this information and the positive results obtained in both groups, we believe that SVINT should be repeated for a more accurate evaluation and should be included in motion sickness studies to determine its specificity, as in VEMP studies in future.

Although rotational chair and caloric tests are frequently used in studies of motion sickness[5,33,34], few studies have evaluated oculomotor test results. However, Fowler et al.[15] compared the VNG results of people with low, moderate, and high suspicion of motion sickness and observed no statistically significant difference in oculomotor findings between the groups, similar to our study. Similarly, Bilgen and Kirazlı[35] reported no significant difference between the control and motion sickness groups in oculomotor evaluation using electronystagmography. They interpreted this as indicating the absence of pathology in the central vestibular pathways in motion sickness[35]. In addition, in a study in which saccade assessment was performed on participants with space sickness before, during, and after flight, it was observed that saccade latency increased significantly while saccade velocity decreased significantly during flight. However, no significant differences in saccade velocity, accuracy, or latency were observed between the groups with and without space sickness[36]. This suggests that the system is disrupted during movement in people with motion sickness.

The fact that VORs are affected in vestibular pathologies has led researchers to investigate the results of vHIT in the evaluation of motion perception[37,38]. VOR stabilizes the image in the fovea during head movements. Under certain conditions, such as visual tracking of objects moving in sync with the head, VOR must be suppressed to maintain foveal fixation. However, when this suppression is insufficient, retinal image movement results in oscillopsia, the persistence of which can lead to motion sickness-like symptoms[39]. Kılınç et al.[14] reported that a significant decrease was observed in all semicircular canal gains in the motion sickness group and a significant increase was observed only in anterior canal asymmetry. However, Neupane et al.[12] reported that asymmetry rates were statistically more significant in the motion sickness group and that semicircular canal gains were lower in the right anterior-left posterior plane. They stated that this can be explained by intersensory conflict in the semicircular canals in motion sickness and concluded that the asymmetry ratio is a more valuable parameter than the VOR gain[40]. Our study revealed no significant difference between the groups in terms of VOR gains or asymmetry rates.

Similarly, Kumar et al. observed no significant difference between individuals with and without motion sickness in terms of VOR gain and VOR gain asymmetry in the head impulse paradigm and suppression head impulse tests[17]. In individuals with motion sickness, VOR and vestibulocollic reflex dysfunction occur in the presence of a provocative stimulus that elicits symptoms. In our study, none of the participants reported any motion sickness symptoms during or after the vHIT, although Karababa et al.[40] reported that some motion sickness symptoms were observed after a rotational stimulus. These differences between studies were likely due to differences in sensitivity between individuals and whether conditions provoked symptoms during the tests. Greater susceptibility to motion sickness is associated with a more pronounced deterioration of the VOR[12,40].

Because there is no cut-off value for MSSQ-SF scores, we used 0-40 and 60-100 percentile scores to determine the control and patient groups, respectively. One of the study's major limitations is that because motion sickness susceptibility is scored according to self-report, there is a possibility of intertwining data rising during grouping. Another limitation is that tests that include a condition that will trigger motion sickness were not included in our test battery, and smooth pursuit and saccade tests were not performed in the vertical plane during the evaluation of vertical visual perception. In addition, the narrow age range of the participants included in the study is another limitation of our study.

CONCLUSION

There is currently no gold standard test for diagnosing motion sickness; the pathophysiology still needs to be fully elucidated, and the search for appropriate test batteries for diagnosis continues to determine possible effects. In our study, a large vestibular test battery including VNG-oculomotor tests, vHIT, cVEMP, and SVINT evaluations revealed no significant effect on the vestibular test results in motion sickness. The observation of a significant difference only in oVEMP n1-p1 amplitude in our study suggested that the utricular function in the motion sickness group should be emphasized in further studies. Our study contributes to the literature on vestibular test results in motion sickness, which remains a subject of controversy. In addition, our study reports the first use of SVINT to evaluate motion sickness. On the basis of our findings, we believe that tests for the diagnosis of motion sickness should be performed under conditions that will create a significant sensory conflict.

Acknowledgements: The authors thank Bezmialem Vakif University for support.

Ethics

Ethics Committee Approval: Approval for the study was obtained from the Non-Interventional Ethics Committee of Bezmialem Vakif University on 08/02/2022 (no: 2022/2).

Informed Consent: An informed consent form was obtained from the individuals who volunteered to participate in the study.

Author Contributions

Concept: O.G.T., Design: O.G.T., M.B.B., N.B., F.A., Data Collection and/or Processing: E.K., S.O., B.R., E.T., S.A., Analysis and/or Interpretation: O.G.T., E.K., S.O., M.B.B., N.B., F.A., Literature Search: O.G.T., E.K., S.O., Writing: O.G.T., E.K., S.O.

Conflict of Interest: The authors have no conflict of interest to declare.

Financial Disclosure: This work was supported by Bezmialem Vakif University Fund (project number: 20210808).

REFERENCES

1. Golding JF. Motion sickness. Handb Clin Neurol. 2016;137:371-90.
2. Leung AK, Hon KL. Motion sickness: an overview. Drugs Context. 2019;8:2019-9-4.
3. Gahlinger PM. Motion sickness. How to help your patients avoid travel travail. Postgrad Med. 1999;106:177-84.
4. Koch A, Cascorbi I, Westhofen M, Dafotakis M, Klapa S, Kuhtz-Buschbeck JP. The Neurophysiology and Treatment of Motion Sickness. Dtsch Arztebl Int. 2018;115:687-96.
5. Buyuklu F, Tarhan E, Ozluoglu L. Vestibular functions in motion sickness susceptible individuals. Eur Arch Otorhinolaryngol. 2009;266:1365-71.
6. Henriques IF, Douglas de Oliveira DW, Oliveira-Ferreira F, Andrade PM. Motion sickness prevalence in school children. Eur J Pediatr. 2014;173:1473-82.
7. Paillard AC, Quarck G, Paolino F, et al. Motion sickness susceptibility in healthy subjects and vestibular patients: effects of gender, age and trait-anxiety. J Vestib Res. 2013;23:203-9.
8. Oman CM. Sensory conflict in motion sickness: an observer theory approach. Pictorial communication in virtual and real environments. 1991:362-76.
9. Bos JE, Bles W. Modelling motion sickness and subjective vertical mismatch detailed for vertical motions. Brain Res Bull. 1998;47:537-42.
10. Cheung BS, Howard IP, Money KE. Visually-induced sickness in normal and bilaterally labyrinthine-defective subjects. Aviat Space Environ Med. 1991;62:527-31.
11. Cha YH, Golding JF, Keshavarz B, et al. Motion sickness diagnostic criteria: Consensus Document of the Classification Committee of the Bárány Society. J Vestib Res. 2021;31:327-44.
12. Neupane AK, Gururaj K, Sinha SK. Higher Asymmetry Ratio and Refixation Saccades in Individuals with Motion Sickness. J Am Acad Audiol. 2018;29:175-86.

13. Xie SJ, Chen W, Jia HB, Wang ZJ, Yao Q, Jiang YY. Ocular vestibular evoked myogenic potentials and motion sickness susceptibility. Aviat Space Environ Med. 2012;83:14-8.
14. Kılınç FM, Kaya M, Emekci T, Cengiz DU. Evaluation of semicircular canal functions by the Video Head Impulse Test (vHIT) in individuals with motion sickness. Evaluation. 2020;79:31-5.
15. Fowler CG, Dallapiazza M, Hadsell KT. Vestibular Function and Motion Sickness Susceptibility: Videonystagmographic Evidence From Oculomotor and Caloric Tests. Am J Audiol. 2020;29:188-98.
16. Ma Y, Ou Y, Chen L, Zheng Y. [Vestibular testing abnormalities in individuals with motion sickness]. Lin Chuang Er Bi Yan Hou Tou Jing Wai Ke Za Zhi. 2009;23:728-30.
17. Kumar RT, Sinha SK. Head Impulse Test Paradigm and Suppression Head Impulse Test Paradigm in Individuals With and Without Motion Sickness. Am J Audiol. 2021;30:518-23.
18. Dumas G, Curthoys IS, Lion A, Perrin P, Schmerber S. The Skull Vibration-Induced Nystagmus Test of Vestibular Function-A Review. Front Neurol. 2017;8:41.
19. Reason JT, Brand JJ. Motion Sickness. Academic press; 1975.
20. Golding JF. Motion sickness susceptibility. Auton Neurosci. 2006;129:67-76.
21. Ugur E, Konukseven BO, Topdag M, Cakmakci ME, Topdag DO. Expansion to the Motion Sickness Susceptibility Questionnaire-Short Form: A Cross-Sectional Study. J Audiol Otol. 2022;26:76-82.
22. Golding JF. Predicting individual differences in motion sickness susceptibility by questionnaire. Pers Individ Dif. 2006;41:237-48.
23. Dumas G, Quatre R, Schmerber S. How to do and why perform the skull vibration-induced nystagmus test. Eur Ann Otorhinolaryngol Head Neck Dis. 2021;138:287-90.
24. Johnson WH, Sunahara FA, Landolt JP. Importance of the vestibular system in visually induced nausea and self-vection. J Vestib Res. 1999;9:83-7.
25. Singh NK, Pandey P, Mahesh S. Assessment of otolith function using cervical and ocular vestibular evoked myogenic potentials in individuals with motion sickness. Ergonomics. 2014;57:1907-18.
26. Fowler CG, Sweet A, Steffel E. Effects of motion sickness severity on the vestibular-evoked myogenic potentials. J Am Acad Audiol. 2014;25:814-22.
27. Nooij SAE, Vanspauwen R, Bos JE, Wuyts FL. A re-investigation of the role of utricular asymmetries in space motion sickness. J Vestib Res. 2011;21:141-51.
28. Satar B, Akin Ocal FC, Karacayli C, Coban VK. Routine Vestibular Tests May Point Out Vestibular Subtype of Seasickness Only. Aerosp Med Hum Perform. 2020;91:852-60.
29. Tal D, Gilbey P, Bar R, Shupak A. Seasickness pathogenesis and the otolithic organs: vestibular evoked myogenic potentials study--preliminary results. Isr Med Assoc J. 2007;9:641-4.
30. Dumas G, Karkas A, Perrin P, Chahine K, Schmerber S. High-frequency skull vibration-induced nystagmus test in partial vestibular lesions. Otol Neurotol. 2011;32:1291-301.
31. Naghibi N, Shaabani M, Bakhshi E. Comparing mastoid and posterior cervical muscles vibration effects on eye movement in normal subjects. Aud Vestib Res. 2019;28:242-8.
32. Zamora EG, Araújo PES, Guillén VP, et al. Parameters of skull vibration-induced nystagmus in normal subjects. Eur Arch Otorhinolaryngol. 2018;275:1955-61.
33. Dornhoffer J, Chelonis JJ, Blake D. Stimulation of the semicircular canals via the rotary chair as a means to test pharmacologic countermeasures for space motion sickness. Otol Neurotol. 2004;25:740-5.
34. Yu J, Wan Y, Zhao J, Huang R, Wu P, Li W. Normative data for rotational chair considering motion susceptibility. Front Neurol. 2022;13:978442.
35. Bilgen C, Kirazlı T. Hareket Hastalığında Elektronistagmografinin Değeri. KBB ve BBC Dergisi. 2002;10:125-30.
36. Thornton WE, Uri JJ. Oculomotor function during space flight and susceptibility to space motion sickness. Acta Astronaut. 1991;23:53-61.
37. MacDougall HG, McGarvie LA, Halmagyi GM, et al. A new saccadic indicator of peripheral vestibular function based on the video head impulse test. Neurology. 2016;87:410-8.
38. Weber KP, Aw ST, Todd MJ, McGarvie LA, Curthoys IS, Halmagyi GM. Head impulse test in unilateral vestibular loss: vestibulo-ocular reflex and catch-up saccades. Neurology. 2008;70:454-63.
39. Demer JL, Goldberg J, Jenkins HA, Porter FI. Vestibulo-ocular reflex during magnified vision: adaptation to reduce visual-vestibular conflict. Aviat Space Environ Med. 1987;58:A175-9.
40. Karababa E, Satar B, Genç H. Evaluation of effects of optokinetic and rotational stimuli with functional head impulse test (fHIT) in individuals with motion sickness. Eur Arch Otorhinolaryngol. 2023;280:3149-56.

DOI: 10.4274/MMJ.galenos.2024.27243
Medeni Med J 2024;39:101-108

Original Article

Investigation of the Effect of Astaxanthin on Autophagy in Renal Ischemia-reperfusion Modeled Rats

Böbrek İskemi-reperfüzyon Modeli Oluşturulan Sıçanlarda Astaksantinin Otofaji Üzerine Etkisinin Araştırılması

Aysegul KISAOGLU[1], Evren KOSE[1], Nesibe YILMAZ[2], Kevser TANBEK[3], Azibe YILDIZ[4], Umit YILMAZ[5], Rumeyza Hilal CIRIK[4], Davut OZBAG[6]

[1]Inonu University Faculty of Medicine, Department of Anatomy, Malatya, Türkiye
[2]Karabuk University Faculty of Medicine, Department of Anatomy, Karabuk, Türkiye
[3]Inonu University Faculty of Medicine, Department of Physiology, Malatya, Türkiye
[4]Inonu University Faculty of Medicine, Department of Histology and Embryology, Malatya, Türkiye
[5]Karabuk University Faculty of Medicine, Department of Physiology, Karabuk, Türkiye
[6]Adiyaman University Faculty of Medicine, Department of Anatomy, Adiyaman, Türkiye

ABSTRACT

Objective: The aim of this study was to investigate the effect of various astaxanthin (ATX) doses on oxidative damage and autophagy in renal ischemia-reperfusion (I/R) injury-modeled rats.

Methods: The rats were divided into five groups: sham group (n=8), I/R (n=8), I/R + 5 mg/kg ATX (n=8), I/R + 10 mg/kg ATX (n=8), and I/R + 25 mg/kg ATX (n=8) groups. ATX was dissolved in 5 mg/kg, 10 mg/kg, and 25 mg/kg olive oil for 7 days and administered to the rats in the experimental group. Sham and I/R groups were also administered ATX solution (olive oil) via oral gavage for 7 days. Renal ischemia reperfusion was induced in all rats except the sham group after the last dose was administered on the 7th day. Reperfusion was conducted for 24 hours after 45 minutes of ischemia.

Results: Blood samples were collected, and kidney tissue were incised for biochemical and histological analyses. Superoxide dismutase (SOD) and total antioxidant status (TAS) were significantly lower in the I/R group than in the sham group ($p<0.05$), whereas malondialdehyde (MDA) and total oxidant status (TOS) values were higher ($p<0.05$). It was determined that SOD and TAS increased and MDA and TOS decreased in the ATX-administration groups compared with the I/R group, independent of the dose ($p<0.05$). In the 25 mg/kg ATX + I/R group, Beclin-1 and LC3β immunoreactivities were significantly higher than those in the other groups ($p<0.05$). The lowest p62 immunoreactivity was observed in the 25 mg/kg ATX + I/R group.

Conclusions: ATX had a protective effect on kidney function and against oxidative damage. Furthermore, high-dose ATX administration protected kidney tissue via autophagy induction in this study.

Keywords: Astaxanthin, renal, ischemia/reperfusion, oxidative stress, autophagy

ÖZ

Amaç: Bu çalışmanın amacı böbrek iskemi-reperfüzyon (İ/R) hasarı olan sıçanlarda astaksantinin (ATX) otofaji üzerine etkisinin araştırılmasıdır.

Yöntemler: Sıçanlar 5 gruba ayrıldı: Sham grubu (n=8), İ/R (n=8), ATX 5 mg/kg + İ/R (n=8), ATX 10 mg/kg + İ/R (n=8), ATX 25 mg/kg + İ/R (n=8). Deney grubundaki sıçanlara zeytinyağında çözdürülmüş ATX 5 mg/kg, 10 mg/kg ve 25 mg/kg, Sham ve İ/R grubundaki sıçanlara ise ATX çözücüsü (zeytinyağı) gavaj yoluyla 7 gün boyunca verildi. Sham grubu dışındaki tüm sıçanlara 7. gün son doz uygulandıktan sonra İ/R uygulandı. Kırk beş dakikalık böbrek iskemisinden sonra 24 saat süreyle reperfüzyon yapıldı.

Bulgular: Biyokimyasal ve histolojik analizler için kan ve doku örnekleri toplandı. Sham grubunda göre İ/R grubunda süperoksit dismutaz (SOD) ve toplam antioksidan durumu (TAS) anlamlı olarak düşükken ($p<0,05$), malondialdehid (MDA) ve toplam oksidan durumu (TOS) değerleri daha yüksekti ($p<0,05$). ATX uygulanan gruplarda doz miktarından bağımsız olarak SOD ve TAS düzeylerinin arttığı, MDA ve TOS düzeylerinin azaldığı tespit edildi ($p<0,05$). ATX 25 mg/kg + İ/R grubunda Beclin-1 ve LC3β immünreaktiviteleri diğer gruplarla karşılaştırıldığında istatistiksel olarak anlamlı derecede yüksekti ($p<0,05$). En düşük p62 immünreaktivitesi ATX 25 mg/kg + İ/R grubunda tespit edildi ($p<0,05$).

Sonuçlar: ATX'in böbrek fonksiyonlarını ve oksidatif hasara karşı koruyucu etkisi vardı. Ayrıca bu çalışmada yüksek doz ATX uygulaması böbrek dokularını otofaji indüksiyonu yoluyla korumuştur.

Anahtar kelimeler: Astaksantin, böbrek, iskemi/reperfüzyon, oksidatif stres, otofaji

Address for Correspondence: E. Kose, Inonu University Faculty of Medicine, Department of Anatomy, Malatya, Türkiye
E-mail: evren.kose@inonu.edu.tr **ORCID ID:** orcid.org/0000-0002-0246-2589

Received: 23 October 2023
Accepted: 04 May 2024
Online First: 07 June 2024

Cite as: Kisaoglu A, Kose E, Yilmaz N, Tanbek K, Yildiz A, Yilmaz U, Cirik RH, Ozbag D. Investigation of the Effect of Astaxanthin on Autophagy in Renal Ischemia-reperfusion Modeled Rats. Medeni Med J Medeni Med J 2024;39:101-108

INTRODUCTION

The kidney is an organ susceptible to ischemia-reperfusion (I/R) damage. Renal ischemia is the major cause of acute kidney injury induced by various conditions such as low cardiac output, renal vascular occlusion or obstruction, sepsis, and kidney transplantation. Acute kidney injury can lead to morbidity and mortality, affecting approximately 5-30% of inpatients and intensive care patients[1].

I/R injury induces certain structural and metabolic changes in tissues[2]. Thus, tissues require a defense mechanism to maintain vitality. Antioxidant defense is one of these mechanisms. There is a balance between the oxidant and antioxidant systems. An increase in the oxidant level and inadequate antioxidant system leads to oxidative damage[3]. There are various antioxidants in nature. Astaxanthin (ATX) is a red-orange antioxidant in the ketone group of carotenoids[4]. The effects of ATX on living organisms include the promotion of the immune system, anti-inflammatory properties, and protection against neurodegenerative diseases[5]. Certain studies have emphasized the protective effect of ATX against I/R injury[6-8].

Autophagy is a catabolic event that literally means self-eating. It is observed at the basal level in most cells and promotes the transformation of perennial organelles and proteins to maintain intracellular homeostasis[9]. The induction of autophagy during cellular stress is an effective mechanism for cellular survival. Certain empirical studies have reported that the inhibition of autophagy increases kidney damage, demonstrating the protective effect of autophagy against ischemic kidney damage[5]. Various studies have demonstrated that activation of autophagy triggered necrosis pathways and increased kidney damage[10]. Induction of autophagy increases Beclin-1 and LC3β protein activities, whereas it decreases p62 protein activity. Thus, Beclin-1, LC3β and p62 proteins are among the most frequently used parameters to analyze autophagy[11-13].

ATX has a protective effect against oxidative damage due to its antioxidant properties. Furthermore, it could induce and inhibit the autophagy mechanism. The role of autophagy in I/R-induced kidney damage has not yet been clarified. Thus, this study investigated the effects of various ATX doses on oxidative damage and autophagy in renal I/R injury modeled rats.

MATERIALS and METHODS

Study Settings

This study was approved (protocol no: 2019/A-48, date: 23.10.2019) by Inonu University, Animal Experiments Local Ethics Committee. During the study, the experimental animals were cared for and all experimental procedures conducted at Inonu University Faculty of Medicine Experimental Animal Breeding and Research Center.

Experimental Animals and Groups

This study was conducted with 40 male Sprague-Dawley rats with an average weight of 250 g. During the experiments, animals were kept at 21±1 ˚C temperature and 12 hours (h) of light and 12 h of darkness and fed standard rat chow ad libitum and regular tap water. The rats were divided into five groups: sham group (n=8), I/R (n=8), I/R + 5 mg/kg ATX (n=8), I/R + 10 mg/kg ATX (n=8), and I/R + 25 mg/kg ATX (n=8) groups. ATX[14] (Galenik, Cas no: 742-61-7) was dissolved in 5 mg/kg, 10 mg/kg, and 25 mg/kg[15] olive oil for 7 days[16] and administered to the rats in the experimental group. Sham and I/R groups were also administered ATX solution (olive oil) via oral gavage for 7 days. Renal ischemia reperfusion was induced in all rats except the sham group after the last dose was administered on the 7th day. Reperfusion was conducted for 24 h after 45 minutes (min) of ischemia. After 24 h, blood samples were drawn from the animals. The rats were then decapitated. Blood samples were collected for blood urea nitrogen (BUN) and creatinine measurements, and kidney tissue were incised for biochemical and histological analyses.

Rat Kidney I/R Damage Model

All rats were anesthetized with intramuscular 70 mg/kg ketamine (Richter Pharma AG, Australia) and 8 mg/kg xylazine (Bioveta PLC, Czech Republic) administration. Both renal arteries were revealed in the abdominal wall of the rats. A clamp was attached to the renal arteries, and ischemia was induced by obstructing blood flow to the kidneys for 45 min[17]. After 45 min of ischemia, the renal artery clamps were removed and blood flow was restored to the kidneys. After 24 h of reperfusion, the rats were sacrificed under anesthesia, and blood samples and kidney tissue samples were collected.

Blood Urea Nitrogen and Creatinine Measurements

BUN and creatinine levels were measured to determine the kidney function of the experimental group. Analyses were conducted based on the protocol described by commercial ELISA kits (SunRed Biotechnology, China)

with a microplate reader and BioTek HT Synergy Gen 5 software.

Superoxide Dismutase and Malondialdehyde Measurements

Kidney tissue superoxide dismutase (SOD) enzyme activity was determined using the method described by Sun et al.[18]. Malondialdehyde (MDA) was measured using the Esterbauer and Cheeseman[19] method, the most common lipid peroxidation determination method.

Total Antioxidant Status and Total Oxidant Status

The kidney tissue total antioxidant status (TAS) and total oxidant status (TOS) were determined based on the protocol provided in commercial ELISA kits (SunRed Biotechnology, China) with a microplate reader and BioTek HT Synergy Gen 5 software in the experimental groups.

Histochemical Analysis

The kidneys were removed at the end of the experiment and fixed in 10% formaldehyde. After tissue follow-up procedures, 4-5 µm sections were incised from the paraffin blocks. Sections were stained with hematoxylin-eosin (H&E) to determine the general morphological structure. Kidney sections were evaluated for tubular degeneration (tubular necrosis and dilatation) in the cortical and medullary regions. Ten randomly selected areas were examined, and the regions were scored on the basis of the degree of histological changes as follows: 0: no change, 1: mild, 2: moderate, 3: severe change. Analyses were performed using a Leica DFC-280 research microscope and the Leica Q Win Image Analysis System (Leica Micros Imaging Solutions Ltd., Cambridge, UK).

Immunohistochemical Analysis

The deparaffinized and rehydrated sections were placed in a pressure cooker and boiled in 0.01 M citrate (pH 6.0) for 15-20 min. To inhibit endogenous peroxidase enzyme activity, 3% hydrogen peroxide was applied to the sections for 12 min. A protein block (ultra V block) was applied to the sections that were washed with phosphate buffered saline (PBS) for 5 min. The sections were then incubated with primary antibody (GnRH and kispeptin) at 37 °C for 60 min. Biotin-based secondary antibody was applied to the tissues that were washed with PBS for 10 min at 37 °C. The sections were then incubated at 37 °C for 10 min with streptavidin peroxidase. Subsequently, chromogen-applied sections were stained with hematoxylin and covered with a water-based sealer. Brown staining was observed in tubule epithelial cells because of the immunoreactivity with Beclin-1, LC3β and p62. Staining, extent of immunoreactivity (0: 0-25%, 1: 26-50%, 2: 51-75%, 3: 76-100%), and severity (0: none, +1: mild, +2: moderate, +3: severe) were scored semi-quantitatively. The total staining score was calculated by 'prevalence x severity'[20]. The analysis was conducted using a Leica DFC-280 research microscope and a Leica Q Win Image Analysis System (Leica Micros Imaging Solutions Ltd., Cambridge, UK).

Statistical Analysis

Statistical analyses were conducted using the Kruskal-Wallis test on IBM SPSS Statistics 25.0 software. The Conover test was used for Kruskal-Wallis in multiple comparisons. $p<0.05$ was accepted as statistically significant. Data are presented as medians (minimum-maximum). Statistical histological analyses were conducted using statistical software developed by Inonu University Faculty of Medicine, Department of Biostatistics and Medical Informatics. It was determined that measurable variables in all study groups did not exhibit a normal distribution in the normality tests. Thus, Kruskal-Wallis analysis of variance, a non-parametric test, was employed in the general intergroup comparisons of all variables. Paired-group comparisons were determined using the Mann-Whitney U test and Bonferroni correction. $P<0.05$ was accepted as statistically significant. Data are presented as medians (minimum-maximum) based on distribution.

RESULTS

Astaxanthin Preserves Kidney Function

BUN and creatinine levels were measured to determine rat kidney functions. BUN and creatinine levels were significantly higher in the I/R group than in the sham group ($p<0.05$). BUN and creatinine levels were found to be significantly lower in animals given ATX and performed I/R than in the I/R group ($p<0.05$) (Table 1).

Astaxanthin Protects Against Oxidative Stress

SOD, MDA, TAS, and TOS were measured to determine oxidative stress in kidney tissue. SOD and TAS were significantly lower in the I/R group than in the sham group ($p<0.05$), whereas MDA and TOS values were higher ($p<0.05$). It was determined that SOD and TAS increased and MDA and TOS decreased in the ATX-administration groups compared with the I/R group, independent of the dose ($p<0.05$) (Table 1).

Histopathological Changes in Kidney Tissues

The kidney tissues of the sham group had normal histological appearance, except for mild tubular dilatation. However, necrotic changes and dilatation were observed in both cortical and medullar tubules in the I/R group. Another prominent finding in this group was local and diffuse inflammatory cell infiltration in the interstitial tissues. The difference between the I/R and sham groups was statistically significant ($p<0.0001$). It was observed that the histopathological changes observed in the 5 mg/kg ATX + I/R group were similar to those in the I/R group. The histopathological changes observed in the I/R group were significantly lower in the 10 mg/kg ATX + I/R and 25 mg/kg ATX + I/R groups ($p<0.0001$). The most significant decrease in infiltration was observed in the 25 mg/kg ATX + I/R group (Figure 1, Table 2).

Astaxanthin Induces Autophagy

Immunoreactivity of Beclin-1, LC3β and p62 proteins was analyzed to investigate autophagy. Beclin-1 and LC3β immunoreactivities were prominent in the tubule epithelial cell cytoplasm. Statistically, Beclin-1 and LC3β immunoreactivities were similar in the sham, I/R, 5 mg/kg ATX + I/R, and 10 mg/kg ATX + I/R groups. In the 25 mg/kg ATX + I/R group, Beclin-1 and LC3β immunoreactivities were significantly higher than those in the other groups ($p<0.05$) (Figures 2, 3). p62 immunoreactivity was observed in the nuclei cytoplasm of the tubular epithelial cells. Although the lowest immunoreactivity was observed in the 25 mg/kg ATX + I/R group, the difference was not statistically significant (Figure 4). The immunohistochemical analysis findings are shown in Table 3.

DISCUSSION

In our study, the effect of ATX pretreatment on autophagy was investigated in I/R rats. It was determined that I/R induced oxidative damage in the kidneys. It was observed that ATX administration protected the kidneys against oxidative damage in the groups in which ATX was administered before I/R independent of the dose. However, in the high-dose ATX group, the protection was via autophagy induction.

BUN and creatinine are employed to analyze kidney function, and an increase in BUN and creatinine levels indicates a decrease in kidney functions[21]. The H&E staining method is employed to monitor histopathological changes in kidney tissue. Various studies have reported that ATX administration significantly reduced high BUN and creatinine levels and improved histopathological changes induced by kidney damage[22,23]. Li et al.[24] reported that BUN increased because of kidney damage; however, the change in creatinine was not significant, ATX decreased the high

Table 1. The Kruskal-Wallis test was used to analyze the data, and the Conover test was used for the Kruskal-Wallis test in multiple comparisons. Figures are presented as medians (min-max).

Parameter	Group				
	Sham	I/R	5 mg/kg ATX + I/R	10 mg/kg ATX + I/R	25 mg/kg ATX + I/R
SOD (U/mg)	14.49 (9.57-20.65)	7.75 (5.12-9.92)[a]	13.99 (12.14-16.73)	11.87 (7.67-24.69)	13.75 (9.41-18.61)
MDA (µmol/g tissue)	1.70 (1.47-3.130)	5.66 (3.10-12.14)[b]	2.45 (1.40-4.21)	2.35 (1.33-3.32)	2.01 (1.14-2.81)
TAS (µmol trolox equivalent /L)	11.12 (8.72-13.35)	8.40 (5.73-11.23)[a]	12.60 (8.15-15.81)	13.37 (8.50-17.97)	12.45 (9.81-15.06)
TOS (µmol H_2O_2 equivalent/L)	2.21 (1.96-3.27)	4.54 (3.08-5.57)[b]	2.75 (2.03-3.62)	3.00 (1.76-3.83)	2.91 (2.02-3.98)
BUN (mg/dL)	5.04 (4.10-5.45)	5.59 (5.05-6.99)[b]	4.61 (3.75-5.88)	4.59 (3.84-5.21)	4.77 (4.31-5.74)
Creatinine (mg/dL)	69.51 (54.16-81.18)	78.28 (71.93-91.77)[b]	67.69 (36.86-93.15)	72.20 (28.15-97.96)	54.04 (41.13-73.88)

[a]Significant decrease compared with other groups ($p<0.05$), [b]Significant increase compared with other groups ($p<0.05$). ATX: Astaxanthin, I/R: Ischemia-reperfusion, SOD: Superoxide dismutase, MDA: Malondialdehyde, TAS: Total antioxidant status, TOS: Total oxidant status, min-max: Minimum-maximum, BUN: Blood urea nitrogen

BUN level, and the pathological changes induced by kidney damage were reduced after ATX administration. In the present study, it was determined that BUN and creatinine increased due to I/R-induced kidney damage, and these values approached normal in the ATX + I/R groups, independent of the administration dose.

As reported by previous studies, the antioxidant properties of ATX neutralize free radicals and protect cell membranes, cells, and tissues against oxidative damage[25]. In the current study, the common biomarkers SOD, MDA, TAS, and TOS were employed to analyze I/R-induced oxidative damage. Rats pretreated with ATX exhibited lower MDA and TOS and higher SOD and TAS levels when compared with the I/R group rats, consistent with previous study findings, indicating a strong antioxidant effect of ATX and its protective effect against oxidative damage[22,25-28].

Autophagy plays a critical role in the maintenance of cellular homeostasis under stress conditions. The protective mechanisms associated with autophagy induction have been emphasized in various experimental kidney damage models[29,30]. While it seems reasonable to induce autophagy to protect kidney tissue based on current evidence, other studies have reported that increased autophagy augmented kidney damage[31,32]. Thus,

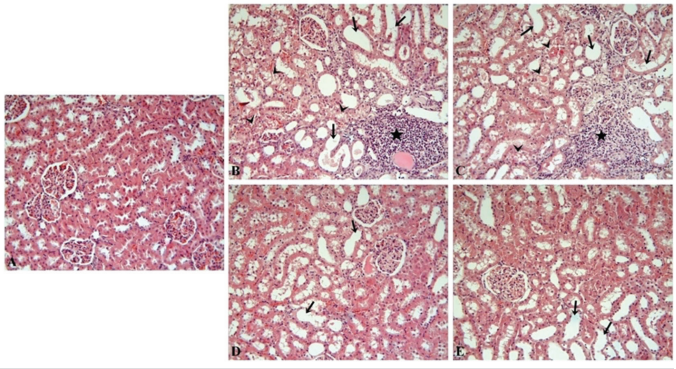

Figure 1. Histopathological findings.

[In the sham group (A), the kidney cortical tissue has a normal histological appearance. In the I/R group (B), necrotic (arrowheads) and dilated (arrows) tubules and inflammatory cell infiltration (star) were noted in the interstitial region. In the 5 mg/kg ATX + I/R group (C), necrotic tubules (arrowheads), dilated tubules (arrows), and inflammatory cell infiltration (star) were observed, similar to the I/R group. In the 10 mg/kg ATX +I/R (D) and 25 mg/kg ATX + I/R (E) groups, significant alleviation in histopathological changes was noted, except for tubular dilatation (arrows)].

ATX: Astaxanthin, I/R: Ischemia-reperfusio

Table 2. Histopathological analysis findings.

Group	Tubular degeneration	Infiltration
Sham	0.0 (0.0-1.0)	0.0 (0.0-0.0)
I/R	2.0 (0.0-3.0)[a]	0.0 (0.0-3.0)[a]
5 mg/kg ATX + I/R	1.0 (0.0-3.0)	0.0 (0.0-3.0)[a]
10 mg/kg ATX + I/R	1.0 (0.0-3.0)[b]	0.0 (0.0-2.0)[b]
25 mg/kg ATX + I/R	1.0 (0.0-3.0)[b]	0.0 (0.0-2.0)[b,c]

[a]Significant increase compared with the sham group (p<0.0001). [b]Significant decrease compared with the I/R group (p<0.0001). [c]Significant decrease compared with the 5 mg/kg ATX +I/R group (p=0.0180). ATX: Astaxanthin, I/R: Ischemia-reperfusion

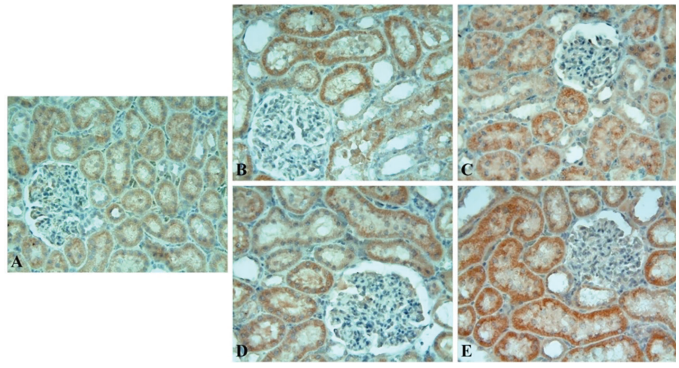

Figure 2. Beclin-1 immunreactivity.

(A: sham group, B: I/R group, C: 5 mg/kg ATX + I/R group, D: 10 mg/kg ATX + I/R group, E: 25 mg/kg ATX + I/R group. Brownish tubule Beclin-1 immunoreactivity in epithelial cells. In the 25 mg/kg ATX + I/R group, immunoreactivity intensity was higher than that in the other groups. Beclin-1 immunoreactivity, 40).

ATX: Astaxanthin, I/R: Ischemia-reperfusion

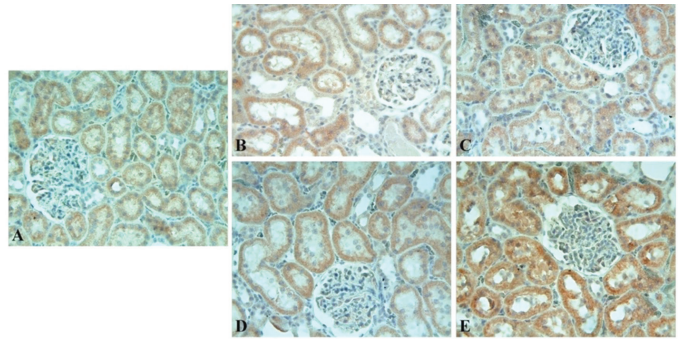

Figure 3. LC3b immunreactivity.

(A: sham group, B: I/R group, C: 5 mg/kg ATX + I/R group, D: 10 mg/kg ATX + I/R group, E: 25 mg/kg ATX + I/R group. Brownish tubule LC3b immunoreactivity in epithelial cells. Immunoreactivity intensity was higher in the 25 mg/kg ATX + I/R group than in the other groups. LC3b immunoreactivity, 40).

there are contradicting views on the protective properties of autophagy in tissues and whether it contributes to I/R induced damages[29,31,32]. ATX also protects tissues against damage via autophagy upregulation. In an experimental study, ATX had protective effects against pancreatic tissue damage by inhibiting autophagy in rats with acute pancreatitis[33]. An experimental study by Shen et al.[34] Reported that autophagy induced liver fibrosis, and ATX had a protective effect on liver tissue via the inhibition of autophagy. Autophagy increased due to dysregulated energy metabolism after I/R in the liver, and ATX reduced the damage caused by autophagy-induced cell necrosis[35]. When these results were evaluated together, ATX protected tissues by inhibiting autophagy. Lee et al.[36] reported that ATX induced autophagy in gastric adenocarcinoma cells induced by *Helicobacter pylori* and protected gastric tissues. In another study, it was reported that ATX augmented autophagy after spinal cord injury and reduced histopathological changes and neuronal degeneration in spinal tissue[37]. It has also been reported in an experimental study that ATX delays the decline in learning and memory ability caused by aging by alleviating cell damage in the brain, i.e., ATX delays age-related cognitive decline by inducing autophagy[38]. These results suggest that ATX protects tissues against damage by inducing autophagy. In our study, ATX protected tissues against damage by inducing autophagy.

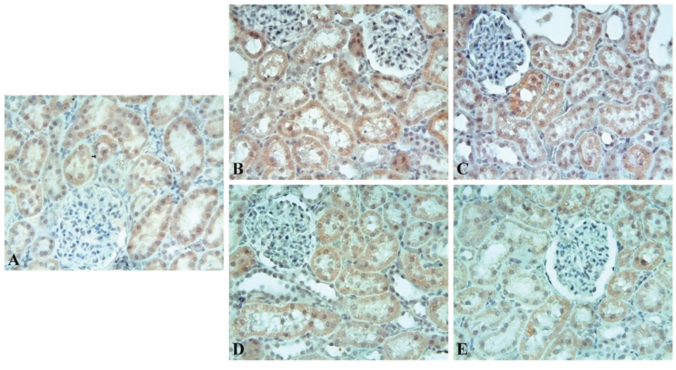

Figure 4. p62 immunoreactivity.

(A: sham group, B: I/R group, C: 5 mg/kg ATX + I/R group, D: 10 mg/kg ATX + I/R group, E: 25 mg/kg ATX + I/R group. Brownish tubule p62 immunoreactivity in epithelial cells. Immunoreactivity intensity was milder in the 25 mg/kg ATX + I/R group than in the other groups. p62 immunoreactivity, 40).

ATX: Astaxanthin, I/R: Ischemia-reperfusion

In our study, histological and biochemical analyses were conducted to monitor kidney tissue damage, and Beclin-1, LC3b and p62 immunoreactivities were analyzed to determine autophagy. Biochemical findings demonstrated that ATX was effective in preserving kidney function and protecting against oxidative damage. Based on the biochemical data, the effects of ATX administration were dose-independent; however, histological analysis revealed no improvement in the 5 mg/kg ATX + I/R group in parallel with the biochemical parameters. It could be suggested that this was due to the need for longer or higher dose administration for histological improvement. Furthermore, high Beclin-1 and LC3b immunoreactivities and low p62 immunoreactivity demonstrated autophagy activation in the 25 mg/kg ATX + I/R group. The decrease in infiltration in the 25 mg/kg ATX + I/R group demonstrated that autophagy induced in the 25 mg/kg ATX + I/R group also protected the tissues against damage.

CONCLUSION

In conclusion, ATX had a protective effect on kidney function and against oxidative damage. Furthermore, high-dose ATX administration protected kidney tissue via autophagy induction in this study.

Table 3. Immunohistochemical analysis findings.

Group	Beclin-1	LC3β	p62
Sham	8.0 (4.0-12.0)	8.0 (4.0-12.0)	4.0 (0.0-12.0)
I/R	8.0 (4.0-12.0)	8.0 (4.0-12.0)	4.0 (0.0-12.0)
5 mg/kg ATX + I/R	8.0 (4.0-12.0)	8.0 (4.0-12.0)	4.0 (0.0-12.0)
10 mg/kg ATX + I/R	8.0 (4.0-12.0)	8.0 (4.0-12.0)	4.0 (0.0-12.0)
25 mg/kg ATX + I/R	12.0 (4.0-12.0)[a]	8.5 (4.0-12.0)[b]	4.0 (0.0-9.0)

[a]Significant increase compared with Sham, I/R, 5 mg/kg ATX + I/R, 10 mg/kg ATX + I/R, and 25 mg/kg ATX + I/R groups ($p<0.05$). [b]Significant increase compared with I/R, 5 mg/kg ATX + I/R, 10 mg/kg ATX + I/R, and 25 mg/kg ATX + I/R groups ($p<0.05$). ATX: Astaxanthin, I/R: Ischemia-reperfusion

Ethics

Ethics Committee Approval: The experimental protocol was examined and approved by the Animal Experiments Local Ethics Committee of Inonu University Faculty of Medicine (protocol no: 2019/A-48) on 23.10.2019.

Informed Consent: Animal experiment study.

Author Contributions

Surgical and Medical Practices: A.K., E.K., N.Y., K.T., U.Y., Concept: A.K., E.K., N.Y., D.O., Design: A.K., E.K., D.O., Data Collection and/or Processing: A.K., E.K., N.Y., K.T., A.Y., U.Y., R.H.C., Analysis and/or Interpretation: A.K., E.K., N.Y., K.T., A.Y., U.Y., R.H.C., Literature Search: A.K., E.K., Writing: A.K., E.K.

Conflict of Interest: The authors have no conflict of interest to declare.

Financial Disclosure: This study was supported by the Research Fund of Inonu University, Project No: TYL-2020-2009.

REFERENCES

1. Wei Q, Dong Z. Mouse model of ischemic acute kidney injury: technical notes and tricks. Am J Physiol Renal Physiol. 2012;303:F1487-94.
2. Jennings RB, Reimer KA. The cell biology of acute myocardial ischemia. Annu Rev Med. 1991;42:225-46.
3. Ahmadiasl N, Banaei S, Alihemmati A. Combination antioxidant effect of erythropoietin and melatonin on renal ischemia-reperfusion injury in rats. Iran J Basic Med Sci. 2013;16:1209-16.
4. Karuppuswamy R. Extraction and Characterization of Major Valuable Compounds From Prawn Waste [dissertation]. University of New South Wales; 2008.
5. Jiang M, Liu K, Luo J, Dong Z. Autophagy is a renoprotective mechanism during in vitro hypoxia and in vivo ischemia-reperfusion injury. Am J Pathol. 2010;176:1181-92.
6. Mentese A, Turkmen S, Karaguzel E, et al. The predictive value of ischemia-modified albumin in long-term results of ischemia-reperfusion injury in an experimental testicular torsion model. Urology. 2012;80:689-94.
7. Li S, Takahara T, Fujino M, et al. Astaxanthin prevents ischemia-reperfusion injury of the steatotic liver in mice. PLoS One. 2017;12:e0187810.
8. Lee DH, Lee YJ, Kwon KH. Neuroprotective Effects of Astaxanthin in Oxygen-Glucose Deprivation in SH-SY5Y Cells and Global Cerebral Ischemia in Rat. J Clin Biochem Nutr. 2010;47:121-9.
9. Levine B, Yuan J. Autophagy in cell death: an innocent convict? J Clin Invest. 2005;115:2679-88.
10. Lin TA, Wu VC, Wang CY. Autophagy in Chronic Kidney Diseases. Cells. 2019;8:61.
11. Chen L, Fu H, Lu T, et al. An Integrated Nomogram Combining Clinical Factors and Microtubule-Associated Protein 1 Light Chain 3B Expression to Predict Postoperative Prognosis in Patients with Intrahepatic Cholangiocarcinoma. Cancer Res Treat. 2020;52:469-80.
12. Komatsu M, Kageyama S, Ichimura Y. p62/SQSTM1/A170: physiology and pathology. Pharmacol Res. 2012;66:457-62.
13. Liang XH, Jackson S, Seaman M, et al. Induction of autophagy and inhibition of tumorigenesis by beclin 1. Nature. 1999;402:672-6.
14. Brendler T, Williamson EM. Astaxanthin: How much is too much? A safety review. Phytother Res. 2019;33:3090-111.
15. Qiu X, Fu K, Zhao X, et al. Protective effects of astaxanthin against ischemia/reperfusion induced renal injury in mice. J Transl Med. 2015;13:28.
16. Pan L, Zhou Y, Li XF, Wan QJ, Yu LH. Preventive treatment of astaxanthin provides neuroprotection through suppression of reactive oxygen species and activation of antioxidant defense pathway after stroke in rats. Brain Res Bull. 2017;130:211-20.
17. Chen CC, Liu ZM, Wang HH, He W, Wang Y, Wu WD. Effects of ulinastatin on renal ischemia-reperfusion injury in rats. Acta Pharmacol Sin. 2004;25:1334-40.
18. Sun Y, Oberley LW, Li Y. A simple method for clinical assay of superoxide dismutase. Clin Chem. 1988;34:497-500.
19. Esterbauer H, Cheeseman KH. Determination of aldehydic lipid peroxidation products: malonaldehyde and 4-hydroxynonenal. Methods Enzymol. 1990;186:407-21.
20. Ozer EA, Kumral A, Ozer E, et al. Effect of retinoic acid on oxygen-induced lung injury in the newborn rat. Pediatr Pulmonol. 2005;39:35-40.
21. Hosten AO. BUN and Creatinine. In Walker HK, Hall WD, Hurst JW, editors. Clinical Methods: The History, Physical, and Laboratory Examinations. 3rd edition. Boston: Butterworths; 1990. Chapter 193.
22. Gao D, Wang H, Xu Y, Zheng D, Zhang Q, Li W. Protective effect of astaxanthin against contrast-induced acute kidney injury via SIRT1-p53 pathway in rats. Int Urol Nephrol. 2019;51:351-8.
23. Iskender H, Yenice G, Dokumacioglu E, et al. Astaxanthin alleviates renal damage of rats on high fructose diet through modulating NFκB/SIRT1 pathway and mitigating oxidative stress. Arch Physiol Biochem. 2020;126:89-93.
24. Li L, Chen Y, Jiao D, Yang S, Li L, Li P. Protective Effect of Astaxanthin on Ochratoxin A-Induced Kidney Injury to Mice by Regulating Oxidative Stress-Related NRF2/KEAP1 Pathway. Molecules. 2020;25:1386.
25. Palozza P, Krinsky NI. Astaxanthin and canthaxanthin are potent antioxidants in a membrane model. Arch Biochem Biophys. 1992;297:291-5.
26. Akca G, Eren H, Tumkaya L, et al. The protective effect of astaxanthin against cisplatin-induced nephrotoxicity in rats. Biomed Pharmacother. 2018;100:575-82.
27. Naito Y, Uchiyama K, Aoi W, et al. Prevention of diabetic nephropathy by treatment with astaxanthin in diabetic db/db mice. Biofactors. 2004;20:49-59.
28. Liu N, Chen J, Gao D, Li W, Zheng D. Astaxanthin attenuates contrast agent-induced acute kidney injury in vitro and in vivo via the regulation of SIRT1/FOXO3a expression. Int Urol Nephrol. 2018;50:1171-80.
29. Mei S, Livingston M, Hao J, Li L, Mei C, Dong Z. Autophagy is activated to protect against endotoxic acute kidney injury. Sci Rep. 2016;6:22171.

30. Xu X, Pan J, Li H, et al. Atg7 mediates renal tubular cell apoptosis in vancomycin nephrotoxicity through activation of PKC-δ. FASEB J. 2019;33:4513-24.

31. Wu HH, Hsiao TY, Chien CT, Lai MK. Ischemic conditioning by short periods of reperfusion attenuates renal ischemia/reperfusion induced apoptosis and autophagy in the rat. J Biomed Sci. 2009;16:19.

32. Isaka Y, Suzuki C, Abe T, et al. Bcl-2 protects tubular epithelial cells from ischemia/reperfusion injury by dual mechanisms. Transplant Proc. 2009;41:52-4.

33. Zhang H, Yang W, Li Y, et al. Astaxanthin ameliorates cerulein-induced acute pancreatitis in mice. Int Immunopharmacol. 2018;56:18-28.

34. Shen M, Chen K, Lu J, et al. Protective effect of astaxanthin on liver fibrosis through modulation of TGF-β1 expression and autophagy. Mediators Inflamm. 2014;2014:954502.

35. Li J, Wang F, Xia Y, et al. Astaxanthin Pretreatment Attenuates Hepatic Ischemia Reperfusion-Induced Apoptosis and Autophagy via the ROS/MAPK Pathway in Mice. Mar Drugs. 2015;13:3368-87.

36. Lee H, Lim JW, Kim H. Effect of Astaxanthin on Activation of Autophagy and Inhibition of Apoptosis in Helicobacter pylori-Infected Gastric Epithelial Cell Line AGS. Nutrients. 2020;12:1750.

37. Abbaszadeh F, Jorjani M, Joghataei MT, Mehrabi S. Astaxanthin Modulates Autophagy, Apoptosis, and Neuronal Oxidative Stress in a Rat Model of Compression Spinal Cord Injury. Neurochem Res. 2022;47:2043-51.

38. Fu M, Liang X, Zhang X, et al. Astaxanthin delays brain aging in senescence-accelerated mouse prone 10: inducing autophagy as a potential mechanism. Nutr Neurosci. 2023;26:445-55.

DOI: 10.4274/MMJ.galenos.2024.60308
Medeni Med J 2024;39:109-116

Original Article

Clinical and Sonographic Evaluation of the Effectiveness of Extracorporeal Shock Wave Therapy in Patients with Lateral Epicondylitis

Lateral Epikondilitli Hastalarda Ekstrakorporeal Şok Dalga Tedavisi Etkinliğinin Klinik ve Sonografik Değerlendirmesi

Sadiye MURAT[1], Bilinc DOGRUOZ KARATEKIN[2], Melisa ZENGIN[2]

[1]Istanbul Medeniyet University Faculty of Medicine, Department of Physical Medicine and Rehabilitation, Istanbul, Türkiye
[2]Goztepe Prof. Dr. Suleyman Yalcin City Hospital, Clinic of Physical Medicine and Rehabilitation, Istanbul, Türkiye

ABSTRACT

Objective: This study assessed and compare the clinical and sonographic outcomes of extracorporeal shock wave therapy (ESWT) in patients with lateral epicondylitis (LE).

Methods: Forty-two LE patients were randomly divided into two groups: the ESWT group (n=21) and the sham-ESWT control group (n=21). Both groups underwent wrist resting splinting, stretching, strengthening exercises for wrist extensors, and ice application. Grip strength, pain, and functionality were assessed by various tests, and common extensor tendon (CET) thickness was measured sonographically before, after, and 1 month after treatment by a blind examiner.

Results: At baseline, there was no significant difference between the groups. Significant differences were observed in pain pressure threshold, grip strength, visual analog scale, and Patient-Rated Tennis Elbow Evaluation (PRTEE) scores between baseline, post-treatment, and 1 month after treatment in both groups ($p<0.05$). However, the Short Form-12 (SF-12) physical scores showed a significant difference only 1 month after treatment ($p<0.01$). In the SF-12 mental score tests, no significant difference was found. CET thickness in the ESWT group significantly decreased after treatment and 1 month after treatment ($p<0.05$), whereas no significant difference was observed in the control group.

Conclusions: Both the ESWT and control groups showed a reduction in pain and improvement in function. However, the ESWT group showed statistically superior results in terms of pain reduction and functional improvement compared with the control group. In addition, sonographic evaluation revealed a significant reduction in CET thickness in the ESWT group, whereas no significant change was noted in the control group.

Keywords: Lateral epicondylitis, extracorporeal shock wave therapy (ESWT), sonographic assessment

ÖZ

Amaç: Bu çalışmanın amacı lateral epikondilit (LE) tanılı hastalarda ekstrakorporeal şok dalga tedavisinin (ESWT) klinik ve sonografik sonuçlarını değerlendirmek ve karşılaştırmaktır.

Yöntemler: Kırk iki LE hastası rastgele iki gruba ayrıldı: ESWT grubu (n=21) ve sham-ESWT kontrol grubu (n=21). Her iki gruba da el bileği istirahat ateli, germe, el bileği ekstansörleri için güçlendirme egzersizleri ve buz uygulaması yapıldı. Grupların kavrama gücü Jamar el dinamometresi, ağrı, fonksiyonellik çeşitli testlerle ve ortak ekstansör tendon (CET) kalınlığı sonografik olarak tedaviden önce, tedaviden sonra ve tedaviden bir ay sonra kör bir denetçi tarafından ölçülmüştür.

Bulgular: Başlangıçta, gruplar arasında anlamlı bir fark yoktu. Her iki grupta ağrı basınç eşiği (PPT), kavrama gücü, görsel analog skalası (VAS), Hasta-değerlendirmeli Tenisçi Dirseği Değerlendirmesi (PRTEE) skorları başlangıç, tedavi sonrası ve tedaviden bir ay sonraki ölçümler arasında anlamlı farklılıklar gözlenmiştir ($p<0,05$). Ancak Kısa Form-12 (SF-12) fiziksel skorlar tedaviden sadece bir ay sonra anlamlı farklılık göstermiştir ($p<0,01$). SF-12 mental skor testinde her iki grupta da ölçümler arasında anlamlı fark bulunmamıştır. ESWT grubunda, CET kalınlığı tedavi sonrasında ve tedaviden bir ay sonra önemli ölçüde azalmıştır ($p<0,05$), ancak kontrol grubunda önemli bir fark gözlenmemiştir.

Sonuçlar: Hem ESWT hem de kontrol grupları ağrıda azalma ve işlevsellikte iyileşme göstermiştir. Ancak, ESWT grubu kontrol grubuna kıyasla ağrı azalması ve fonksiyonel iyileşme açısından istatistiksel olarak daha üstün sonuçlar sergilemiştir. Ek olarak, sonografik değerlendirme ESWT grubunda CET kalınlığında anlamlı bir azalma olduğunu ortaya koyarken, kontrol grubunda anlamlı bir değişiklik kaydedilmemiştir.

Anahtar kelimeler: Lateral epikondilit, ekstrakorporeal şok dalga tedavisi (ESWT), sonografik değerlendirme

Address for Correspondence: M. Zengin, Goztepe Prof. Dr. Suleyman Yalcin City Hospital, Clinic of Physical Medicine and Rehabilitation, Istanbul, Türkiye
E-mail: melisazngn@gmail.com **ORCID ID:** orcid.org/0009-0005-4462-5154
Presented in: Presented as an oral presentation at the 17th Congress of the European Forum for Research in Rehabilitation (EFRR) in Antalya/Türkiye on November 2-5, 2023.

Received: 17 March 2024
Accepted: 20 May 2024
Online First: 30 May 2024

Cite as: Murat S, Dogruoz Karatekin B, Zengin M. Clinical and Sonographic Evaluation of the Effectiveness of Extracorporeal Shock Wave Therapy in Patients with Lateral Epicondylitis. Medeni Med J 2024;39:109-116

INTRODUCTION

Lateral epicondylitis (LE), commonly known as tennis elbow, is a prevalent musculoskeletal condition characterized by pain and tenderness around the lateral epicondyle of the humerus[1].

Its incidence affects approximately 1-3% of the global population annually, with individuals aged 35 years being predominantly affected. It is also noteworthy that the prevalence is higher and the duration is longer in women than in men[2,3].

Although the exact cause of LE is often nonspecific, it is frequently associated with overuse of the elbow, particularly in the dominant arm and among tennis players, leading to repetitive micro-tears, degeneration, and tendinosis[4].

Reduced grip and upper extremity strength, as well as pain that travels from the lateral side of the elbow to the forearm and possibly the upper arm, are signs of LE. Pain is typically exacerbated by activities that involve contraction of the common extensor muscle mass, such as resisted dorsiflexion of the wrist[5].

The severity of pain can range from intermittent and mild to constant and severe, significantly impacting functional ability and performance in occupational and sport activities and even disrupting sleep patterns[6]. The duration of symptoms ranges from 6 months to 2 years, with a general tendency to be self-limiting, and approximately 70-90% of affected patients experience complete resolution within 1 year[7]. However, the overall discomfort and functional disability experienced during the 6-month to 2-year duration can be substantial[8]. Clinical and radiological evaluations are used in the diagnosis[9]. Tenderness with palpation on the lateral epicondyle, positive Cozen's test, and decrease in hand grip strength are important physical examination findings[5]. A significant relationship was also determined between clinical symptoms of LE and diagnostic ultrasonography (USG) findings. USG findings may reveal changes such as increased common extensor tendon (CET) thickness, focal hypoechogenicity, intratendinous calcification, and bone abnormalities[10]. It has been stated that clinical features in patients with chronic LE are associated with the pain threshold value and structural changes in USG[11]. However, in many intervention group studies, the correlation between maximum tendon thickness and clinical parameters, hand grip strength, and pain threshold value varied[3,12,13].

Various treatments have been used for LE[3,7,13,14], and conservative management recommended initially[14]. Some of the treatments available for this condition include physical therapy (such as rest, limited movement, modifying activities, using hot or cold compresses, electrotherapy, massage, and USG), splinting, injections directly into the affected area [such as corticosteroids or platelet-rich plasma (PRP)], oral or topical nonsteroidal anti-inflammatory drugs, and extracorporeal shock wave therapy (ESWT)[3,7,13-15]. Surgery is also considered in severe cases[15].

ESWT is a safe and noninvasive option, known to have minimal side effects like discomfort during treatment and minor bruising[15]. The mechanism of ESWT is not exactly understood, but it appears to involve mechanotransduction triggering cellular changes, increasing collagen synthesis, accelerating vascularization, which promote the healing process and reduce pain in musculoskeletal conditions[4,16]. ESWT has demonstrated efficacy in treating a wide range of musculoskeletal conditions, such as pseudoarthrosis, delayed fracture healing, bone marrow edema, early-stage osteonecrosis, insertional tendinopathies, calcifying tendonitis, tennis elbow, and wound healing issues[15].

There are many studies on the positive effects of radial ESWT (rESWT) on pain and functional status in LE[1,17,18]. However, studies investigating the effect of rESWT on ultrasonographically measured CET thickness in LE are insufficient and yield different results[3,19].

Therefore, the present study aimed to investigate the effects of ESWT on pain, pain-pressure threshold, functional status, quality of life, and ultrasonographically measured CET thickness in patients with LE.

MATERIALS and METHODS

Patients and Methods

Study Design

The present study is a prospective, randomized, and controlled study conducted in a single center. Patients diagnosed with LE who visited the Istanbul Medeniyet University Goztepe Training and Research Hospital between the years 2020 and 2021 were included in the study. This study was approved by the Istanbul Medeniyet University Goztepe Training and Research Hospital Clinical Research Ethics Committee (decision no: 2020/0657, date: 18.11.2020) (Clinical Trial registration number: NCT06342518). All participants willingly provided their signed consent to participate in this project. All medical inquiries adhered to the ethical guidelines set forth in the Declaration of Helsinki.

The participants between the ages of 18 and 60 who applied to the university's physical medicine and rehabilitation outpatient clinic with the complaint of elbow pain were assessed for the study. Those who met the criteria of experiencing pain and tenderness in the lateral epicondyle while extending their wrist and fingers against resistance for at least 3 months were included in the study.

Patients who were pregnant or have a coagulation disorder, cervical radiculopathy, peripheral neuropathy, peripheral vasculopathy in the upper extremity, complex regional pain syndrome, local infections, systemic inflammatory disease, fibromyalgia syndrome, arthritis (including rheumatoid arthritis, spondylarthritis, and crystal-induced arthropathies), malignancy, or those who have been treated with corticosteroids, PRP, or autologous blood injection, as well as those who have received physical therapy agents, undergone upper extremity surgical interventions, or had a history of direct trauma to the elbow or a history of fracture, were excluded from the study.

Forty-two patients who met the inclusion criteria were randomized into two groups using a computer-generated random number list: the ESWT group (n=21) and the sham-ESWT control group (n=21) (Figure 1). A wrist resting splint, wrist extensor strengthening and stretching exercises, and ice treatment were administered to both groups. Ensuring proper usage of the resting splint by the patient was confirmed during follow-up visits. The physician instructed the patients on stretching and strengthening exercises for wrist extensors, which they were asked to perform three times a day. Application of ice for 20 min every 3-4 hours during painful periods was recommended. During follow-up visit, patients confirmed their adherence to exercises and recommendations.

Baseline, post-treatment, and 1-month post-treatment assessments were conducted by a blinded researcher. Hand grip strength was measured using a Jamar hand dynamometer. Measurements were made while the patients were sitting in a chair with their arms supported, shoulder in adduction and neutral position, elbow in 90° flexion, forearm in neutral position, and wrist in 0-30° extension and 0-15° ulnar deviation position, and the average measurement was recorded. Pain severity was evaluated using the visual analog scale (VAS), which was scored from 0 (no pain) to 10 (extremely severe). Functionality was assessed using the Patient-rated Tennis Elbow Evaluation (PRTEE), quality of life was measured using the Short Form-12 (SF-12), deep muscular tissue sensitivity was measured using the pain pressure threshold (PPT), and the thickness of the CET was measured sonographically.

ESWT Protocol

The ESWT group received rESWT on the painful lateral epicondyle once per week for 3 sessions, with 2000 pulses at a frequency of 10 Hz. A gel was used at the interface, and the air pressure was set at 1.8 bar per session.

The sham-ESWT group also received sham-rESWT on the painful lateral epicondyle once per week for 3 sessions, but without actual contact of the applicator. To enhance the illusion of treatment, a gel was applied, and the device emitted a sound at every shock. Throughout the study, the patient, the physician responsible for the patient's assessment, and the physician conducting the USG evaluation remained unaware of the patient's assigned group.

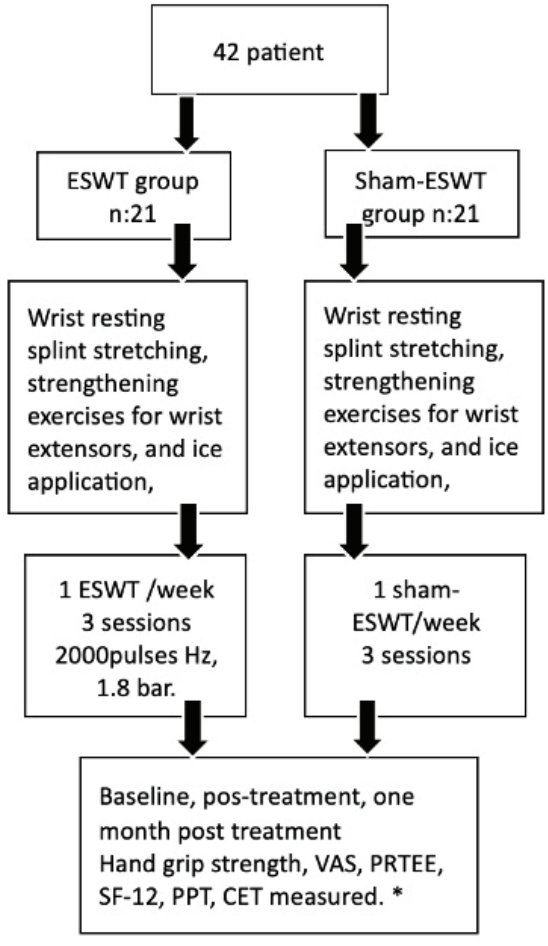

Figure 1. Flow diagram of the study.

VAS: Visual analog scale, PRTEE: Functionality was assessed using the Patient-rated Tennis Elbow Evaluation, SF-12: Quality of life was measured using the Short Form-12, PPT: Pain pressure threshold, CET: Common extensor tendon, ESWT: Extracorporeal shock wave therapy

Ultrasonographic Evaluation

The extensor digitorum, extensor carpi ulnaris, extensor digiti minimi, and extensor radialis brevis tendons join the anterior portion of the lateral epicondyle of the humerus to form the CET. Ultrasonographic examination of tendinosis in the CET typically reveals thickening of the tendon, focal hypoechoic areas, peritendinous fluid, linear intrasubstance tears, bone irregularities, calcifications, enteropathies, and diffuse tendon heterogeneity[20]. During USG for LE, the elbow is positioned at 90° of flexion and the wrist is in pronation. The USG probe is placed longitudinally on the radial surface of the elbow (Figure 2)[20]. The CET thickness is measured.

Statistical Analysis

Statistical analyses were performed using SPSS software version 25.0 (IBM Corp., Chicago, IL). Descriptive statistics are presented as mean ± standard deviation (range) for continuous variables, whereas frequency values (number of cases) are reported for categorical variables. The Mann-Whitney U test was used to evaluate differences between groups for continuous variables due to the non-normal distribution of the data. Within-group comparisons of continuous variables across different time periods were performed using the Wilcoxon signed-rank test. A significance level of $p<0.05$ was considered statistically significant.

Figure 2. Ultrasonographic measurement of common extensor tendon thickness.

RESULTS

This study included 42 patients diagnosed with chronic LE. Half of the patients received sham-ESWT (n=21) and the other half received ESWT treatment (n=21). The mean age of the patients was 41.40±8.30 years (27-56).

Baseline characteristics of patients in the ESWT and sham-ESWT groups were analyzed separately in Table 1. There were no statistically significant differences observed between the groups with respect to the variables analyzed.

Differences Between the Control Group and ESWT Group

The test scores of the two groups were obtained before treatment, after treatment, and 1 month after treatment.

There was no significant difference in baseline test scores between the control and ESWT groups. However,

Table 1. Baseline data prior to treatment.

	Control group* (n=21)	ESWT group* (n=21)	p-value
Age (years)	41.09±9.17	41.71±7.56	0.81
Gender (F/M)	15/6	12/9	0.34
Side (R/L)	15/6	10/11	0.12
Pain pressure threshold	10.42±5.91	13.57±8.34	0.16
Grip strength	42.23±18.97	54.38±24.57	0.08
Common extensor tendon thickness	5.90±0.94	5.55±1.19	0.30
SF-12 PCS	37.71±8.48	39.42±7.35	0.48
SF-12 MCS	48.80±11.57	49.68±9.59	0.24
VAS	6.71±1.34	7.04±1.43	0.44
PRTEE pain	26.28±7.57	28.42±8.56	0.39
PRTEE function	29.02±7.92	28.23±8.39	0.75
PRTEE total	55.30±14.99	56.66±15.66	0.77

*Mean ± standard deviation. SF-12 PCS: Short Form-12 physical scores, SF-12 MCS: Short Form-12 mental score, VAS: Visual analog scale, PRTEE: Patient-rated Tennis Elbow Evaluation, ESWT: Extracorporeal shock wave therapy

there was a significant difference between the groups, except for the SF-12 physical scores (SF-12 PCS) at the 6th week and 3rd month (Table 2).

While there was no significant difference between the groups in terms of SF-12 PCS score at the beginning and after the treatment, a significant difference was found between the two groups 1 month after the treatment ($p<0.01$) (Table 2).

Differences Between Groups at Baseline, Post-treatment, and 1 Month Post-treatment

Test results obtained at baseline, after treatment, and 1 month after treatment were compared to determine the effect of treatment in the control and ESWT groups.

A statistically significant difference was found between the measurements of PPT, grip strength, SF-12 PCS, VAS, PRTEE pain, PRTEE function, and PRTEE total tests at baseline, post-treatment, and 1 month after treatment in both groups (Table 3).

In the SF-12 mental score test, no statistically significant difference was found between the measurements at the beginning, after treatment, and 1 month after treatment in both groups (Table 3).

In the measurement of CET thickness, there was no statistically significant difference between the measurements at the beginning, after the treatment, and 1 month after the treatment in the control group, whereas a significant difference was found in the ESWT group (Table 3).

DISCUSSION

In this study, we investigated the clinical and ultrasonographic effects of rESWT in patients with LE. LE, commonly known as tennis elbow, is a painful condition that can significantly affect an individual's quality of life and functional capacity[4]. While various treatment modalities have been explored, the use of rESWT in the management of LE has shown promise[17].

This study demonstrated that rESWT has several advantages as a conservative treatment for LE. First, a significant increase in grip strength was observed in the rESWT group compared with the control group, which indicates an improvement in functional capacity. Additionally, the VAS scores for pain significantly decreased in the rESWT group, highlighting its efficacy in pain management. This aligns with the results of the systematic review and meta-analysis conducted by Yao et al.[1]. Their meta-analysis of pain evaluation, including 14 trials with

Table 2. Descriptive statistics and Mann-Whitney U test results.

	Group		Before treatment			After treatment			After 1st month		
		n	Median	IQR	p	Median	IQR	p	Median	IQR	p
PPT	Control	21	10.00	7.00	0.24	13.00	6.00	**<0.001**	14.00	7.50	**<0.001**
	ESWT	21	11.00	13.00		17.00	11.00		20.00	11.00	
Grip strength	Control	21	40.00	17.50	0.10	40.00	22.50	**<0.05**	40.00	22.50	**<0.01**
	ESWT	21	50.00	40.00		50.00	35.00		60.00	37.50	
CET thickness	Control	21	6.00	1.00	0.40	6.00	1.10	**<0.01**	6.00	1.15	**<0.01**
	ESWT	21	5.90	1.55		5.00	1.65		5.00	1.55	
SF-12 PCS	Control	21	40.25	13.36	0.40	40.00	14.84	0.07	40.00	11.75	**<0.01**
	ESWT	21	41.67	13.59		45.03	12.07		50.49	8.02	
SF-12 MCS	Control	21	50.85	19.29	0.21	46.60	18.78	**<0.01**	48.68	10.87	**<0.01**
	ESWT	21	51.78	14.17		51.00	8.42		51.68	7.66	
VAS	Control	21	7.00	2.50	0.43	6.00	2.00	**<0.001**	6.00	2.00	**<0.001**
	ESWT	21	7.00	2.00		3.00	2.50		3.00	2.50	
PRTEE pain	Control	21	24.00	12.50	0.43	24.00	9.50	**<0.05**	22.00	9.50	**<0.01**
	ESWT	21	27.00	12.00		17.00	8.00		14.00	10.00	
PRTEE function	Control	21	32.00	14.75	0.68	29.00	13.50	**<0.01**	29.00	14.00	**<0.001**
	ESWT	21	32.00	12.00		18.50	17.00		16.00	16.00	
PRTEE total	Control	21	55.00	25.75	0.82	55.00	19.50	**<0.01**	52.00	20.00	**<0.001**
	ESWT	21	60.00	25.50		33.50	25.00		27.00	24.00	

PPT: Pain pressure threshold, CET: Common extensor tendon, SF-12 PCS: Short Form-12 physical scores, SF-12 MCS: Short Form-12 mental score, VAS: Visual analog scale, PRTEE: Patient-rated Tennis Elbow Evaluation, IQR: Interquartile range, ESWT: Extracorporeal shock wave therapy

Table 3. Descriptive statistics and Wilcoxon signed-rank test and Friedman test results.

	Measurement	n	Control group			n	ESWT group		
			Median	IQR	p		Median	IQR	p
PPT	Before treatment	21	10.00[a]	7.00	**<0.001**	21	11.00[a]	13.00	**<0.001**
	After treatment	21	13.00	6.00		21	17.00[b]	11.00	
	After 1st month	21	14.00[c]	7.50		21	20.00[c]	11.00	
Grip strength	Before treatment	21	40.00[a]	17.50	**<0.01**	21	50.00[a]	40.00	**<0.001**
	After treatment	21	40.00	22.50		21	50.00[b]	35.00	
	After 1st month	21	40.00	22.50		21	60.00[c]	37.50	
CET thickness	Before treatment	21	6.00	1.00	0.58	21	5.90[a]	1.55	**<0.001**
	After treatment	21	6.00	1.10		21	5.00	1.65	
	After 1st month	21	6.00	1.15		21	5.00[c]	1.55	
SF-12 PCS	Before treatment	21	40.25[a]	13.36	**<0.01**	21	41.67[a]	13.59	**<0.001**
	After treatment	21	40.00	14.84		21	45.03[b]	12.07	
	After 1st month	21	40.00[c]	11.75		21	50.49[c]	8.02	
SF-12 MCS	Before treatment	21	50.85	19.29	1.00	21	51.78	14.17	0.11
	After treatment	21	46.60	18.78		21	51.00	8.42	
	After 1st month	21	48.68	10.87		21	51.68	7.66	
VAS	Before treatment	21	7.00[a]	2.50	**<0.001**	21	7.00[a]	2.00	**<0.001**
	After treatment	21	6.00	2.00		21	3.00[b]	2.50	
	After 1st month	21	6.00[c]	2.00		21	3.00[c]	2.50	
PRTEE pain	Before treatment	21	24.00[a]	12.50	**<.001**	21	27.00[a]	12.00	**<0.001**
	After treatment	21	24.00	9.50		21	77.00[b]	8.00	
	After 1st month	21	22.00[c]	9.50		21	14.00[c]	10.00	
PRTEE function	Before treatment	21	32.00[a]	14.75	**<.001**	21	32.00[a]	12.00	**<0.001**
	After treatment	21	29.00	13.50		21	18.50[b]	17.00	
	After 1st month	21	29.00[c]	14.00		21	16.00[c]	16.00	
PRTEE total	Before treatment	21	55.00[a]	25.75	**<.001**	21	60.00[a]	25.50	**<0.001**
	After treatment	21	55.00[b]	19.50		21	33.50[b]	25.00	
	After 1st month	21	52.00[c]	20.00		21	27.00[c]	24.00	

[a]Before and after treatment (p<0.05), [b]After treatment and 1 month after treatment (p<0.05), [c]Before treatment and 1 month after treatment (p<0.05). PPT: Pain pressure threshold, CET: Common extensor tendon, SF-12 PCS: Short Form-12 physical scores, SF-12 MCS: Short Form-12 mental score, VAS: Visual analog scale, PRTEE: Patient-rated Tennis Elbow Evaluation, IQR: Interquartile range, ESWT: Extracorporeal shock wave therapy

950 patients, revealed significantly lower VAS scores in the ESWT group than in the other therapies. Additionally, the meta-analysis of grip strength, encompassing eight articles with 458 patients, demonstrated a significant increase in grip strength among patients receiving ESWT. Overall, their pooled results suggest that ESWT leads to better long-term grip strength improvement and faster pain relief. when compared to alternative therapies[1].In a study by Özmen et al.[19] on 40 patients diagnosed with LE, they divided the patients into three groups. Clinical and sonographic comparisons were made between the effects of kinesio taping, ESWT, and ultrasound therapy. While pain significantly decreased in all groups, grip strength only increased in the kinesio taping group. PRTEE scores significantly decreased in all groups by the 8th week. CET thickness significantly decreased only in the ESWT group. Although there was no superiority among the groups, the significant reduction in pain and decrease in CET thickness in LE with ESWT are consistent with our study results[19].Utilization of USG findings as an effective tool for assessing outcomes was also aimed in our study. The advancement of technology has magnified the significance of incorporating radiological images into the diagnostic process, and the diagnostic validity of musculoskeletal USG in LE has been a subject of extensive research[9,21]. In this context, a review conducted by Dones et al.[21], which included a meta-analysis of 15 studies, stands out. The analysis revealed that gray-scale

USG is advantageous for objectively diagnosing LE. In this analysis, various factors such as hypoechogenicity, calcifications, neovascularity, thickness, enthesopathy, cortical irregularities, cortical spurs, bone changes, cortical irregularities, partial tears, and full tears were also individually assessed for statistical analysis. Among the various changes examined, hypoechogenicity emerged as the key diagnostic finding with the highest sensitivity and specificity, whereas significant differences in thickness were also observed. According to the meta-analysis, the sensitivity of thickness was 0.51 (0.47-0.55) and the specificity was 0.80 (0.75-0.84)[21]. Although its sensitivity may not be sufficiently high for exclusive diagnostic purposes, its remarkable specificity is notable. Furthermore, our study detected a significant reduction in tendon thickness following treatment. This aligns with the results of the meta-analysis, and our research provides promising evidence for the use of tendon thickness as a radiological indicator of recovery in LE. This raises hope for future assessments of treatment effectiveness.

However, it is essential to acknowledge the limitations of this study, including the relatively small sample size and short follow-up period. Future research with larger cohorts and longer-term follow-up is needed to further explore the efficacy and safety of rESWT in treating LE. Additionally, more extensive investigations should be conducted to establish a stronger correlation between USG findings and clinical scores, potentially providing valuable information for predicting disease prognosis and treatment outcomes.

CONCLUSION

In conclusion, this study suggests that rESWT is a promising treatment modality for LE, offering benefits in terms of grip strength improvement and pain reduction. The use of USG as a diagnostic tool in LE assessment and treatment monitoring has been reinforced by the findings of previous studies. It provides valuable insights for further research to expand the understanding of rESWT's role in LE management and the potential implications of USG findings on disease prognosis and healing time.

Acknowledgement: We would like to give our special thanks to Prof. Dr. Afitap Icagasioglu for her support, and supervision.

Ethics

Ethics Committee Approval: This study was approved by the Istanbul Medeniyet University Goztepe Training and Research Hospital Clinical Research Ethics Committee (decision no: 2020/0657, date: 18.11.2020).

Informed Consent: All participants willingly provided their signed consent to participate in this project.

Author Contributions

Surgical and Medical Practices: S.M., B.D.K., M.Z., Concept: S.M., B.D.K., M.Z., Design: S.M., B.D.K., M.Z., Data Collection and/or Processing: S.M., B.D.K., M.Z., Analysis and/or Interpretation: S.M., B.D.K., M.Z., Literature Search: S.M., B.D.K., M.Z., Writing: S.M., B.D.K., M.Z.

Conflict of Interest: The authors have no conflict of interest to declare.

Financial Disclosure: The authors declared that this study has received no financial support.

REFERENCES

1. Yao G, Chen J, Duan Y, Chen X. Efficacy of Extracorporeal Shock Wave Therapy for Lateral Epicondylitis: A Systematic Review and Meta-Analysis. Biomed Res Int. 2020;2020:2064781.
2. Trentini R, Mangano T, Repetto I, et al. Short- to mid-term follow-up effectiveness of US-guided focal extracorporeal shock wave therapy in the treatment of elbow lateral epicondylitis. Musculoskelet Surg. 2015;99(Suppl 1):91-7.
3. Gündüz R, Malas FÜ, Borman P, Kocaoğlu S, Özçakar L. Physical therapy, corticosteroid injection, and extracorporeal shock wave treatment in lateral epicondylitis. Clinical and ultrasonographical comparison. Clin Rheumatol. 2012;31:807-12.
4. Ahmad Z, Siddiqui N, Malik SS, Abdus-Samee M, Tytherleigh-Strong G, Rushton N. Lateral epicondylitis: a review of pathology and management. Bone Joint J. 2013;95:1158-64.
5. Zwerus EL, Somford MP, Maissan F, Heisen J, Eygendaal D, van den Bekerom MP. Physical examination of the elbow, what is the evidence? A systematic literature review. Br J Sports Med. 2018;52:1253-60.
6. Gorski JM. Evaluation of Sleep Position for Possible Nightly Aggravation and Delay of Healing in Tennis Elbow. J Am Acad Orthop Surg Glob Res Rev. 2019;3:e082.
7. Kim GM, Yoo SJ, Choi S, Park YG. Current Trends for Treating Lateral Epicondylitis. Clin Shoulder Elb. 2019;22:227-34.
8. Bot SD, van der Waal JM, Terwee CB, van der Windt DA, Bouter LM, Dekker J. Course and prognosis of elbow complaints: a cohort study in general practice. Ann Rheum Dis. 2005;64:1331-6.
9. du Toit C, Stieler M, Saunders R, Bisset L, Vicenzino B. Diagnostic accuracy of power Doppler ultrasound in patients with chronic tennis elbow. Br J Sports Med. 2008;42:872-6.
10. Levin D, Nazarian LN, Miller TT, et al. Lateral epicondylitis of the elbow: US findings. Radiology. 2005;237:230-4.
11. Palaniswamy V, Ng SK, Manickaraj N, et al. Relationship between ultrasound detected tendon abnormalities, and sensory and clinical characteristics in people with chronic lateral epicondylalgia. PLOS ONE. 2018;13:e0205171.
12. Clarke AW, Ahmad M, Curtis M, Connell DA. Lateral elbow tendinopathy: correlation of ultrasound findings with pain and functional disability. Am J Sports Med. 2010;38:1209-14.

13. Krogh TP, Fredberg U, Stengaard-Pedersen K, Christensen R, Jensen P, Ellingsen T. Treatment of lateral epicondylitis with platelet-rich plasma, glucocorticoid, or saline: a randomized, double-blind, placebo-controlled trial. Am J Sports Med. 2013;41:625-35.
14. Bowen RE, Dorey FJ, Shapiro MS. Efficacy of nonoperative treatment for lateral epicondylitis. Am J Orthop (Belle Mead NJ). 2001;30:642-6.
15. Auersperg V, Trieb K. Extracorporeal shock wave therapy: an update. EFORT Open Rev. 2020;5:584-92.
16. Wang CJ, Wang FS, Yang KD, et al. Shock wave therapy induces neovascularization at the tendon-bone junction. A study in rabbits. J Orthop Res. 2003;21:984-9.
17. Karaca İ, Gül H, Erel S. Comparison of extracorporeal shock wave therapy and high-intensity laser therapy on pain, grip strength, and function in patients with lateral epicondylalgia: a randomized controlled study. Lasers Med Sci. 2022;37:3309-17.
18. Aldajah S, Alashram AR, Annino G, Romagnoli C, Padua E. Analgesic Effect of Extracorporeal Shock-Wave Therapy in Individuals with Lateral Epicondylitis: A Randomized Controlled Trial. 2022;7.29.
19. Özmen T, Koparal SS, Karataş Ö, Eser F, Özkurt B, Gafuroğlu TÜ. Comparison of the clinical and sonographic effects of ultrasound therapy, extracorporeal shock wave therapy, and Kinesio taping in lateral epicondylitis. Turk J Med Sci. 2021;51:76-83.
20. Obuchowicz R, Bonczar M. Ultrasonographic Differentiation of Lateral Elbow Pain. Ultrasound Int Open. 2016;2:38-46.
21. Dones VC 3rd, Grimmer K, Thoirs K, Suarez CG, Luker J. The diagnostic validity of musculoskeletal ultrasound in lateral epicondylalgia: a systematic review. BMC Med Imaging. 2014;14:10.

DOI: 10.4274/MMJ.galenos.2024.55060
Medeni Med J 2024;39:117-121

Original Article

Correlation Between Vestibular Disorders and Superior Semicircular Dehiscence on High-resolution Computed Tomography at Tam Anh Ho Chi Minh General Hospital

Tam Anh Ho Chi Minh Genel Hastanesi'nde Yüksek Çözünürlüklü Bilgisayarlı Tomografide Vestibüler Bozukluklar ve Superior Semisirküler Dehissans Arasındaki Korelasyon

Cong Trinh TRAN[1], Thi Lan Huong LE[1], Tran Thi Thuy HANG[1], Nghi Hai MA[2], Ho Hoang PHUONG[1], Tran Phanchung THUY[3]

[1]Tam Anh Ho Chi Minh City General Hospital, Ho Chi Minh City, Vietnam
[2]Vietnamese Society of Otorhinolaryngology, Ho Chi Minh City, Vietnam
[3]Vietnam National University Ho Chi Minh City, School of Medicine, Ho Chi Minh City, Vietnam

ABSTRACT

Objective: Superior semicircular canal dehiscence (SSCD) is a pathologic condition within the inner ear characterized by various vestibular manifestations. Numerous studies have reported an incidence rate of SSCD ranging from 3.6% to 9% in the general population. The objective of this medical study was to evaluate the prevalence of superior SSCD and investigate its correlation with vestibular symptoms among patients who underwent high-resolution computed tomography (HRCT) scans. To the best of our knowledge, there is limited research and awareness regarding SSCD in Vietnam. In addition, the secondary aim of our investigation is to assess the prevalence of SSCD in Vietnam and compare it with findings from previous studies worldwide.

Methods: This retrospective study was conducted at Tam Anh Ho Chi Minh General Hospital from March 2022 to February 2024. Medical records and HRCT scans of the patients were collected. Patients were categorized into two groups: those with and without vestibular disorders. SSCD was defined as the absence of bone overlying the superior semicircular canal facing toward the dura of the middle cranial fossa. Statistical analysis was performed to determine the correlation between vestibular symptoms and the presence of SSCD.

Results: A total of 362 patients (including 151 men and 211 women) were recruited. The prevalence of SSCD was 10.2% according to the HRCT scan results. The study found that 18.33% of patients with vestibular disorders had SSCD on HRCT scans, whereas only 6.2% of patients without vestibular disorders exhibited SSCD, indicating a significant association (p-value <0.001).

Conclusions: These findings highlight the importance of considering SSCD as a potential etiology in patients presenting with vestibular symptoms and emphasize the diagnostic utility of HRCT.

Keywords: Vestibular disorders, superior semicircular canal dehiscence (SSCD), high-resolution computed tomography (HRCT)

ÖZ

Amaç: Superior semisirküler kanal dehisansı (SSKD), iç kulakta çeşitli vestibüler belirtilerle karakterize patolojik bir durumdur. Çok sayıda çalışma, genel popülasyonda %3,6 ila %9 arasında değişen bir SSKD insidans oranı bildirmiştir. Bu tıbbi çalışmanın amacı, yüksek çözünürlüklü bilgisayarlı tomografi (YÇBT) taramaları yapılan hastalarda SSKD prevalansını değerlendirmek ve vestibüler semptomlarla korelasyonunu araştırmaktır. Bildiğimiz kadarıyla, Vietnam'da SSKD ile ilgili sınırlı araştırma ve farkındalık bulunmaktadır. Buna ek olarak, araştırmamızın ikincil amacı Vietnam'da SSKD prevalansını değerlendirmek ve bunu dünya çapında daha önce yapılan çalışmalardan elde edilen bulgularla karşılaştırmaktır.

Yöntemler: Bu retrospektif çalışma Tam Anh Ho Chi Minh Genel Hastanesi'nde Mart 2022 ile Şubat 2024 tarihleri arasında gerçekleştirildi. Hastaların tıbbi kayıtları ve YÇBT taramaları toplandı. Hastalar iki gruba ayrıldı: Vestibüler bozukluğu olan ve olmayanlar. SSKD, orta kraniyal fossanın durasına doğru bakan superior semisirküler kanalın üzerinde kemik yokluğu olarak tanımlandı. Vestibüler semptomlar ile SSKD varlığı arasındaki korelasyonu belirlemek için istatistiksel analiz yapıldı.

Bulgular: Toplam 362 hasta (151 erkek ve 211 kadın) çalışmaya dahil edildi. YÇBT tarama sonuçlarına göre SSKD prevalansı %10,2 idi. Çalışmada, vestibüler bozukluğu olan hastaların %18,33'ünde YÇBT taramalarında SSKD bulunurken, vestibüler bozukluğu olmayan hastaların yalnızca %6,2'sinde SSKD görüldü ve bu da anlamlı bir ilişkiye işaret etmektedir (p-değeri <0,001).

Sonuçlar: Bu bulgular, vestibüler semptomlarla başvuran hastalarda SSKD'nin potansiyel bir etiyoloji olarak değerlendirilmesinin önemini ve YÇBT'nin tanısal faydasını vurgulamaktadır.

Anahtar kelimeler: Vestibüler bozukluklar, superior semisirküler kanal dehissansı (SSKD), yüksek çözünürlüklü bilgisayarlı tomografi (YÇBT)

Address for Correspondence: T. P. Thuy, Vietnam National University Ho Chi Minh City, School of Medicine, Ho Chi Minh City, Vietnam
E-mail: drthuytranent@gmail.com **ORCID ID:** orcid.org/0009-0002-1154-2262

Received: 04 April 2024
Accepted: 28 May 2024
Online First: 12 June 2024

Cite as: Tran CT, Le TLH, Hang TTT, Ma NH, Phuong HH, Thuy TP. Correlation Between Vestibular Disorders and Superior Semicircular Dehiscence on High-resolution Computed Tomography at Tam Anh Ho Chi Minh General Hospital. Medeni Med J 2024;39:117-121

INTRODUCTION

Superior semicircular canal dehiscence (SSCD) refers to an osseous arch defect of the superior semicircular canal[1], first described by Minor et al.[2] in 1998, and is associated with vestibular syndrome, presenting symptoms such as vertigo, dizziness, lightheadedness, tinnitus, hearing loss, and vertigo induced by loud sounds, known as the Tullio phenomenon[3]. These manifestations arise due to an abnormal opening in the osseous roof of the canal, creating a "third window" phenomenon with aberrant sound conduction and pressure dynamics[4]. Diagnosis involves audiometric evaluation, vestibular assessment, and identification on temporal bone computed tomography (CT)[5] and supports management strategies such as pharmacotherapy or surgical intervention[6]. While autopsy studies indicate a low prevalence of SSCD (0.5%)[7], imaging studies report higher rates (3.0% to 9.0%)[8-12], underscoring the sensitivity of CT in detecting SSCD. Incidental findings of canal dehiscence in asymptomatic individuals prompt investigations into its association with vestibular dysfunction. Consequently, CT imaging is recommended for patients with vestibular symptoms to facilitate early detection and management[1]. However, research and awareness regarding SSCD remain limited in Vietnam. The objectives of this study were to assess the incidence and features of SSCD using high-resolution computed tomography (HRCT) and to evaluate the relationship between SSCD and vestibular disorder symptoms.

MATERIALS and METHODS

The study was conducted at Tam Anh Ho Chi Minh General Hospital and received ethics approval from Tam Anh General Hospital, Ho Chi Minh City Review Board (reg. no: 371/CV- TAHCM, date: 25.03.2024).

Study and Patients

This retrospective study, conducted at Tam Anh General Hospital in Ho Chi Minh City between June 2023 and January 2024, included all patients visiting the Otorhinolaryngology Department who underwent HRCT scans of the temporal bone. Participants of all ages who underwent temporal bone CT scans had their comprehensive data documented within the electronic medical record system (Hsoft). The exclusion criteria comprised patients not undergoing CT scans following high-resolution temporal bone protocols, the visualization of the semicircular canal being obscured due to pathological conditions or foreign bodies or insufficient clinical information within the dataset. Sample size calculation, based on a significance level of 0.05 and previous research by Williamson et al.[12] in 2003, indicated a minimum requirement of 125 patients. However, our retrospective examination of electronic medical records reviewed a total of 362 patients. CT scans were performed using 32, 128, and 768-slice CT scanners from Siemens Healthcare, Germany, with a slice thickness of ≤1 mm, distance of 0.375 mm, 120 kV (peak), 195 mA, pitch of 0.53, bone window, and matrix of 512x512. image acquisition was conducted in the axial plane with coronal orientation reconstructions (≤1 mm thick, ≤1 mm distance), chosen as previous studies have demonstrated their adequacy in accurately determining the dehiscence of the superior semicircular canal (Figure 1,2) compared with the reconstructions according to the planes of Stenver (Figure 3) and Poschl (Figure 4)[5].

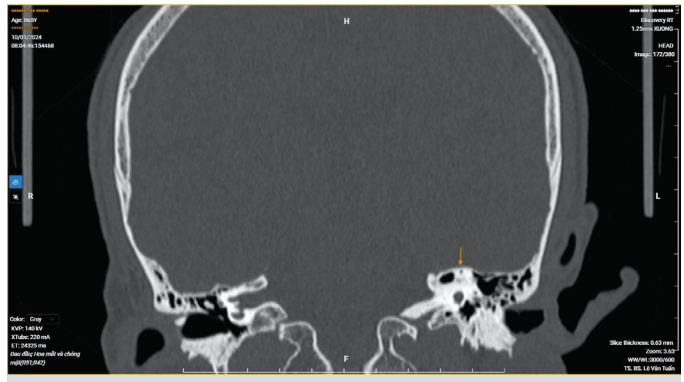

Figure 1. The superior semicircular canal appears intact. Coronal reconstruction of the temporal bone CT scan demonstrates an intact bony roof of the superior semicircular canal (arrow).

CT: Computed tomography

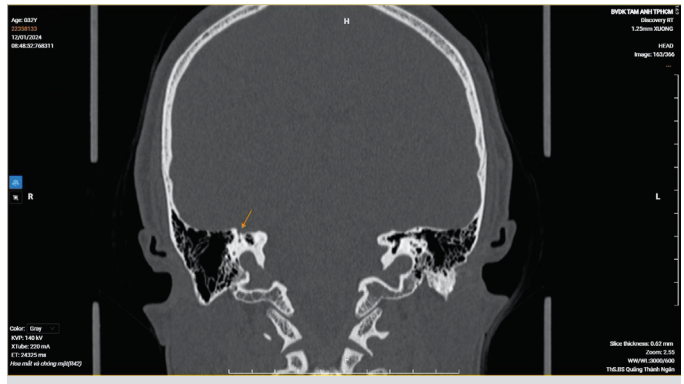

Figure 2. Superior semicircular canal dehiscence. Coronal reconstruction of the temporal bone CT scan in another patient reveals the absence of the bony roof of the superior semicircular canal (arrow).

CT: Computed tomography

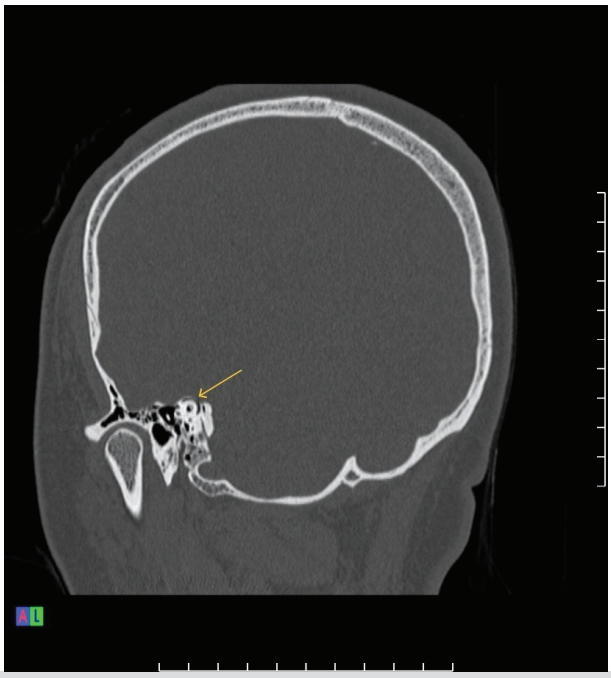

Figure 3. Superior semicircular canal dehiscence in Stenvers view. Coronal CT reconstruction in the Stenvers plane of the same patient reveals a defect in the bony roof of the superior semicircular canal (arrow).

CT: Computed tomography

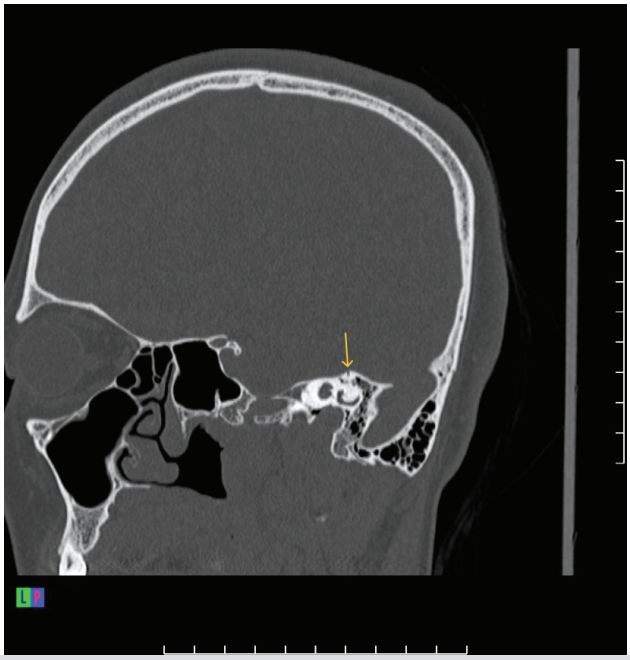

Figure 4. Superior semicircular canal dehiscence in Pöschl view. Coronal CT reconstruction in the Pöschl plane of the same patient reveals a defect in the bony roof of the superior semicircular canal (arrow).

CT: Computed tomography

Data Collection

Electronic medical records were accessed to gather patient data along with HRCT imaging details. Following the interpretation of the scan results, subjects were categorized into two groups based on symptomatology: those exhibiting symptoms aligning with vestibular syndrome, as indicated by the International Classification of Diseases (ICD) code H81 documented by clinicians, and those lacking symptoms indicative of vestibular syndrome, as per the ICD code (patients without vestibular syndrome). Symptoms such as vertigo, dizziness, lightheadedness, tinnitus, hearing loss, and acoustic vertigo (Tullio phenomenon) were deemed consistent with vestibular syndrome.

Statistical Analysis

In our study, we determined the prevalence of radiologic SSCD in both asymptomatic and symptomatic patient cohorts and estimated 95% confidence intervals using the Newcombe method for extreme percentages. To assess differences between these patient groups, we employed the Fisher Exact test for categorical variables and the Student t-test for continuous variables. We set a significance threshold of $p<0.05$ for all statistical tests. These calculations were executed using the Rstudio programing environment.

RESULTS

Information from 365 patients was recorded at Tam Anh General Hospital between June 2023 and January 2024, resulting in the following findings:

Population Demographics

In our study, the median age was determined to be 45.7±18.6 years, with the youngest participant being 1 year old and the oldest being 89 years old. Females constituted 58.3% of the cohort, whereas males comprised 41.7%. No significant age discrepancy was observed between genders, with a median age of 45 years for males and 46.2 years for females. The study population was categorized into two groups: 120 cases (33.1%) presenting with vestibular syndrome and 242 cases (66.9%) without vestibular syndrome. Upon comparison of ages, it was noted that individuals without vestibular syndrome were younger than those with vestibular syndrome, with median ages of 43.7±19.4 years and 49.8±16.5 years ($p=0.003$). Among the 120 cases exhibiting vestibular syndrome, symptoms included dizziness in 75% (90 cases), hearing loss in 16.67% (20 cases), tinnitus in 6.67% (8 cases), dizziness in 0.83% (1 case), and vestibular disorders in 0.83% (1 case).

Prevalence of Superior Semicircular Canal Dehiscence and its Association with Vestibular Syndrome

In our study, the prevalence of SSCD was found to be 10.2% (37 of 362 cases). Among these cases, the incidence of SSCD in the group presenting with vestibular syndrome was 18.3% (22 out of 120 cases), whereas it was 6.2% (15 out of 242 cases) in the group without vestibular syndrome, as shown in Table 1. Notably, the prevalence of SSCD was nearly three times higher in individuals with vestibular syndrome than in those without (p=0.001), demonstrating a statistically significant difference, as shown in Table 2. Gender-based analysis revealed no significant variation in SSCD prevalence. Furthermore, no association between SSCD and age was observed. However, within the vestibular syndrome group, the presence of SSCD was significantly associated with dizziness (p<0.001).

DISCUSSION

The prevalence of SSCD in our study was found to be 10.2% (37 out of 362 patients), which aligns closely with the reported frequency of 9% in a study conducted by Williamson et al.[12]. Despite a higher representation of females in our study cohort (58.3% vs. 41.7%), no significant association was observed between the occurrence of SSCD and gender, consistent with prior research findings.

Among patients presenting with vestibular syndrome, the prevalence of SSCD detected via HRCT was 18.3%, resembling the findings reported by Ghany and Osman[13] who identified SSCD in 28 patients through HRCT scans. In contrast, Berning et al.[14] examined 610 patients, including 500 asymptomatic and 110 symptomatic individuals, who underwent HRCT scans, revealing a prevalence of 13.6% among those with vestibular symptoms and 2% among those without. Our study demonstrated a higher frequency of SSCD among symptomatic patients compared with that reported by Berning et al.[14], which may be attributed to differences in sample size and patient population characteristics.

In patients without vestibular syndrome, the prevalence of SSCD detected via HRCT was 6.3%, similar to the findings reported by Nadgir et al.[10]. However, our study revealed a higher prevalence of SSCD among asymptomatic individuals compared with Crovetto et al.'s[15] study, which reported a frequency of 3.6%. These variations could be influenced by differences in sample size and demographic factors among the study populations.

Our retrospective analysis revealed a significantly higher prevalence of SSCD among patients with vestibular syndrome (18.3%) than among those without (6.2%), with a statistically significant difference (p<0.001).

Consequently, we recommend that patients presenting with vestibular symptoms, particularly dizziness, undergo HRCT scanning to assess for SSCD.

Table 1. Comparison of superior semicircular canal dehiscence rates between groups with and without vestibular syndrome.

	SSCD		p-value (x^2)	OR (CI 95%)
	Present (n=37)	Absent (n=325)		
Symptomatic	18.3% (22)	6.2% (98)	0.001	2.95
Asymptomatic	81.7% (15)	93,8% (227)		

SSCD: Superior semicircular canal dehiscence, OR: Odds ratio, CI: Confidence interval

Table 2. Correlation between superior semicircular canal dehiscence and symptoms in the vestibular syndrome groups.

	SSCD		p-value (x^2)
	Present (n=22)	Absent (n=98)	
Dizziness	86.3% (19)	72.4% (71)	<0.001
Hearing loss	9% (2)	18.5% (18)	1
Tinnitus	4.7% (1)	7.1% (7)	1
Lightheadedness	0% (0)	1% (1)	1
Vestibular disorders	0% (0)	1% (1)	1

SSCD: Superior semicircular canal dehiscence

However, our study has several limitations inherent to its retrospective design, potentially leading to incomplete data collection and misclassification of patients with vestibular symptoms. In addition, the diverse clinical manifestations of SSCD and the possibility of other conditions mimicking its symptoms necessitate cautious interpretation of HRCT findings. Moreover, the ratio of SSCD cases to temporal bone HRCT scans in patients with vestibular syndrome should be interpreted with caution because of the relatively small sample size.

CONCLUSION

The prevalence of SSCD detected via HRCT in our study did not differ significantly from prior research findings. Radiologists should remain vigilant in identifying this pathology during temporal bone HRCT imaging, particularly when it is correlated with clinical symptoms. Ultimately, we advocate the inclusion of HRCT scans in the diagnostic workup of patients presenting with vestibular syndrome, especially those experiencing symptoms such as dizziness. This approach facilitates the detection and evaluation of SSCD.

Ethics

Ethics Committee Approval: The study was conducted at Tam Anh Ho Chi Minh General Hospital and received ethics approval from Tam Anh General Hospital, Ho Chi Minh City Review Board (reg. no: 371/CV- TAHCM, date: 25.03.2024).

Informed Consent: Retrospective study.

Author Contributions

Surgical and Medical Practices: C.T.T., T.P.T., Concept: C.T.T., H.H.P., T.P.T., Design: C.T.T., H.H.P., T.P.T., Data Collection and/or Processing: C.T.T., T.L.H.L., T.T.T.H., N.H.M., H.H.P., T.P.T., Analysis and/or Interpretation: C.T.T., T.L.H.L., T.T.T.H., N.H.M., H.H.P., T.P.T., Literature Search: C.T.T., T.L.H.L., T.T.T.H., N.H.M., H.H.P., T.P.T., Writing: C.T.T., T.L.H.L., T.T.T.H., H.H.P., T.P.T.

Conflict of Interest: The authors have no conflict of interest to declare.

Financial Disclosure: The authors declared that this study has received no financial support.

REFERENCES

1. Bhatt AA, Lundy LB, Middlebrooks EH, Vibhute P, Gupta V, Rhyner PA. Superior Semicircular Canal Dehiscence : Covering Defects in Understanding from Clinical to Radiologic Evaluation. Clin Neuroradiol. 2021;31:933-41.
2. Minor LB, Solomon D, Zinreich JS, Zee DS. Sound- and/or pressure-induced vertigo due to bone dehiscence of the superior semicircular canal. Arch Otolaryngol Head Neck Surg, 1998;124:249-58.
3. Watson SR, Halmagyi GM, Colebatch JG. Vestibular hypersensitivity to sound (Tullio phenomenon): structural and functional assessment. Neurology. 2000;54:722-8.
4. Rosowski JJ, Songer JE, Nakajima HH, Brinsko KM, Merchant SN. Clinical, experimental, and theoretical investigations of the effect of superior semicircular canal dehiscence on hearing mechanisms. Otol Neurotol. 2004;25:323-32.
5. Branstetter BF 4th, Harrigal C, Escott EJ, Hirsch BE. Superior semicircular canal dehiscence: oblique reformatted CT images for diagnosis. Radiology. 2006;238:938-42.
6. Minor LB. Clinical manifestations of superior semicircular canal dehiscence. Laryngoscope. 2005;115:1717-27.
7. Carey JP, Minor LB, Nager GT. Dehiscence or thinning of bone overlying the superior semicircular canal in a temporal bone survey. Arch Otolaryngol Head Neck Surg. 2000;126:137-47.
8. Gartrell BC, Gentry LR, Kennedy TA, Gubbels SP. Radiographic features of superior semicircular canal dehiscence in the setting of chronic ear disease. Otol Neurotol. 2014;35:91-6.
9. Masaki Y. The prevalence of superior canal dehiscence syndrome as assessed by temporal bone computed tomography imaging. Acta Otolaryngol. 2011;131:258-62.
10. Nadgir RN, Ozonoff A, Devaiah AK, Halderman AA, Sakai O. Superior semicircular canal dehiscence: congenital or acquired condition? AJNR Am J Neuroradiol. 2011;32: 947-9.
11. Stimmer H, Hamann KF, Zeiter S, Naumann A, Rummeny EJ. Semicircular canal dehiscence in HR multislice computed tomography: distribution, frequency, and clinical relevance. Eur Arch Otorhinolaryngol. 2012;269:475-80.
12. Williamson RA, Vrabec JT, Coker NJ, Sandlin M. Coronal computed tomography prevalence of superior semicircular canal dehiscence. Otolaryngol Head Neck Surg. Coronal computed tomography prevalence of superior semicircular canal dehiscence. Otolaryngol Head Neck Surg. 2003;129:481-9.
13. Ghany AFA, Osman NM. Superior Semicircular Canal Dehiscence: A Missed Finding in Temporal Bone Multidetector CT Scans in Symptomatic Patients Presenting with Vertigo. Int Adv Otol. 2011;7:157-64.
14. Berning AW, Arani K, Branstetter BF 4th. Prevalence of Superior Semicircular Canal Dehiscence on High-Resolution CT Imaging in Patients without Vestibular or Auditory Abnormalities. AJNR Am J Neuroradiol. 2019;40:709-12.
15. Crovetto M, Whyte J, Rodriguez OM, Lecumberri I, Martinez C, Eléxpuru J. Anatomo-radiological study of the Superior Semicircular Canal Dehiscence Radiological considerations of Superior and Posterior Semicircular Canals. Eur J Radiol. 2010;76:167-72.

DOI: 10.4274/MMJ.galenos.2024.53822
Medeni Med J 2024;39:122-131

Review

A Meta-analysis of the Effect of Probiotic *Lactobacillus* sp. as Immunomodulating Inflammatory Responses

Probiyotik Lactobacillus sp.'nin İmmünomodülatör Enflamatuvar Yanıtlar Üzerindeki Etkisinin Meta-analizi

Waode Fifin ERVINA[1,2], Sri Pantja MADYAWATI[3], Iswinarno Doso SAPUTRO[4], Dodi SAFARI[2], Rury Eryna PUTRI[5], Salma ZULQAIDA[1]

[1]Postgraduate School of Universitas Airlangga, Master of Immunology Program, Surabaya, Indonesia
[2]National Research and Innovation Agency, Cibinong, Indonesia
[3]Post Graduate School of Universitas Airlangga, Surabaya, Indonesia
[4]Soetomo General Academic Hospital, Surabaya, Indonesia
[5]Postgraduate School of Universitas Airlangga, Master of Forensic Program, Surabaya, Indonesia

ABSTRACT

Lactobacillus sp. is considered an indispensable probiotic, and this probiotic has an effective role in maintaining the immune system. We evaluated the effect of the probiotic *Lactobacillus* sp. on modulating inflammation in several cases. In collecting the literature, we used databases from the Web of Science, the Cochrane Central Register of Controlled Trials, PubMed, and Embase. Studies that met the inclusion criteria were analyzed using Review Manager (version 5.4). A p-value of <0.05 of the total effect is considered statistically significant. Finally, 1895 references were retrieved and 20 were included in the meta-analysis. This meta-analysis suggested that most cases in this study were healthy elderly who received treatment with *Lactobacillus* sp. *Lactobacillus* sp. has a positive effect on B cells, eosinophils, IgE, NK cells, TNF-α, and IL-10. *Lactobacillus* could regulate the immune system by modulating inflammation in the healthy elderly.

Keywords: Good health and well-being, inflammation response, immune system, *Lactobacillus* sp.

ÖZ

Lactobacillus sp. vazgeçilmez bir probiyotik olarak kabul edilimektedir ve bağışıklık sisteminin korunmasında etkili bir role sahiptir. Çalışmamızda probiyotik *Lactobacillus* sp.'nin çeşitli vakalarda enflamasyonu modüle etme üzerindeki etkisini değerlendirdik. Literatür taramasında Web of Science, Cochrane Central Register of Controlled Trials, PubMed ve Embase veri tabanlarını kullandık. Dahil edilme kriterlerini karşılayan çalışmalar Review Manager (versiyon 5.4) ile analiz edildi. Toplam etkinin p-değerinin <0,05 olması istatistiksel olarak anlamlı kabul edildi. Son olarak, toplam 1895 referansa ulaşıldı ve 20 tanesi meta-analize dahil edildi. Bu meta-analiz, bu çalışmadaki olguların çoğunun *Lactobacillus* sp. ile tedavi gören sağlıklı yaşlılar olduğunu göstermiştir. *Lactobacillus* sp. B hücreleri, eozinofiller, IgE, NK hücreleri, TNF-α ve IL-10 üzerinde olumlu bir etkiye sahiptir ve sağlıklı yaşlılarda enflamasyonu modüle ederek bağışıklık sistemini düzenleyebilir.

Anahtar kelimeler: İyi sağlık ve iyilik hali, enflamasyon yanıtı, bağışıklık sistemi, *Lactobacillus* sp.

INTRODUCTION

Many studies have shown that probiotics, especially *Lactobacillus* sp., play an effective role in maintaining the immune system. This role is evidenced by the interaction between probiotics and commensal organisms in modulating mucosal immune cells or epithelial cells. The number of *Lactobacillus* sp. in the small intestine in adults is small, but this number can be increased through food fermentation assisted by short-chain fatty acids. The amount of microbiota found in feces is small, ranging from 0.01% to 0.6% of total counts[1]. Some *Lactobacilli*, such as *Ligilactobacillus salivarius*, *Lactobacillus rhamnosus*, and *Lacticaseibacillus paracasei*, were also

Address for Correspondence: S.C. Madyawati, Postgraduate School of Universitas Airlangga, Master of Immunology Program, Surabaya, Indonesia
E-mail: sri-p-m@fkh.unair.ac.id **ORCID ID:** orcid.org/0000-0002-5864-439X

Received: 28 March 2024
Accepted: 03 June 2024
Online First: 13 June 2024

Cite as: Ervina WF. Madyawati SP. Saputro ID. Safari D. Putri RE. Zulqaida S. A Meta-analysis of the Effect of Probiotic *Lactobacillus* sp. as Immunomodulating Inflammatory Responses. Medeni Med J 2024;39:122-131

detected in infants with amounts ranging from 10^5 to 10^8 CFU/g[2].

Lactobacillus is a genus of rod-shaped, Gram-positive, non-spore forming, facultatively anaerobic bacteria from the phylum *Firmicutes*[3]. In March 2020, 261 *Lactobacillus* species had been identified and reclassified into 25 genera (including 23 new genera); this was due to their high genotypic, phenotypic, and ecological diversity[4].

Inflammation occurs not only in diseased conditions but also in aging and obesity. Consuming probiotics can modulate inflammation to balance it. Today, the use of probiotics is becoming popular because many studies have proven the benefits of probiotics in modulating human health. *Lactobacillus* has been widely used in both children and the elderly, and probiotics are not only used as a treatment for disease but also as a prevention. One of the probiotics that is often used in research is *Lactobacillus* sp. and *Bifidobacterium* however this study limits the effectiveness of *Lactobacillus* sp. on the immune system, and the mechanism of *Lactobacillus* sp. in modulating the immune system through the gut microbiome is still unknown.

There have been many studies on *Lactobacillus* probiotics with different strains, proving that *Lactobacillus* has great potential for use in human and murine models. While some clinical studies have been negative or inconclusive[5], other studies have shown positive results[6-8]. *Lactobacillus* has shown significant and promising results in treating acute infectious diarrhea and in the prevention of antibiotic-associated diarrhea in human clinical trials[6]. Recent research has examined the use of the probiotic *Lactobacillus* in the treatment and prevention of allergic diseases and allergic rhinitis/asthma. There have been many studies proving the role of *L. rhamnosus GG* in the prevention of atopic eczema or dermatitis[9].

Lactobacillus sp. maintains intestinal homeostasis by stimulating regulatory T-cells to produce interleukin (IL)-10 and increasing the expression in a TLR2-dependent manner, thereby inducing B cell production. In some cases of inflammation, *Lactobacillus* sp. has been shown to significantly influence dendritic cells, thereby activating NK cells. *Lactobacillus* sp. plays a dual role, one of which is inhibiting IkB phosphorylation and degradation, thereby preventing NF-κb translocation which results in decreasing tumor necrosis factor alpha (TNF-α) expression. In allergic cases, *Lactobacillus* sp. inhibits Th2 cytokine production, thereby reducing eosinophil infiltration.

The aim of this meta-analysis study was to analyze whether probiotic *Lactobacillus* sp. affects the modulation of the immune system, especially on B cells, eosinophils, immunoglobulin (Ig)E, NK cells , TNF-α, and IL-10, under inflammatory conditions. This study provides more reliable evidence for clinical decisions.

MATERIALS and METHODS

Study Strategy

Four databases serve as reference sources for this analysis: Cochrane Library , Web of Science, Embase, and PubMed. All basic research from this source takes *Lactobacillus* sp. probiotic intervention against the immune system taken from 1992 to 2022. The keywords used for the literature search are "*Lactobacillus*", "Probiotic", "Immune System", and "Immunity".

Inclusion criteria: (1) clinical study of *Lactobacillus* sp. administered to humans; (2) research using immunological parameters; (3) the data have a mean, standard deviation, and total of samples. Exclusion criteria: (1) meta-analysis studies, reports, reviews, and meeting conclusions; (2) tests on experimental animals, *in vitro* tests, and research other than clinical trials; (3) research without original data; (4) research using prebiotics or other ingredients; (5) non-randomized controlled trials; (6) no measure of immune outcome; (7) not relevant to *Lactobacillus* sp. probiotics and immune system.

Publication bias uses the value from Egger's test; if $p>0.05$, then there is no publication bias. The determination of publication bias fulfills the following requirements: (1) Random sequence generation; (2) allocation concealment; (3) blinding of participants and personnel; (4) blinding of outcome assessments; (5) incomplete outcome data; (6) selective reporting.

Data Collection

The supporting PRISMA 2019 checklist for this study is available as supporting information[10]. Data extracted from journals filtered based on inclusion and exclusion criteria. Some authors independently extracted data, made decisions, and compared their conclusions with those of other studies. If there is a disagreement between studies, a third person (a member of the writing team) is needed to solve the problem through discussion and consultation. During the extraction process of the original data, authentication and reliability are required to avoid bias. Bias caused by the subject will be evaluated as soon as possible. To ensure the reliability of data

extraction and minimize bias and error, the authors conducted systematic training of the experts. The information data obtained from this study were as follows: the type of *Lactobacillus* sp. obtained, the type of disease, and the dose used *Lactobacillus* sp. effect on B cells, NK cells, eosinophils, IgE, IL-10, and TNF-α.

Data Organization and Analysis

Before conducting the meta-analysis, several indicators were standardized. The meta-analysis used Review Manager 5.4 (Cochrane Collaboration Network, London, UK). This study used the Cohen's method, and the effect measure was std. Mean difference. Forest plots were used to detect heterogeneity from the collection of journals obtained. Funnel plots are used for possible publication bias. Sample size, mean difference, and 95% confidence interval (CI) were calculated to analyze the results of the acquired immunological parameters. A p-value <0.05 of the total effect was assumed to be statistically significant. I^2 is an indicator that measures the degree of heterogeneity of the total data obtained. If I^2 <50%, the heterogeneity of the total data obtained is low, so the fixed-effects model is used. Conversely I^2>50%, then the heterogeneity of the total data obtained is high so that it uses a random-effects model.

RESULTS

A total of 1895 references were obtained from the four databases shown in Figure 1. A total of 604 references were excluded because they were not relevant =325, duplications =96, and journal reviews =870. Furthermore, several exclusion criteria from references obtained animal trial results =237, no measure immune outcome =160, not randomized clinical trials =187. This meta-analysis study originally used 20 references; however, 10 references have the same authors and title but different parameters of the immune system in Tables 1, 2. Review Manager 5.4 (Cochrane Collaboration Network, London, UK) was used to perform statistical analysis on six indicators: Eosinophils (five studies), B cells (four studies), IgE (seven studies), NK cells (four studies) TNF-α (six studies), and IL-10 (four studies). The mean difference and 95% CI of these indicators are shown in Figures 2-4.

Effect of the Disease

This meta-analysis pooled studies examining several inflammatory diseases and conditions such as atopic dermatitis[11-13], allergic rhinitis[14-16], Japanese cedar pollinosis[17,18], human immunodeficiency virus (HIV)[19], healthy elderly[20-25], inflammatory bowel disease (IBD)[26], and hypercholesterolaemic adults. Our study shows that the most popular reaction to inflammation was in the healthy elderly.

Effect of Probiotic Species

Lactobacillus probiotics have many strains, the most commonly used of which is *Lactobacillus casei Shirota* (*LcS*)[16,25,27]. In addition, the type of strain used to test the effectiveness of *Lactobacillus* probiotics on the immune system was *Lactobacillus plantarum* CJLP133[11], *L. plantarum* YIT 0132[14], *Lactobacillus acidophilus* strain L-92[15], *Lactobacillus GG* and *Lactobacillus gasseri* TMC0356[17], *L. rhamnosus* GR-1[19], *L. casei* DNl14001[20-28], *L. paracasei* NCC 2461[21], *L. gasseri* TMC0356[22], *Lactobacillus reuteri* DSM 17938[23], *L. salivarius* LS01[13], *L. plantarum* HSK201[18], *L. plantarum* L-137[24], *L. plantarum* ECGC 13110402[29], *Lactobacillus pentosus*[12], *L. rhamnosus* GR-1 and *L. reuteri* RC-14[26], and *L. acidophilus*[30].

Effects of Age

The majority of the population in this study was >50 years old and found in healthy elderly cases[20-25,30]. Meanwhile, in other studies, the population was 1-13 years old[11,12] and 18-45 years old[13,15,16,18,27].

Effect of Treatment Length Probiotic was Administered

This study shows that the length treatment of *Lactobacillus* probiotic on the immune system was administered 8 weeks, because it considered effective to modulate eosinophil[14], B cell[20,23], IgE,[15,18,27], NK cell[20], IL-10[23], and TNF-α[23].

Effect of the Probiotic Form

The most popular forms of *Lactobacillus* probiotic was yogurt[11,16,19,20,26,28], and milk[15,17,18,25,27] than other supplement forms such as juice[14], powder[13,21,30], tablet[12,22,23], and capsule[24].

Effect by Country

The results of the meta-analysis of data collection showed that most countries that intervened with the probiotic *Lactobacillus* are Japan[14,15,17,18,22,24,27].

Effect of the Immune System

After an intervention, the 95% CI of eosinophils was -0.50 (the lower limit was <0 and the upper limit was >0). The significant p=0.05 means that *Lactobacillus* has an effect on eosinophils. The mean difference of the total effect was -0.50/mm^3, and its 95% CI was -0.99 to -0.01/mm^3 (Figure 2a), indicating that *Lactobacillus* could effectively decrease the level of eosinophils and regulate host immunity.

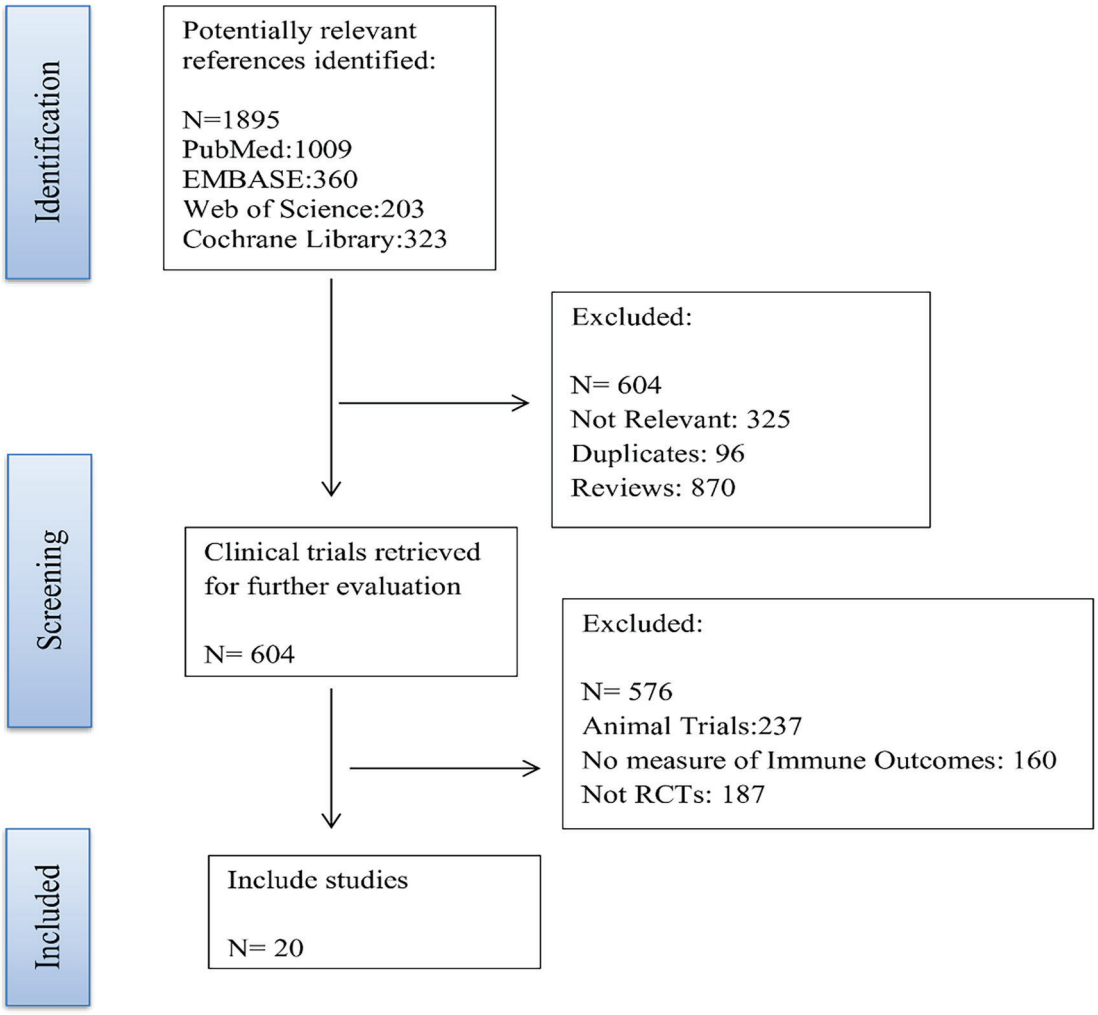

Figure 1. Flowchart of study selection in the meta-analysis.

RCT: Randomized controlled trials

For IgE, the 95% CI of IgE was -0.10 (the lower limit was <0 and the upper limit was >0). A significant p=0.56 means that *Lactobacillus* has no significant effect on IgE. The mean difference of the total effect was -0.10/mm^3, and its 95% CI was -0.42 to 0.23 pg/mL (Figure 2b), indicating that *Lactobacillus* could effectively decrease the level of IgE but not significance.

The forest plot of B cells showed that the significant p=0.02 suggests that *Lactobacillus* has an effect on B cells. The mean difference of the total effect was -0,37/uL, its 95% CI was -0.69 to -0.05/uL in Figure 3a, indicating that *Lactobacillus* could effectively decrease the level of B cells in the treatment group.

The forest plot of NK cells showed that the significant p=0.77 mean that *Lactobacillus* had no significant effect on NK cells, the mean difference of the total effect was -0.04/mm^3, its 95% CI was -0.30 to 0.22/mm^3 in Figure 3b, indicating that *Lactobacillus* could effectively decrease the level of NK cells in the treatment group but not significant.

IL-10, the 95% CI was -0.25 (the lower limit was <0 and the upper limit was >0). The significant p=0.10 indicates that *Lactobacillus* has no significant effect on IL-10. The mean difference of the total effect was -0.25 pg/mL, and its 95% CI was -0.55 to 0.05 pg/mL (Figure 4a), indicating that *Lactobacillus* could effectively increase the level of IL-10 in the treatment group, but the difference was not significant.

After the intervention, the 95% CI of TNF-α -0.12 were -0.50 (the lower limit was <0 and the upper limit was >0). The significant p=0.39 means that *Lactobacillus* has no significant effect on TNF-α. The mean difference of the total effect was -0.12 pg/mL, and its 95% CI was 0.40 to 0.16 pg/mL (Figure 4b), indicating that

Table 1. Characteristics of the included studies about country, type of disease, form of supplement, age, and duration consumption probiotic.

No	Author (Reference)	Country	Type of disease	Form of supplement	Age (y)	Duration (weeks)
1	Han et al.[11], 2012	Korea	Atopic dermatitis	Yogurts	1-13	12
2	Harima-Mizusawa et al.[14], 2016	Japan	Allergic rhinitis	Juice	16-65	8
3	Ishida et al.[15], 2005	Japan	Allergic rhinitis	Milk	34-36	8
4	Kawase et al.[17], 2009	Japan	Japanese cedar pollinosis	Milk	20-57	10
5	Hummelen et al.[19], 2011	Canada	HIV	Yogurts	>18	4
6	Parra et al.[20], 2004	Spain	Healthy person	Yoghurt	51-58	8
7	Bunout et al.[21], 2004	Switzerland	Healthy eldery	Powder	>70	16
8	Miyazawa et al.[22], 2015	Japan	Healthy eldery	Tablet	50-70	4
9	Mangalat et al.[23], 2012	America	Healthy adults	Tablet	19-60	8
10	Drago et al.[13], 2011	Italy	Atopic dermatitis	Powder	10-46	16
11	Tamura et al.[27], 2007	Japan	Allergic rhinitis	Milk	x=39	8
12	Hasegawa et al.[18], 2009	Japan	Japanese cedar polinosis	Milk	x=35	8
13	Ivory et al.[16], 2008	UK	Allergic rhinitis	Yogurt	18-45	2
14	Hirose et al.[24], 2006	Japan	Healthy subjects	Capsule	40-64	12
15	Seifert et al.[25] 2011	Germany	Healthy individuals	Milk	18-60	4
16	Meyer et al.[28] 2007	Austria	Healthy young women	Yogurt	22-29	2
17	Costabile et al.[29], 2017	UK	Hypercholesterolaemic	Capsular	30-65	12
18	Ahn et al.[12], 2020	Korea	Atopic Dermatitis	Tablet	2-13	12
19	Baroja et al.[26], 2007	Canada	Inflammatory bowel disease	Yogurt	26-63	4
20	Ouwehand et al.[30], 2008	Finland	Healthy elderly	Powder	>65	2

x= mean of age. HIV: Human immunodeficiency virus

Table 2. Characteristics of the included studies about gebus of *Lactobacillus*, dose, and outcome.

No	Author (Reference)	Genus of Lactobacillus	Dose	Type of immune
1	Han et al.[11], 2012	*L. plantarum*CJLP133	$1x10^{10}$ CFU	Eosinophil & IgE
2	Harima-Mizusawa et al.[14],2016	*L. plantarum* YIT 0132	100 mL	Eosinophil
3	Ishida et al.[15], 2005	*L. acidophilus* strain L-92	$3x10^{10}$ CFU	Eosinophils & IgE
4	Kawase et al.[17], 2009	*L.GG* and *L. gasseri* TMC0356	$1.4×10^{8}$ CFU and $1.0×10^{7}$ CFU	Eosinophils & IgE
5	Hummelen et al.[19], 2011	*L. rhamnosus* GR-1	$15.38×10^{10}$ CFU	Eosinophils
6	Parra et al.[20], 2004	*L. casei* DNl14001	$10^{8}x10^{10}$ CFU	B cell & NK cell
7	Bunout et al.[21], 2004	*L. paracasei* NCC 2461	10^{9} CFU	B cell & NK cell
8	Miyazawa et al.[22], 2015	*L. gasseri* TMC0356	$1.0×10^{9}$ CFU	B cell
9	Mangalat et al.[23], 2012	*L. reuteri* DSM 17938	$5x10^{8}$ CFU	B cell, IL-10 & TNF-α
10	Drago et al.[13], 2011	*L. salivarius* LS01	$1 x 10^{9}$ CFU	IgE
11	Tamura et al.[27], 2007	*L. casei* strain *Shirota*	$4x10^{10}$ CFU	IgE
12	Hasegawa et al.[18], 2009	*L. plantarum* strain HSK201	$6x10^{10}$ CFU	IgE
13	Ivory et al.[16], 2008	L. casei Shirota	$6.5x10^{9}$ CFU	IgE & TNF-α
14	Hirose et al.[24], 2006	*L. plantarum* L-137	10 mg	NK cell
15	Seifert et al.[25], 2011	L. casei Shirota	$1.95x10^{10}$ CFU	NK cell
16	Meyer et al.[28], 2007	*L. casei* DN114 001	$3.7x10^{8}$ CFU	IL-10 & TNF-α
17	Costabile et al.[29], 2017	*L. plantarum* ECGC13110402	$2x10^{9}$ CFU	IL-10 & TNF-α
18	Ahn et al.[12], 2020	L. pentosus	$1.0×10^{10}$ CFU	IL-10
19	Baroja et al.[26], 2007	*L. rhamnosus* GR-1 and *L. reuteri* RC-14	$1x10^{3}$ CFU and $2x10^{7}$ CFU	TNF-α
20	Ouwehand et al.[30], 2008	L. acidophilus	$2x10^{9}$ CFU	TNF-α

x=mean of age, IL-10: Interleukin 10, TNF-α: Tumor necrosis factor alpha, IgE: Immunoglobulin E

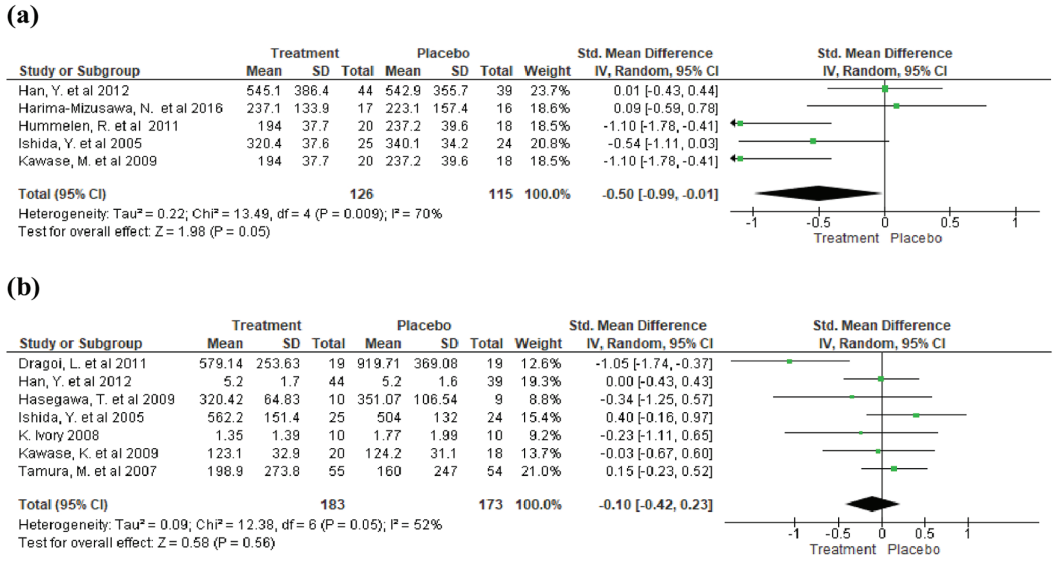

Figure 2. Forest plot effect of *Lactobacillus* supplementation on (a) eosinophils and (b) IgE comparing between *Lactobacillus* group (treatment) and placebo group. The statistical method used was Cohen'd, the effect measure was standard mean difference, and the analysis method was the random effects model.

SD: Standard deviation, CI: Confidence interval, *IgE: Immunoglobulin E*

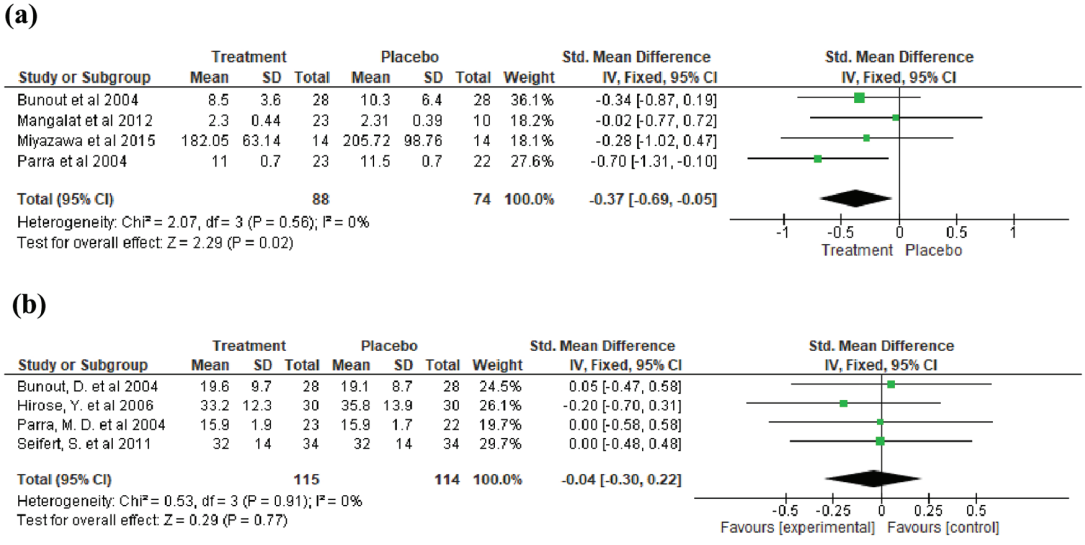

Figure 3. Forest plot effect of *Lactobacillus* supplementation on (a) B cells and (b) NK cells comparing between *Lactobacillus* group (treatment) and placebo group. The statistical method used was Cohen'd, the effect measure was standard mean difference, and the analysis method was the fixed effects model.

SD: Standard deviation, CI: Confidence interval

Lactobacillus could effectively decrease the level of TNF-α and regulate host immunity. Only 20 studies met the requirements of Egger's test. Overall, these studies have a low risk of bias due to the incomplete outcome requirements in Figure 5.

DISCUSSION

In recent years, probiotics have attracted extensive attention for treatment because of their low cost and minimal adverse reactions. However, previous studies regarding probiotics have shown limitations such as a small sample size, lack of medical evidence, and

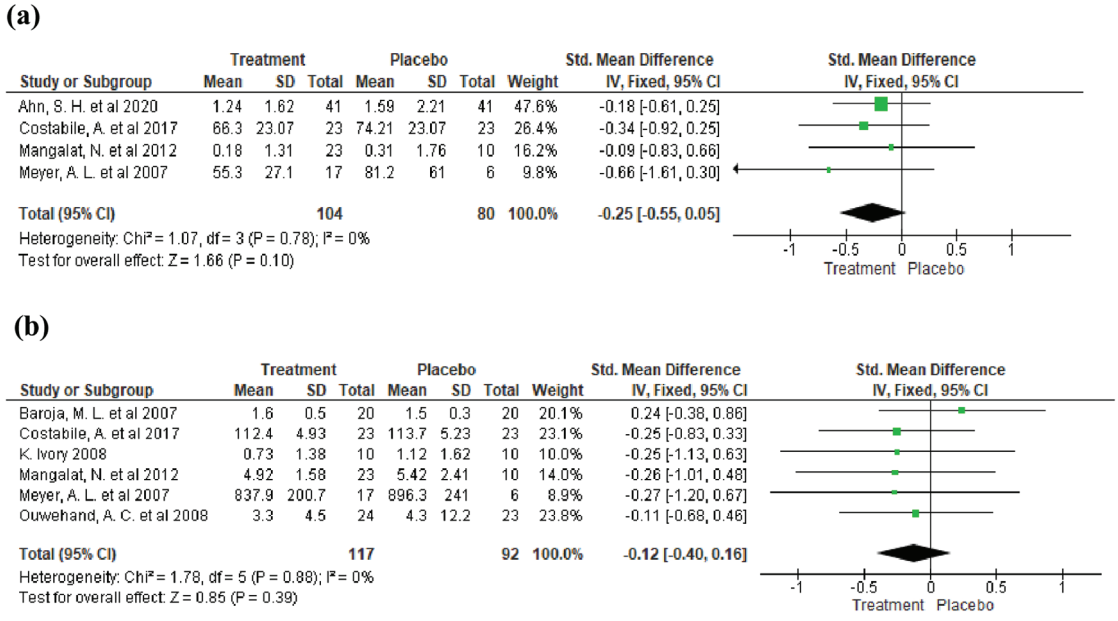

Figure 4. Forest plot effect of *Lactobacillus* supplementation on (a) IL-10 and (b) TNF-α comparing between *Lactobacillus* group (treatment) and placebo group. The statistical method used was Cohen'd, the effect measure was standard mean difference, and the analysis method was the fixed effects model.

SD: Standard deviation, CI: Confidence interval, IL-10: Interleukin 10, TNF-α: Tumor necrosis factor

Figure 5. Risk of bias. Quality evaluation of included trials.

incomplete evaluation indicators. Our meta-analysis study mainly focused on the systematic evaluation of the efficacy of *Lactobacillus* on the immune system. This study gathered 20 studies, 10 of which have the same references but different immune cells that have proven the effect of *Lactobacillus* on the immune system, such as B cells, eosinophils, IgE, NK cells, TNF-α, and IL-10. Currently, research proves the immunomodulatory effect of *Lactobacillus* on several diseases such as allergies, IBD, and atopic dermatitis.

Lactobacillus probiotic strains improve the integrity of intestinal defenses, thereby maintaining immune cell tolerance, reducing translocation of bacteria across the intestinal mucosa, and causing disease-coding phenotypes such as gastrointestinal infections, IBD, and irritable bowel syndrome[31]. Probiotics have a significant influence on the intestinal microbiota, which has been proven in experimental animal studies and clinical trials in humans. *Lactobacillus* also plays a significant role in the modulation and production of B cells, eosinophils, IgE, NK cells, TNF-α, and IL-10.

Many studies have proven that consumption of *Lactobacillus* has a good effect on the body. The probiotic effect is commonly accepted with daily consumption of a minimum of 10^6 CFU/mL or gram of probiotics[32]. Consumption of probiotics has different effects on each individual. The effect was based on immunological reactions and symptomatic parameters caused by the amount of *Lactobacillus* probiotic consumption. Probiotics can be administered orally in the form of capsules[33,34], yoghurt[35,36], dairy drinks or milk[15,16,37,38], and tablets[39,40]. Our data suggest that the majority of *Lactobacillus* probiotics are administered in the form of milk. Factors that influence the effectiveness of probiotic consumption are the duration and timing of intake. Moreover, the duration of *Lactobacillus* consumption in human trials differed from 2 to 12 weeks, and 8 weeks is the most popular time for *Lactobacillus* treatment. *LcS* is the most popular strain used for *Lactobacillus* treatment.

Our data show that age is the inflammatory reaction that triggers the activation of immunological cells. The majority of them are >50 years old. In several studies, aged >50 years, there has been an inflammatory reaction such as activation of TNF-α and IL-6[41-43]. This study proves the effect of *Lactobacillus* probiotics can modulate inflammatory reactions in healthy 50-year-olds. It showed that *Lactobacillus* probiotics could modulate the activity of B cells, eosinophils, IgE, NK cells, TNF-α, and IL-10.

B cells play a role in eliminating incoming bacteria. On the other hand, B cells can also cause autoimmune and allergic diseases[44]. This study proves that *Lactobacillus* impacts reducing the number of B cells. This decrease in B cells is necessary because antibodies can damage the intestinal mucosa. In some cases, such as allergies and autoimmune diseases, B cell activation is very high and can attack other immune cells. The results of our meta-analysis prove that a decrease in *Lactobacillus* plays a role in reducing the activation of B cells.

Several studies using probiotics have proven effective in increasing NK cell activity. Studies have shown that the administration *of L. rhamnosus* HN001 supplements for 3 weeks shows the activity of NK cells in middle-aged and elderly populations[45]. Our analysis proves that *Lactobacillus* positivity increases NK cell activation, which means that NK cells are effective for the treatment group. One probiotic that is often used in research trials is the lactic acid bacteria strain, *LcS*, which is currently manufactured in Japan as a commercial beverage. Many studies have shown the immunomodulatory effects of *LcS* on the gut immune system, particularly NK cell activity within the innate immune system[46].

Our analysis also showed that *Lactobacillus* had a positive result on TNF-α which means that *Lactobacillus* acts as an immunomodulator to decrease TNF-α cells. Probiotics such as *Lactobacillus* can inhibit TNF-α expression, generating an immunosuppressant and anti-inflammatory effect as a response; this statement has been widely reported by other studies. A study showed that the probiotic *Lactobacillus* can reduce TNF-α expression, and treat colitis symptoms[47].

Like TNF-α, we proved that *Lactobacillus* downregulates IgE. This effect is essential in patients with food allergies because it avoids clinical manifestations with vital consequences for allergic patients. IgE is an amply recognized antibody (immunoglobulin) associated with allergic responses. In different cases, IgE antibodies can bind to allergens and increase host resistance against parasites (helminths and protozoans). Mechanism of IgE as a defense through binding to allergen products and FcεRI on basophils and mast cells, antigen and IgE-induced aggregation of FcεRI can trigger the release of histamine, proteases, prostaglandins, leukotrienes, chemokines and cytokines[48].

IL-10 plays a central role in downregulating inflammatory cascades by suppressing the secretion of proinflammatory cytokines. *Lactobacillus* was positive for IL-10 expression. Some studies have revealed the positive effect of *Lactobacillus* sp. in stimulating IL-10.

Current research has demonstrated that administering *L. casei* can modify intestinal microbiota composition and TLR expression and increase IL-10 levels in the colonic mucosa of patients with mild ulcerative colitis[49].

The strength of this study was that the probiotic *Lactobacillus* sp. is highly effective in the elderly who are >50 years old through modulation of eosinophils and B cells. The limitations of this study: (1) Many studies have examined the effects of *Lactobacillus* sp. probiotics but did not include the mean, standard deviation, and the number of samples, so that studies were excluded from this study; (2) There is little evidence of the effect of probiotic *Lactobacillus* sp. on anti-inflammatory parameters; (3) Only collects a few cases (atopic dermatitis, allergic rhinitis, Japanese cedar pollinosis, HIV, healthy eldery, hypercholestrolaemic, and IBD), so the role of probiotic *Lactobacillus* sp. in other cases is not known.

CONCLUSION

In conclusion, our meta-analysis demonstrated that most cases in this study were healthy elderly patients who received treatment with *Lactobacillus* sp. *Lactobacillus* sp. positively affects B cells, eosinophils, IgE, NK cells, TNF-α, and IL-10. This means that *Lactobacillus* could regulate the immune system by modulating inflammation in the healthy elderly.

Acknowledgements: Thank you to the Center of Women Empowerment in Law Enforcement Research Found for funding this study.

Ethics

Author Contributions

Concept: W.F.E., S.P.M., I.D.S., D.S., R.E.P., S.Z., Design: W.F.E., S.P.M., I.D.S., D.S., R.E.P., S.Z., Data Collection and/or Processing: W.F.E., I.D.S., D.S., Analysis and/or Interpretation: W.F.E., S.P.M., D.S., R.E.P., Literature Search: W.F.E., R.E.P., Writing: W.F.E., S.P.M., I.D.S., D.S., R.E.P., S.Z.

Conflict of Interest: The authors have no conflict of interest to declare.

Financial Disclosure: This study was funded by the Center of Women Empowerment in Law Enforcement Research Found, Postgraduate School, Airlangga University, for funding this study (project no: 3899/UN3.SPS/PT.01.03/2023).

REFERENCES

1. Lebeer S, Vanderleyden J, De Keersmaecker SC. Genes and molecules of lactobacilli supporting probiotic action. Microbiol Mol Biol Rev. 2008;72:728-64.
2. Mackie RI, Sghir A, Gaskins HR. Developmental microbial ecology of the neonatal gastrointestinal tract. Am J Clin Nutr. 1999;69:1035S-45S.
3. Ibrahim SA. Lactic acid bacteria: Lactobacillus spp.: Other species. 2016. Available from: https://www.sciencedirect.com/science/article/abs/pii/B978008100596500857X?via%3Dihub
4. Zheng J, Wittouck S, Salvetti E, et al. A taxonomic note on the genus Lactobacillus: Description of 23 novel genera, emended description of the genus Lactobacillus Beijerinck 1901, and union of Lactobacillaceae and Leuconostocaceae. Int J Syst Evol Microbiol. 2020;70:2782-858.
5. Ligaarden SC, Axelsson L, Naterstad K, Lydersen S, Farup PG. A candidate probiotic with unfavourable effects in subjects with irritable bowel syndrome: a randomised controlled trial. BMC Gastroenterol. 2010;10:16.
6. Sazawal S, Hiremath G, Dhingra U, Malik P, Deb S, Black RE. Efficacy of probiotics in prevention of acute diarrhoea: a meta-analysis of masked, randomised, placebo-controlled trials. Lancet Infect Dis. 2006;6:374-82.
7. Isolauri E, Arvola T, Sütas Y, Moilanen E, Salminen S. Probiotics in the management of atopic eczema. Clin Exp Allergy. 2000;30:1604-10.
8. Viljanen M, Savilahti E, Haahtela T, et al. Probiotics in the treatment of atopic eczema/dermatitis syndrome in infants: a double-blind placebo-controlled trial. Allergy. 2005;60:494-500.
9. Kalliomäki M, Antoine J-M, Herz U, Rijkers GT, Wells JM, Mercenier A. Guidance for substantiating the evidence for beneficial effects of probiotics: prevention and management of allergic diseases by probiotics. J Nutr. 2010;140:713S-21S.
10. Moher D, Liberati A, Tetzlaff J, Altman DG; PRISMA Group. Preferred reporting items for systematic reviews and meta-analyses: the PRISMA statement. Ann Intern Med. 2009;151:264-9, W64.
11. Han Y, Kim B, Ban J, et al. A randomized trial of L actobacillus plantarum CJLP 133 for the treatment of atopic dermatitis. Pediatr Allergy Immunol. 2012;23:667-73.
12. Ahn SH, Yoon W, Lee SY, et al. Effects of Lactobacillus pentosus in children with allergen-sensitized atopic dermatitis. J Korean Med Sci. 2020;35:e128.
13. Drago L, Iemoli E, Rodighiero V, Nicola L, De Vecchi E, Piconi S. Effects of Lactobacillus salivarius LS01 (DSM 22775) treatment on adult atopic dermatitis: a randomized placebo-controlled study. Int J Immunopathol Pharmacol. 2011;24:1037-48.
14. Harima-Mizusawa N, Kano M, Nozaki D, Nonaka C, Miyazaki K, Enomoto T. Citrus juice fermented with Lactobacillus plantarum YIT 0132 alleviates symptoms of perennial allergic rhinitis in a double-blind, placebo-controlled trial. Benef Microbes. 2016;7:649-58.
15. Ishida Y, Nakamura F, Kanzato H, et al. Clinical effects of Lactobacillus acidophilus strain L-92 on perennial allergic rhinitis: a double-blind, placebo-controlled study. J Dairy Sci. 2005;88:527-33.
16. Ivory K, Chambers SJ, Pin C, Prieto E, Arqués JL, Nicoletti C. Oral delivery of Lactobacillus casei Shirota modifies allergen-induced immune responses in allergic rhinitis. Clin Exp Allergy. 2008;38:1282-9.
17. Kawase M, He F, Kubota A, et al. Effect of fermented milk prepared with two probiotic strains on Japanese cedar pollinosis in a double-blind placebo-controlled clinical study. Int J Food Microbiol. 2009;128:429-34.

18. Hasegawa T, Hirakawa K, Matsumoto T, Toki S, Maeyama Y, Morimatsu F. Efficacy of Lactobacillus plantarum strain HSK201 in relief from Japanese cedar pollinosis. Biosci Biotechnol Biochem. 2009;73:2626-31.

19. Hummelen R, Hemsworth J, Changalucha J, et al. Effect of micronutrient and probiotic fortified yogurt on immune-function of anti-retroviral therapy naive HIV patients. Nutrients. 2011;3:897-909.

20. Parra M, Martinez de Morentin B, Cobo J, Mateos A, Martinez J. Daily ingestion of fermented milk containing Lactobacillus casei DN114001 improves innate-defense capacity in healthy middle-aged people. J Physiol Biochem. 2004;60:85-91.

21. Bunout D, Barrera G, Hirsch S, et al. Effects of a nutritional supplement on the immune response and cytokine production in free-living Chilean elderly. JPEN J Parenter Enteral Nutr. 2004;28:348-54.

22. Miyazawa K, Kawase M, Kubota A, et al. Heat-killed Lactobacillus gasseri can enhance immunity in the elderly in a double-blind, placebo-controlled clinical study. Benef Microbes. 2015;6:441-9.

23. Mangalat N, Liu Y, Fatheree NY, et al. Safety and tolerability of Lactobacillus reuteri DSM 17938 and effects on biomarkers in healthy adults: results from a randomized masked trial. PLoS One. 2012;7:e43910.

24. Hirose Y, Murosaki S, Yamamoto Y, Yoshikai Y, Tsuru T. Daily intake of heat-killed Lactobacillus plantarum L-137 augments acquired immunity in healthy adults. J Nutr. 2006;136:3069-73.

25. Seifert S, Bub A, Franz CM, Watzl B. Probiotic Lactobacillus casei Shirota supplementation does not modulate immunity in healthy men with reduced natural killer cell activity. J Nutr. 2011;141:978-84.

26. Lorea Baroja M, Kirjavainen P, Hekmat S, Reid G. Anti-inflammatory effects of probiotic yogurt in inflammatory bowel disease patients. Clin Exp Immunol. 2007;149:470-9.

27. Tamura M, Shikina T, Morihana T, et al. Effects of probiotics on allergic rhinitis induced by Japanese cedar pollen: randomized double-blind, placebo-controlled clinical trial. Int Arch Allergy Immunol. 2007;143:75-82.

28. Meyer A, Elmadfa I, Herbacek I, Micksche M. Probiotic, as well as conventional yogurt, can enhance the stimulated production of proinflammatory cytokines. J Hum Nutr Diet. 2007;20:590-8.

29. Costabile A, Buttarazzi I, Kolida S, et al. An in vivo assessment of the cholesterol-lowering efficacy of Lactobacillus plantarum ECGC 13110402 in normal to mildly hypercholesterolaemic adults. PLoS One. 2017;12:e0187964.

30. Ouwehand AC, Tiihonen K, Saarinen M, Putaala H, Rautonen N. Influence of a combination of Lactobacillus acidophilus NCFM and lactitol on healthy elderly: intestinal and immune parameters. Br J Nutr. 2009;101:367-75.

31. Lee BJ, Bak Y-T. Irritable bowel syndrome, gut microbiota and probiotics. J Neurogastroenterol Motil. 2011;17:252-66.

32. Kechagia M, Basoulis D, Konstantopoulou S, et al. Health benefits of probiotics: a review. ISRN Nutr. 2013;2013:481651.

33. Costa D, Marteau P, Amouyal M, et al. Efficacy and safety of the probiotic Lactobacillus paracasei LP-33 in allergic rhinitis: a double-blind, randomized, placebo-controlled trial (GA2LEN Study). Eur J Clin Nutr. 2014;68:602-7.

34. Lin W-Y, Fu L-S, Lin H-K, Shen C-Y, Chen Y-J. Evaluation of the effect of Lactobacillus paracasei (HF. A00232) in children (6–13 years old) with perennial allergic rhinitis: a 12-week, double-blind, randomized, placebo-controlled study. Pediatr Neonatol. 2014;55:181-8.

35. Giovannini M, Agostoni C, Riva E, et al; Felicita Study Group. A randomized prospective double blind controlled trial on effects of long-term consumption of fermented milk containing Lactobacillus casei in pre-school children with allergic asthma and/or rhinitis. Pediatr Res. 2007;62:215-20.

36. Martínez-Cañavate A, Sierra S, et al. A probiotic dairy product containing L. gasseri CECT5714 and L. coryniformis CECT5711 induces immunological changes in children suffering from allergy. Pediatr Allergy Immunol. 2009;20:592-600.

37. Wassenberg J, Nutten S, Audran R, et al. Effect of Lactobacillus paracasei ST11 on a nasal provocation test with grass pollen in allergic rhinitis. Clin Exp Allergy. 2011;41:565-73.

38. Snel J, Vissers YM, Smit BA, et al. Strain-specific immunomodulatory effects of Lactobacillus plantarum strains on birch-pollen-allergic subjects out of season. Clin Exp Allergy. 2011;41:232-42.

39. Perrin Y, Nutten S, Audran R, et al. Comparison of two oral probiotic preparations in a randomized crossover trial highlights a potentially beneficial effect of Lactobacillus paracasei NCC2461 in patients with allergic rhinitis. Clin Transl Allergy. 2014;4:1.

40. Ahmed M, Billoo AG, Iqbal K. Efficacy of probiotic in perennial allergic rhinitis under five year children: A randomized controlled trial. Pak J Med Sci. 2019;35:1538-43.

41. Bian A-L, Hu H-Y, Rong Y-D, Wang J, Wang J-X, Zhou X-Z. A study on relationship between elderly sarcopenia and inflammatory factors IL-6 and TNF-α. Eur J Med Res. 2017;22:25.

42. Koo EG, Lai LM, Choi GY, Chan MT. Systemic inflammation in the elderly. Best Pract Res Clin Anaesthesiol. 2011;25:413-25.

43. De Martinis M, Franceschi C, Monti D, Ginaldi L. Inflammation markers predicting frailty and mortality in the elderly. Exp Mol Pathol. 2006;80:219-27.

44. Kelly-Scumpia KM, Scumpia PO, Weinstein JS, et al. B cells enhance early innate immune responses during bacterial sepsis. J Exp Med. 2011;208:1673-82.

45. Aziz N, Bonavida B. Activation of natural killer cells by probiotics. For Immunopathol Dis Therap. 2016;7:41-55.

46. Matsumoto K, Takada T, Shimizu K, et al. The effects of a probiotic milk product containing Lactobacillus casei strain Shirota on the defecation frequency and the intestinal microflora of sub-optimal health state volunteers: a randomized placebo-controlled cross-over study. Biosci Microflora. 2006;25:39-48.

47. Pena JA, Versalovic J. Lactobacillus rhamnosus GG decreases TNF-α production in lipopolysaccharide-activated murine macrophages by a contact-independent mechanism. Cell Microbiol. 2003;5:277-85.

48. Sariego TH, del Toro DD, Barranco JJ, Arenal A. Can probiotics modulate the cytokines and antibodies levels in food allergy models? A meta-analysis. 2022. DOI:10.21203/rs.3.rs-1777155/v1

49. de Moreno de LeBlanc A, Del Carmen S, Zurita-Turk M, et al. Importance of IL-10 modulation by probiotic microorganisms in gastrointestinal inflammatory diseases. ISRN Gastroenterol. 2011;2011:892971.

DOI: 10.4274/MMJ.galenos.2024.37729
Medeni Med J 2024;39:132-135

Case Report

Solitary Submandibular Schwannoma Mimicking a Salivary Gland Tumor in a Child

Bir Çocukta Tükürük Bezi Tümörünü Taklit Eden Soliter Submandibular Schwannoma

Kim Yew Richard WONG[1], Ikram HAKIM[1], Halimuddin SAWALI[2], Rachel Cui Ai LIM[1], Nur Kamilia MOHD MOHSIN[3]

[1]Hospital Tawau, Department of Otorhinolaryngology-Head and Neck Surgery, Sabah, Malaysia
[2]Hospital Queen Elizabeth, Department of Otorhinolaryngology-Head and Neck Surgery, Sabah, Malaysia
[3]Hospital Queen Elizabeth, Department of Pathology, Sabah, Malaysia

ABSTRACT

Tumors occurring in the submandibular space are infrequent among pediatric patients, and benign peripheral nerve tumors in this region are exceptionally rare. This study describes the uncommon occurrence of a schwannoma in the submandibular space in a child and describes its management. A 7-year-old child presented with a gradually enlarging swelling over a 7-month period in the submandibular region, clinically resembling a salivary gland tumor. There were no associated marginal mandibular, lingual, or hypoglossal nerve palsy. The mass was excised completely, and histopathological examination revealed it to be a schwannoma. It is appropriate to consider benign peripheral nerve tumors, such as schwannoma, in the differential diagnosis of submandibular space tumors in children.

Keywords: Submandibular gland neoplasms, neurilemmoma, salivary gland neoplasms

ÖZ

Submandibular boşlukta meydana gelen tümörler pediatrik hastalar arasında sık görülmez ve bu bölgedeki benign periferik sinir tümörleri son derece nadirdir. Bu çalışmada, bir çocukta submandibular alanda nadir görülen bir schwannoma olgusu ve tedavisi anlatılmaktadır. Yedi yaşında bir çocuk, submandibular bölgede 7 aylık bir süre içinde giderek büyüyen ve klinik olarak tükürük bezi tümörüne benzeyen bir şişlik ile başvurdu. Kitle ile ilişkili marjinal mandibular, lingual veya hipoglossal sinir felci yoktu. Kitle tamamen eksize edildi ve histopatolojik incelemede schwannoma olduğu görüldü. Çocuklarda submandibular boşluk tümörlerinin ayırıcı tanısında schwannoma gibi benign periferik sinir tümörlerinin düşünülmesi gerekmektedir.

Anahtar kelimeler: Submandibular bez neoplazmları, nörilemmoma, tükürük bezi neoplazmları

INTRODUCTION

Salivary masses in children comprise 10% of all tumors affecting the head and neck in the pediatric population. While uncommon, it is about five times more likely to be malignant than in an adult, with rates of 50% and 10%, respectively. The parotid gland (66%) emerged as the most frequently affected site, followed by the submandibular gland (34%). Benign lesions accounted for 94% of submandibular gland tumors. Pleomorphic adenoma was the predominant benign tumor (92%), whereas acinic cell carcinoma stood out as the leading malignancy (64%)[1]. Other benign tumors of the submandibular space include Warthin's tumor, embryoma, monomorphic adenoma, lipoma, and teratoma, listed in decreasing order of occurrence[2].

CASE REPORT

A 7-year-old girl of Bajau descent, with no medical comorbidities, presented to us with a history of painless, slow-growing right submandibular swelling for 7 months. There were no associated skin changes or pus discharge. There were no history of preceding trauma or insect bite. On examination, there was a right submandibular swelling measuring 4x3 cm, which was firm in consistency

Address for Correspondence: K.Y.R. Wong, Hospital Tawau, Clinic of Otorhinolaryngology-Head and Neck Surgery, Sabah, Malaysia
E-mail: richardwky@gmail.com **ORCID ID:** orcid.org/0000-0002-0165-0895

Received: 26 February 2024
Accepted: 02 April 2024
Online First: 15 April 2024

Cite as: Wong KYR, Hakim I, Sawali H, Lim RCA, Mohd Mohsin NK. Solitary Submandibular Schwannoma Mimicking a Salivary Gland Tumor in a Child. Medeni Med J 2024;39:132-135

and non-tender (Figure 1). No punctum or skin changes were noted. There were no remarkable findings in the oral cavity and no associated marginal mandibular, lingual, or hypoglossal nerve palsy. There was no medialization of the lateral pharyngeal wall on flexible nasopharyngolaryngoscopy, with normal supraglottic and glottic structures observed. On the basis of our initial clinical assessment, a provisional diagnosis of a submandibular gland pleomorphic adenoma was made.

Tru-cut needle biopsy of the right submandibular swelling, however; revealed a low-grade spindle cell lesion, with features favoring a benign peripheral nerve sheath tumor.

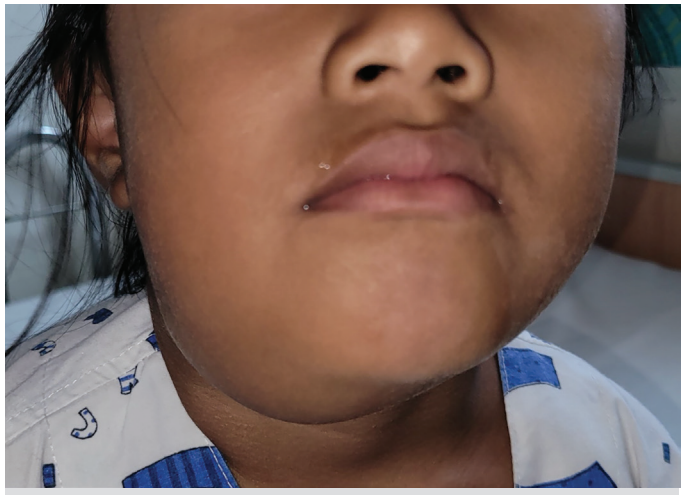

Figure 1. Right submandibular swelling measuring 4x3 cm.

Computed tomography (CT) scan of the neck (Figure 2) showed a large, well-defined, heterogeneously enhancing hypodense mass (45 Hounsfield unit) at the right submandibular space measuring approximately 4.7x3.2x3.5 cm (AP x W x CC). The mass displaces the right submandibular gland posteriorly and extends from the level of the right medial pterygoid muscle superiorly to the level of the hyoid bone inferiorly. No significant cervical lymphadenopathy was observed.

The patient underwent excision of the right submandibular mass under general anesthesia. A skin incision was made 2 cm below the angle of the mandible, and the subplatysmal flap was raised. The marginal mandibular nerve was protected using the Hayes-Martin maneuver. Upon entering the submandibular space, there was a solid whitish mass with a smooth surface measuring 3x5 cm (Figure 3). The lingual nerve and submandibular gland were identified and preserved. The originating nerve of the tumor was not determined in this case. Nonetheless, a meticulous intracapsular dissection was performed to completely excise the mass.

Histopathological examination of the specimen confirmed that it was a benign peripheral nerve sheath tumor, which was consistent with Schwannoma; as sections show a thinly encapsulated lesion composed of proliferation of spindle cells arranged in hypercellular (Antoni A) and hypocellular areas (Antoni B) (Figure 4). Verocay bodies were observed in the hypercellular areas (Figure 5). This tumor was further classified as a conventional schwannoma because it does not exhibit features specific to other special subtypes; for example,

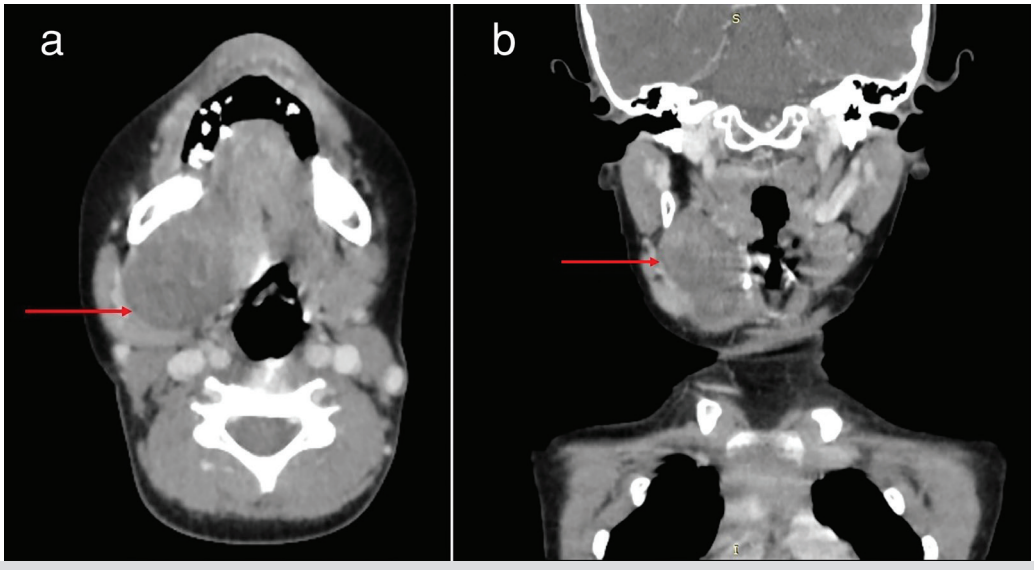

Figures 2. Contrast enhanced computed tomography scan of the neck in axial (a) & coronal (b) views showing the right submandibular mass (red arrow).

the ancient, cellular, plexiform, or microcystic subtypes. The child recovered well postoperatively with no recurrence or nerve deficit within 6 months of follow-up. The patients parents provided written informed consent for the publication of this article.

DISCUSSION

Schwannoma, initially described by Verocay in 1908, typically manifests in individuals aged between 30 and 50 years. They are benign tumors that are solitary and well differentiated and originate from Schwann cells. Approximately 25-45% of extracranial schwannomas are found in the head and neck region; with the temporal bone, lateral neck, and paranasal sinuses being the most frequently affected areas. Schwannomas typically occur as solitary lesions; however, in some cases, they may manifest as multiple lesions as part of neurofibromatosis type 2. The nerve of origin is unidentifiable in approximately 10-40% of schwannomas[3].

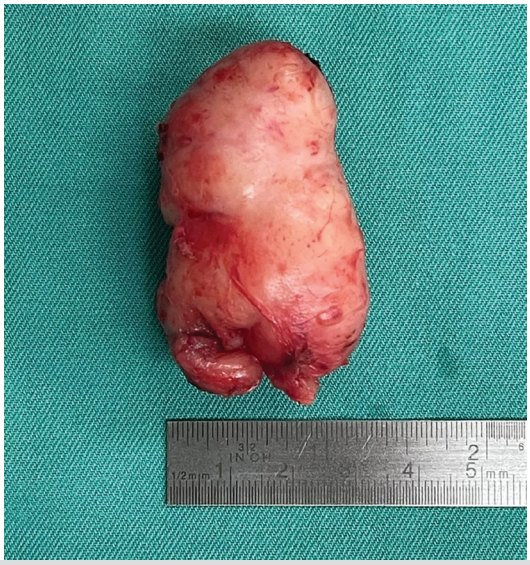

Figure 3. Operative specimen showing a solid whitish mass with smooth surface which was completely excised.

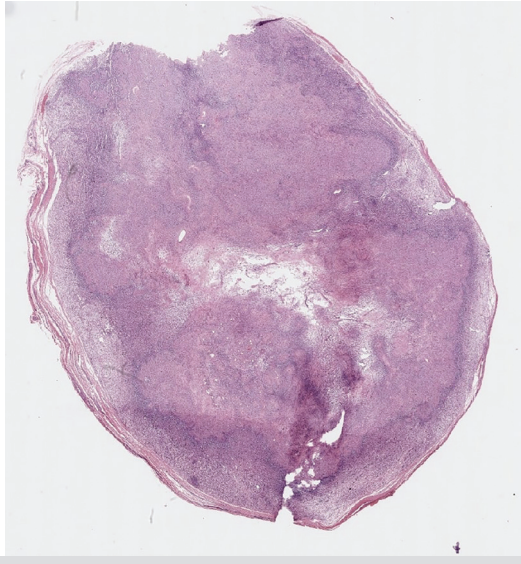

Figure 4. Histopathologic examination of the surgical specimen demonstrated a thinly encapsulated lesion composed of proliferation of spindle cells arranged in hypercellular (Antoni B) and hypocellular areas (Antoni B).

Extracranial schwannomas situated in the salivary glands are infrequent, with the majority arising in the parotid gland from a peripheral branch of the facial nerve. Schwannomas originating in the submandibular space are exceedingly rare, and only a limited number of cases have been reported. Patients present with a painless and mobile mass in the submandibular region. These benign tumors tend to displace rather than infiltrate the associated nerve, which accounts for the absence of nerve palsy[4].

Ultrasonography reveals a well-defined solid hypoechoic mass, not unlike pleomorphic adenomas. CT characteristics of schwannomas include well-defined tumors with low or soft tissue attenuation and either homogeneous or heterogeneous enhancement. Magnetic resonance imaging (MRI) is recognized as the most effective imaging technique for diagnosing schwannomas. On MRI, schwannomas display low signal intensity on T1-weighted images and high signal intensity on T2-weighted images. In T2-weighted images, a distinctive target signal pattern is evident, featuring heightened peripheral signal intensity and reduced central signal intensity[5].

Schwannoma exhibits a distinctive histological profile characterized by an encapsulated lesion originating from a nerve. It is composed of a close intermingling of spindle

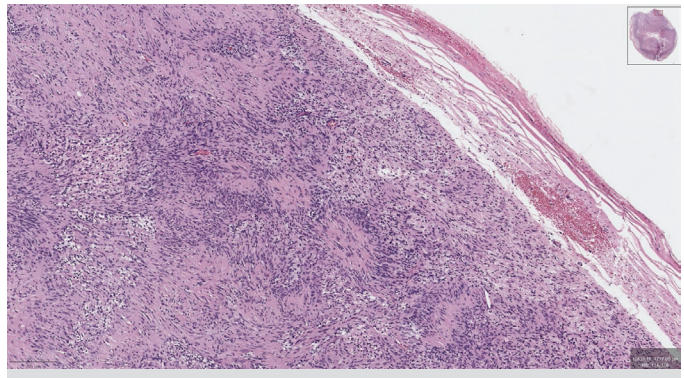

Figure 5. Prominent nuclear palisading forming Verocay bodies are seen in the hypercellular areas.

cells that form highly cellular areas known as Antoni type A, along with less cellular and myxoid Antoni type B areas. Within the palisades of Antoni type A cells, there are regions without nuclei referred to as Verocay bodies[6].

Schwannomas found in various regions of the human body have demonstrated immunoreactivity to proteins S-100 and vimentin. Furthermore, varying immunoreactivity to EMA and GFAP was identified in areas corresponding to the perineurium. Although uncommon, positivity for additional markers like CD56 and CD57 has been noted in both benign and malignant schwannomas[7].

The preferred approach for treating schwannoma typically involves removing the tumor while preserving the associated nerve[8]. The usual challenge lies in the inability to identify the nerve of origin, and even with nerve-preserving intracapsular enucleation, preserved nerve function post-surgery is not guaranteed. In some cases, postoperative neurological deficits may help establish the tumor's origin[9].

After a thorough surgical excision, there is no need for long-term follow-up; as recurrence is rare after surgery. However, in cases of incomplete excision, it is advisable to undergo annual ultrasonography and review[10].

In conclusion, submandibular space schwannoma is a rare entity; and this, to the best of our knowledge; is the first reported case in the pediatric age group. Diagnosis of the lesion is typically achieved through a contrast-enhanced CT scan of the neck coupled with fine needle aspiration cytology. Complete surgical resection is generally considered curative.

Acknowledgments: We would like to thank the Director General of Ministry of Health Malaysia for his permission to publish this article as a case report.

Ethics

Informed Consent: Patient's guardian's written informed consent was obtained.

Author Contributions

Surgical and Medical Practices: K.Y.R.W., I.H., H.S., R.C.A.L., N.K.M.M., Concept: K.Y.R.W., I.H., H.S., R.C.A.L., N.K.M.M., Design: K.Y.R.W., I.H., H.S., R.C.A.L., N.K.M.M., Data Collection and/or Processing: K.Y.R.W., I.H., R.C.A.L., N.K.M.M., Analysis and/or Interpretation: K.Y.R.W., N.K.M.M., Literature Search: K.Y.R.W., Writing: K.Y.R.W., I.H., H.S.

Conflict of Interest: The authors have no conflict of interest to declare.

Financial Disclosure: The authors declared that this study has received no financial support.

REFERENCES

1. Jesberg P, Monzon A, Gitomer SA, Herrmann BW. Pediatric primary salivary gland tumors. Am J Otolaryngol. 2023;44:103948.
2. Lesperance Marci M, Flint PW. Salivary gland disease in children. In: Cummings Pediatric Otolaryngology. 1st ed. Elsevier; 2015. p. 304-5.
3. Ranjan SK, Sinha M, Sharan A, Munda VS, Usha P, Yadav SK. Schwannoma of the submandibular gland: A rare case report. J Clin Diagn Res. 2016;10:PD23-4.
4. Bondy PC, Block RM, Green J. Ancient schwannoma of the submandibular gland: A case report. Ear Nose Throat J. 1996;75:781-3.
5. Park KW, Lee DH, Lee JK, Lim SC. A clinical study of submandibular schwannoma. Oral Surg Oral Med Oral Pathol Oral Radiol. 2022;133:e6-9.
6. Bansal V, Aggarwal P, Wadhwan V, Bansal A, Kapoor S, Yadav M. Giant solitary schwannoma of submandibular salivary gland-a rare entity. J Maxillofac Oral Surg. 2017;16:382-6.
7. dos Santos JN, Silva Gurgel CA, Gonçalves Ramos EA, Pereira Júnior FB, Crusoé-Rebello IM, Oliveira MC. Plexiform schwannoma mimicking a salivary gland tumor: An unusual case report diagnosed in pediatric patient. Int J Pediatr Otorhinolaryngol Extra. 2011;6:317-21.
8. Kang GC, Soo KC, Lim DT. Extracranial non-vestibular head and neck schwannomas: A ten-year experience. Ann Acad Med Singap. 2007;36:233-40.
9. Loterh SS, Prabhu V, O'Brien C. Submandibular schwannoma: Is excision a 'gold standard treatment'? BMJ Case Rep. 2015;2015:bcr2015209900.
10. Patel M, Srinivasan B, Sharma S. The diagnostic dilemma of a parasympathetic schwannoma in the submandibular gland. Ann R Coll Surg Engl. 2015;97:e13-4.

DOI: 10.4274/MMJ.galenos.2024.83652
Medeni Med J 2024;39:136-139

Case Report

The Dual Innervation of the Gluteus Maximus Associated with Other Anatomical Variations of the Gluteal Region

Gluteal Bölgenin Diğer Anatomik Varyasyonları ile İlişkili Gluteus Maksimusun İkili İnnervasyonu

Punnapa RAVITEJA, Mrudula CHANDRUPATLA, Alka V BHINGARDEO, Surraj SUSAI

All India Institute of Medical Sciences Bibinagar, Department of Anatomy, Hyderabad, India

ABSTRACT

The gluteus maximus (GM) is a big quadrilateral musculature that lines the rear portion of the pelvis. It is innervated by the inferior gluteal nerve. The sciatic nerve, inferior gluteal nerve, and posterior cutaneous nerve of the thigh are branches of the sacral plexus. The superior and inferior gluteal arteries are the chief arterial supply to the gluteal region. In the present case, there was a dual innervation of the GM. The superior gluteal artery and the superior gluteal nerve was piercing the piriformis and the inferior gluteal artery was running between the posterior cutaneous nerve of the thigh and the inferior gluteal nerve. According to our literature review, anatomical studies in which this cadaveric procedure has been performed have not been previously reported. The anatomical variations of the gluteal region are important to surgeons, physicians, anatomists, and nurses.

Keywords: Gluteus maximus, sciatic nerve, cadaver, dual innervation, piriformis

ÖZ

Gluteus maksimus (GM) pelvisin arka kısmını kaplayan büyük bir dörtgen kas sistemidir. İnferior gluteal sinir tarafından innerve edilir. Siyatik sinir, inferior gluteal sinir ve uyluğun posterior kutanöz siniri sakral pleksusun dallarıdır. Süperior ve inferior gluteal arterler gluteal bölgenin başlıca arteriyel beslenmesidir. Mevcut olguda, GM ve superior gluteal arterin ikili bir innervasyonu vardı. Superior gluteal sinir piriformisi delmekte ve inferior gluteal arter uyluğun posterior kutanöz siniri ile inferior gluteal sinir arasında seyretmekteydi. Literatür taramamıza göre, bu kadavra prosedürünün uygulandığı anatomik çalışmalar daha önce bildirilmemiştir. Gluteal bölgenin anatomik varyasyonları cerrahlar, hekimler, anatomistler ve hemşireler için önemlidir.

Anahtar kelimeler: Gluteus maksimus, siyatik sinir, kadavra, çift innervasyon, piriformis

INTRODUCTION

The gluteus maximus (GM) is a big quadrilateral musculature that lines the rear portion of the pelvis. It originates from the iliac crest, posterior part of the gluteal surface of the ilium, dorsal part of the sacrum, side of the coccyx, and sacrotuberous ligament. Three-quarters of it is placed into the iliotibial tract, while the other quarter is introduced into the gluteal tuberosity. It is supplied by the inferior gluteal nerve (IGN). GM is a chief extensor of the hip joint and acts as an anti-gravity muscle[1].

The sacral plexus (SP) branch known as the IGN has root values of L5, S1, and S2. The sciatic nerve (SN) is the thickest in the body and is a branch of the SP with root values L4-S3. Another branch of SP with root values of S1-S3 is the posterior cutaneous nerve of the thigh (PCNT). The inferior gluteal artery (IGA) supplies blood to the GM after entering the gluteal region through the greater sciatic foramen. It is a branch from the internal iliac artery's anterior segment. The superior gluteal artery (SGA) is a branch of the posterior segment of the internal iliac artery that reaches the gluteal region via the greater sciatic foramen and passes above the piriformis, accompanied by the superior gluteal nerve[1].

In this case report, we present a unique rare case of dual innervation of the GM and IGA compression. SGA and SGN were piercing the piriformis. Variations in the innervation of GM are exceedingly rare. According to

Address for Correspondence: P. Raviteja, All India Institute of Medical Sciences Bibinagar, Department of Anatomy, Hyderabad, India
E-mail: punnaparaviteja5@gmail.com **ORCID ID:** orcid.org/0009-0007-4839-7122

Received: 09 January 2024
Accepted: 28 April 2024
Online First: 29 May 2024

Cite as: Raviteja P, Chandrupatla M, Bhingardeo AV, Susai S. The Dual Innervation of the Gluteus Maximus Associated with Other Anatomical Variations of the Gluteal Region. Medeni Med J 2024;39:136-139

our literature review, anatomical studies in which this cadaveric procedure has been performed have not been previously reported.

CASE REPORT

During the usual dissection of a 61-year-old female corpse, which had been embalmed in formalin during hands-on training for undergraduate and postgraduate medical students at the department of anatomy, a discrepancy was observed in regular cadaveric dissection; therefore, it was exempted from review by the ethics board. As it was a cadaver, the body would come under a body donation program, the consent was given by the next kin of the deceased.

We dissected the GM into two halves and reflected it as superomedial and inferolateral. We found an incidental finding in the right gluteal region; the GM was innervated by the two nerves. The superomedial half of the GM was innervated by the branch of the SN that gave twigs. The inferolateral half of GM was supplied by IGN. The PCNT received an extra branch from the IGN. The IGA ran between the PCNT and the IGN, which led to the compression of the artery, as shown in Figures 1 and 2. SGA and SGN were piercing the piriformis, as shown in Figure 3. The left gluteal region was normal.

DISCUSSION

Quiñones-Rodríquez et al.[2] reported bilateral dual innervation of GM by the SN and IGN branches. Those with an aberrant branch from the SN to the GM may be more vulnerable to iatrogenic nerve injury because of intramuscular gluteal injection or surgical procedures[2].

Lesser et al.[3] described a case in which the components of the SN distal to the piriformis formed a nerve loop. From the nerve loop, some branches innervated the GM, and one branch communicated with the PCNT. These variations increase iatrogenic nerve injuries.

Inflammation of the piriformis muscle is known as piriformis syndrome. Due to inflammation, the SN is compressed, resulting in pain in the inferomedial portion of the gluteal region, sciatica, and dyspareunia in females[4]. Because of the presence of SN innervation to the GM, the pain may radiate to the entire gluteal region in piriform syndrome cases. In addition, inflammation of the GM strains the aberrant branch of the SN.

Sumalatha et al.[5] reported a higher division of the SN into the common peroneal and tibial nerves. The common peroneal nerve enters the gluteal region as two trunks, medial and lateral. GM is innervated by the medial trunk of the common peroneal nerve[5]. Paval and Nayak[6] noticed that IGN is derived from the two roots. One root pierces the piriformis, and the other root emerges from the lower edge of the piriformis[6].

Golmohammadi and Delbari[7] found a higher division of the SN into the tibial and common peroneal nerves. The IGN originated from the common peroneal nerve[7].

The piriformis receives innervation from the anterior rami of S1 and S2. According to Iwanaga et al.[8], the innervation of the piriformis was primarily the superior gluteal nerve. In this case, the superior gluteal nerve and SGA were piercing the piriformis.

The PCNT received an extra branch from the IGN. If there is any injury to the IGN, the pain may radiate to the area where the PCNT innervates the region. The most common site for gluteal intramuscular injection was the upper outer quadrant of the GM. In this case, there was dual innervation of the GM by the SN and IGN. The gluteal

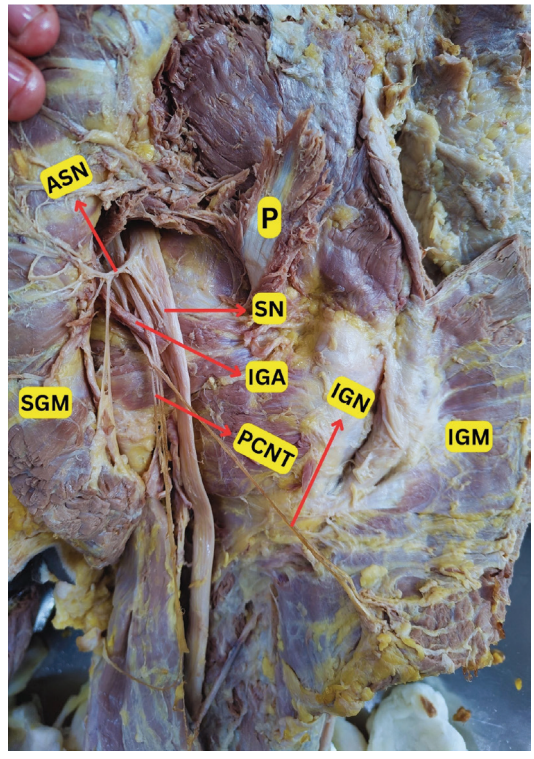

Figure 1. Shows the dual innervation of the gluteus maximus (GM) and the inferior gluteal artery passing between two nerves.

IGM: Inferolateral part of the gluteus maximus, SGM: Superomedial part of the gluteus maximus, IGN: Inferior gluteal nerve, ASN: Abnormal branch of the sciatic nerve, SN: Sciatic nerve, PCNT: The posterior cutaneous nerve of the thigh, IGA: Inferior gluteal artery, P: Piriformis

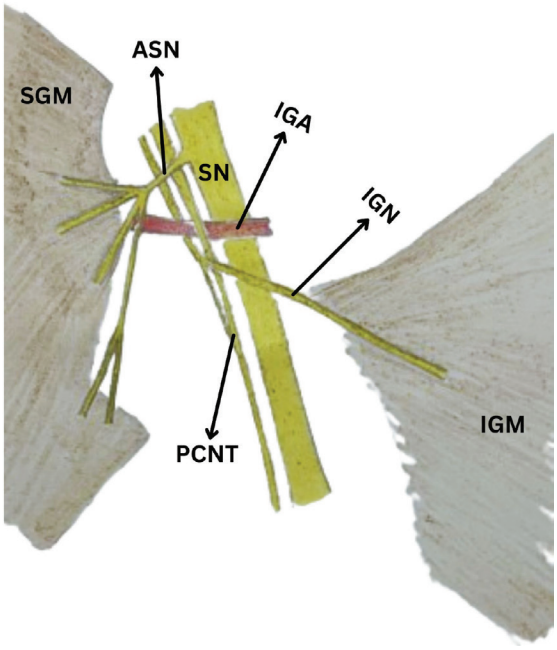

Figure 2. Shows the schematic diagram of the dual innervation of the gluteus maximus (GM).

IGM: Inferolateral part of the gluteus maximus, SGM: Superomedial part of the gluteus maximus, IGN: Inferior gluteal nerve, ASN: Abnormal branch of the sciatic nerve, SN: Sciatic nerve, PCNT: The posterior cutaneous nerve of the thigh, IGA: Inferior gluteal artery

injections may lead to injury of the SN, and the pain may radiate to the area where it innervates the region.

Tillmann and Verlaufsvarianten des[9] explained how the IGN departs the pelvis by piercing the piriformis. Normally, it exits the pelvis distal to the piriformis.

During in utero development, GM originates as two separate parts, the pars-sacroiliaca and pars-coccygea. These two muscle belly fuse in the tenth week of intrauterine life. Usually, these muscles are innervated by one nerve. If the two muscles are innervated by two different nerves, this leads to dual innervation of the GM[10].

According to our literature review, anatomical studies in which this cadaveric procedure has been performed have not been previously reported. The most common site for intramuscular injection is the upper outer region of the gluteal region. These variations increase the risk of iatrogenic nerve injuries. Surgeons, physicians, anatomists, and nurses need to understand the distinctions in the gluteal territory.

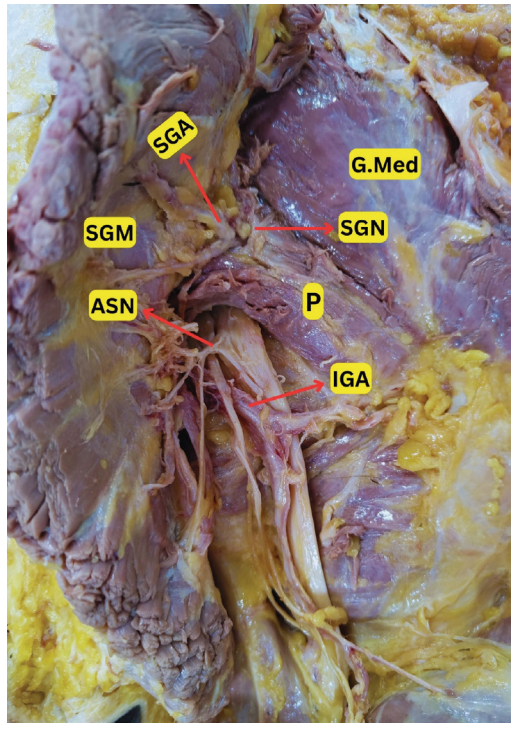

Figure 3. Shows the superior gluteal artery (SGA) and the superior gluteal nerve (SGN) piercing the piriformis.

P: Piriformis, SGM: Superomedial part of the gluteus maximus, G.Med: Gluteus medius, SGA: Superior gluteal artery, SGN: Superior gluteal nerve, IGA: Inferior gluteal artery, ASN: Abnormal branch of the sciatic nerve

Acknowledgments: We would like to thank the cadaver's relatives for giving their relative's corpse for teaching and research. We would also like to recognize the efforts of anatomy laboratory attendees in maintaining the cadavers and the laboratory regularly.

Ethics

Informed Consent: As it was a cadaver, the body would come under a body donation program, the consent was given by the next kin of the deceased.

Author Contributions

Surgical and Medical Practices: P.R., M.C., A.V.B., S.S., Concept: P.R., M.C., A.V.B., S.S., Design: P.R., M.C., A.V.B., S.S., Data Collection and/or Processing: P.R., M.C., A.V.B., S.S., Analysis and/or Interpretation: P.R., M.C., A.V.B., S.S., Literature Search: P.R., M.C., A.V.B., S.S., Writing: P.R., M.C., A.V.B., S.S.

Conflict of Interest: The authors have no conflict of interest to declare.

Financial Disclosure: The authors declared that this study has received no financial support.

REFERENCES

1. Standring S. Gray's anatomy: the anatomical basis of clinical practice. 41st edition. New York: Elsevier Limited, 2016.
2. Quiñones-Rodríguez J, Camacho-Quiñones A, Cárdenas-Suárez NY, Ramírez N. Dual Innervation to the Gluteus Maximus: A Case Report with Clinical Implications. J Clin of Diagn Res. 2022;16:AD01-3.
3. Lesser ER, Kilgore M, Iwanaga J, et al. A Highly Unusual Source and Course of the Inferior Gluteal Nerve With Related Variations: A Case Report. Cureus. 2023;15:e48694.
4. Kirschner JS, Foye PM, Cole JL. Piriformis syndrome, diagnosis and treatment. Muscle Nerve. 2009;40:10-8.
5. Sumalatha S, D Souza AS, Yadav JS, Mittal SK, Singh A, Kotian SR. An unorthodox innervation of the gluteus maximus muscle and other associated variations: A case report. Australas Med J. 2014;7:419-22.
6. Paval J, Nayak S. A case of bilateral high division of sciatic nerve with a variant inferior gluteal nerve. Neuroanatomy. 2006;5:33-4.
7. Golmohammadi R, Delbari A. Report of a Novel Bilateral Variation of Sciatic and Inferior Gluteal Nerve: A Case Study. Basic Clin Neurosci. 2021;12:421-6.
8. Iwanaga J, Eid S, Simonds E, Schumacher M, Loukas M, Tubbs RS. The majority of piriformis muscles are innervated by the superior gluteal nerve. Clin Anat. 2019;32:282-6.
9. Tillmann B. Verlaufsvarianten des N. gluteus inferior [Variations in the pathway of the inferior gluteal nerve (author's transl)]. Anat Anz. 1979;145:293-302.
10. Tichý M, Grim M. Morphogenesis of the human gluteus maximus muscle arising from two muscle primordia. Anat Embryol (Berl). 1985;173:275-7.

DOI: 10.4274/MMJ.galenos.2024.76508
Medeni Med J 2024;39:140-143

Case Report

Association of Dipeptidiyl Peptidase-4 Inhibitors and Bullose Pemphigoid: A Report of Four Cases

Dipeptidil Peptidaz-4 İnhibitörleri ve Büllöz Pemfigoid Arasındaki İlişki: Dört Olgu Raporu

Neslihan USLU, Kagan GUNGOR, Gonca TAMER, Bulent CAN

Istanbul Goztepe Prof. Dr. Suleyman Yalcin City Hospital, Clinic of Internal Medicine, Division of Endocrinology and Metabolic Diseases, Istanbul, Türkiye

ABSTRACT

Dipeptidyl-peptidase 4 inhibitors (DPP4i) are commonly used as antidiabetic medications. Although these drugs are generally recognized for their favorable clinical safety profile, emerging evidence points to the potential for adverse events associated with DPP4i. Notably, cases of bullous pemphigoid (BP) linked to DPP4i therapy have recently been documented in the medical literature. This report presents four cases of BP in elderly patients resulting from DPP4i treatment, involving two cases with ligandliptin and two with vildagliptin use. Successful remission was achieved in all cases through discontinuation of the implicated medication and implementation of topical corticosteroid therapy. It is imperative for clinicians to be vigilant about the potential risk of BP development when employing DPP4i drugs, particularly in the context of elderly patients with diabetes.

Keywords: Bullose pemphigoid, DPP4i, dipeptidyl peptidase 4 inhibitors

ÖZ

Dipeptidil-peptidaz 4 inhibitörleri (DPP4i) yaygın olarak kullanılan antidiyabetik ilaçlardandır. Bu ilaçlar sıklıkla güvenli olarak bilinse de DPP4 inhibitörlerinin yan etki potansiyelini gösteren kanıtlar bulunmaktadır. Özellikle, DPP4i tedavisine bağlı büllöz pemfigoid (BP) olguları son zamanlarda tıbbi literatürde belgelenmiştir. Bu raporda, yaşlı hastalarda DPP4i tedavisine bağlı olarak gelişen, ikisi linagliptin ve ikisi vildagliptin kullanımını içeren dört BP olgusu sunulmaktadır. Tüm olgularda, söz konusu ilacın kesilmesi ve topikal kortikosteroid tedavisinin uygulanmasıyla başarılı bir remisyon elde edilmiştir. Klinisyenlerin özellikle diyabetli yaşlı hastalarda DPP4i ilaçlarını kullanırken, potansiyel BP gelişimi riski konusunda dikkatli olmaları gerekmektedir.

Anahtar kelimeler: Bülloz pemfigoid, DPP4i, dipeptidil peptidaz 4 inhibitörleri

INTRODUCTION

Bullous pemphigoid (BP) is a chronic blistering dermatological disease that predominantly affects elderly individuals. Characterized by the development of autoimmunity against hemi-desmosomal proteins such as BP180 (collagen XVII) and BP230, BP commonly presents as tense blisters, causing pruritic urticarial and eczema-like lesions[1]. The recent literature has highlighted a connection between dipeptidyl-peptidase 4 inhibitors (DPP4i) and drug-induced BP. Notably, differences exist between the classic and DPP4i-induced variants of BP; while the former involves antibodies against the non-collagenous (NC16A) domain, the latter targets another region of NC16A. This report discusses four cases of DPP4i drug-induced BP, involving two cases linked to ligandliptin and two cases linked to vildagliptin.

CASE REPORTS

Patient consent form was obtained.

Case 1

A 77-year-old man presented to our clinic with a 1-week history of erythematous bullous lesions. The patient, previously diagnosed with type 2 diabetes mellitus, sought medical attention because of uncontrolled glucose levels despite intensive insulin

Address for Correspondence: N. Uslu, Istanbul Goztepe Prof. Dr. Suleyman Yalcin City Hospital, Clinic of Internal Medicine, Division of Endocrinology and Metabolic Diseases, Istanbul, Türkiye
E-mail: neslihan.uslu@hotmail.com **ORCID ID:** orcid.org/0000-0001-5688-7008

Received: 20 January 2024
Accepted: 02 June 2024
Online First: 07 June 2024

Cite as: Uslu N, Gungor K, Tamer G, Can B. Association of Dipeptidiyl Peptidase-4 Inhibitors and Bullose Pemphigoid: A Report of Four Cases Medeni Med J 2024;39:140-143

and metformin treatment. Linagliptin was subsequently added to the patient's regimen. Six months later, the patient developed erythematous bullous skin lesions following the introduction of DPP4i therapy. Blisters initially appeared on his legs and later spread across his body. The patient had no history of allergies. Physical examination and differential diagnosis were performed in the dermatology clinic. A skin lesion biopsy confirmed the clinical diagnosis of BP. Upon discontinuation of the DPP4i drug and initiation of topical corticosteroid therapy (klobetasol propionate), the dermatological lesions resolved.

Case 2

A 77-year-old man with a 10-year history of type 2 diabetes mellitus and chronic renal failure due to diabetes was referred to our clinic with a 2-month history of erythematous bullous lesions. The lesions initially presented as pruritic rashes before developing into bullous formations (Figure 1a,b). Linagliptin was the sole medication he had used over the past 6 months. Physical examination and differential diagnosis were performed in the dermatology clinic. A skin lesion biopsy confirmed the clinical diagnosis of BP. Following diagnosis confirmation, linagliptin was discontinued, and treatment with topical corticosteroids (clobetasol propionate) and antihistamine drugs was initiated, resulting in the healing of skin lesions.

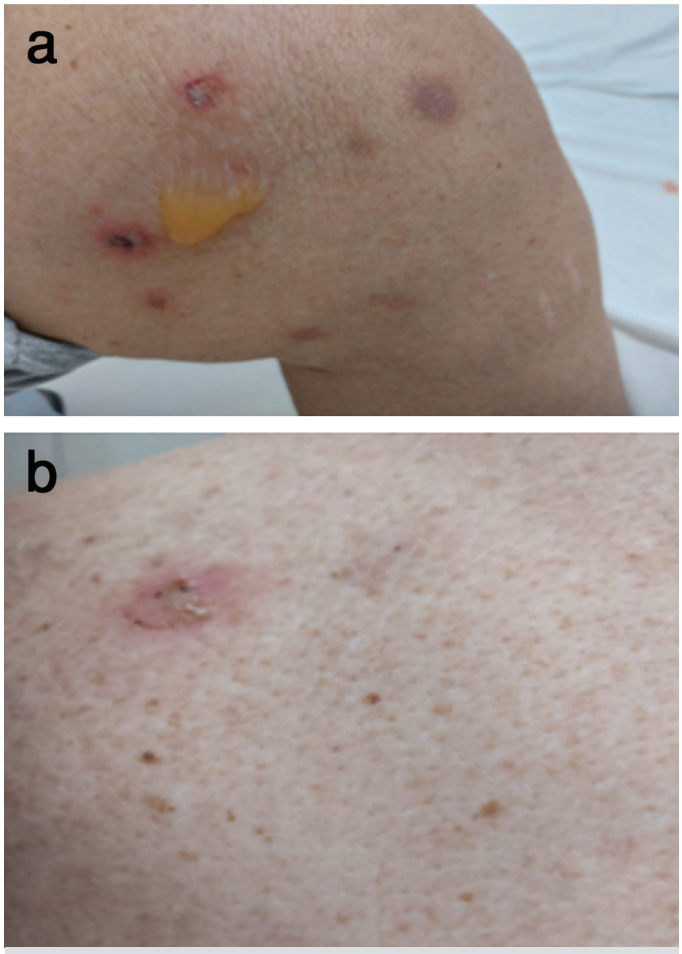

Figure 1a, b. Newly developed and healing erythematous bullous lesions in case 2

Case 3

A 78-year-old woman presented to our clinic with an itchy rash that had appeared on her back a month earlier. Diagnosed with type 2 diabetes mellitus for 5 years, she was on metformin and vildagliptin treatment. Allergy history was negative. Clinical assessment led to a diagnosis of BP attributed to the DPP4i drug vildagliptin. Physical examination and differential diagnosis were performed in the dermatology clinic. A skin lesion biopsy confirmed the diagnosis, prompting the discontinuation of vildagliptin treatment. Topical corticosteroids (clobetasol propionate) and antihistamine drugs were prescribed, resulting in the regression of skin lesions after 1 month and complete healing during the follow-up period.

Case 4

A 71-year-old woman with pruritic lesions on her back was referred to our outpatient clinic from the dermatology clinic. The patient was diagnosed with type 2 diabetes mellitus for 15 years and had been on vildagliptin treatment for 6 months. The itchy erythematous bullous lesions had presented 2 months previously. Allergy history was negative. Physical examination and differential diagnosis were performed in the dermatology clinic. Skin lesion biopsy confirmed the diagnosis, and vildagliptin treatment was discontinued. Corticosteroids and antihistamine drugs were prescribed, resulting in the regression of skin lesions after 2 weeks.

These cases underscore the potential connection between DPP4i and BP, particularly in elderly patients with diabetes. Discontinuation of the DPP4i and appropriate treatment can lead to successful BP remission.

DISCUSSION

The cell surface protein CD26, also known as DPP4, serves as both a T-cell lymphocyte surface glycoprotein and a host of DPP4 enzymatic activity. This CD26/DPP4 antigen is expressed across various cell types in the body, including skin cell membranes and immune cells[2,3]. This dual presence raises the possibility that DPP4i may exert effects on both immune and skin cells.

DPP4i, a class of antidiabetic drugs frequently combined with metformin, operate through the incretin system[2]. They elicit several effects, such as the reduction of Th1 activity and the augmentation of TGF beta 1 production via the Th3 regulatory system[4]. Additionally, DPP4i can induce eosinophil activation in the skin through CCL11/exotoxin signaling[5]. These mechanisms link DPP4i actions with immune responses involved in the pathogenesis of BP[6].

Recent investigations have illuminated an elevated risk of BP associated with DPP4i drug treatment, with a reported increase of nearly two to three times[7]. Several cases related to DPP4i have been reported. Among the DPP4i implicated, ligandliptin, vildagliptin, and Anagliptin are prominent in the induction of BP[8]. Notably, although the less selective DPP4i, vildagliptin, is a common culprit, sitagliptin does not seem to be linked to DPP4i-induced BP[7,9]. The duration of treatment leading to DPP4i-induced BP varies in the literature, ranging from 8 days to 4 years[10-12]. This can cause a delay in diagnosis and treatment. Key risk factors include older age and male gender, with most cases affecting individuals aged 80 years [7,13]. In the presented cases, the age also tended to be older, with a mean age of 75 years; two patients were men and two were women. Consistent with the existing literature, vildagliptin and linagliptin emerged as the DPP4i drugs responsible for drug-induced BP in the presented cases[10,11,13]. Two types of DPP4i drugs (linagliptin and vildagliptin) were also implicated in our cohort of patients.

DPP4i-induced BP typically exhibits lower levels of inflammation and erythema than classical BP[1,9]. However, we did not observe this in our cohort. The diagnosis relies on skin biopsies from the lesions and direct immunofluorescence staining. Skin biopsy and direct immunofluorescence on perilesional skin remains the gold standard for diagnosis even in DPP4i-induced BP. While classic BP involves autoantibodies targeting the NC16A domain, patients with DPP4i-induced BP exhibit autoantibodies against the mid-portion of the BP180 antigen (collagen XVII)[1,9]. A retrospective study suggests that linagliptin-induced BP may be more challenging to treat than vildagliptin-induced BP. The complex and unclear pathological mechanisms underpinning DPP4i-induced BP confer a risk of mortality[14]. The diagnostic process may be complicated by the varying durations of treatment leading to disease onset. Replacing one DPP4i with another is not recommended[12,15]. Persistent cutaneous symptoms despite steroid administration were observed in all presented cases. After cessation of DPP4i, improvement was observed within 2 weeks. Consequently, an early diagnosis and prompt discontinuation of DPP4i drugs are crucial measures. Treatment options include systemic or topical glucocorticoids[8,9]. These findings strongly suggest a causal role for DPP4i in this disease. However, this study has limitations such as the lack of a control group, the observational nature of case reports, and the need for randomized controlled trials to establish causality.

Diagnosing DPP4i drug-induced BP can prove challenging because of the varying durations of treatment precipitating the condition. Clinicians must be alert to this potential complication, particularly in elderly diabetic patients. Swift diagnosis and immediate discontinuation of the offending drug often result in effective treatment and healing of skin lesions.

Ethics

Informed Consent: Patients' consent form was obtained.

Author Contributions

Design: B.C., Data Collection and/or Processing: K.G., Literature Search: N.U., B.C., Writing: N.U.

Conflict of Interest: The authors have no conflict of interest to declare.

Financial Disclosure: The authors declared that this study has received no financial support.

REFERENCES

1. Tasanen K, Varpuluoma O, Nishie W. Dipeptidyl Peptidase-4 Inhibitor-Associated Bullous Pemphigoid. Front Immunol. 2019;10:1238.
2. Someili A, Azzam K, Hilal MA. Linagliptin-Associated Alopecia and Bullous Pemphigoid. Eur J Case Rep Intern Med. 2019;6:001207.
3. Attaway A, Mersfelder TL, Vaishnav S, Baker JK. Bullous pemphigoid associated with dipeptidyl peptidase IV inhibitors. A case report and review of literature. J Dermatol Case Rep. 2014;8:24-8.
4. Bastuji-Garin S, Joly P, Lemordant P, et al. Risk factors for bullous pemphigoid in the elderly: a prospective case-control study. J Invest Dermatol. 2011;131:637-43.
5. Forssmann U, Stoetzer C, Stephan M, et al. Inhibition of CD26/dipeptidyl peptidase IV enhances CCL11/eotaxin-mediated recruitment of eosinophils in vivo. J Immunol. 2008;181:1120-7.
6. Giomi B, Caproni M, Calzolari A, Bianchi B, Fabbri P. Th1, Th2 and Th3 cytokines in the pathogenesis of bullous pemphigoid. J Dermatol Sci. 2002;30:116-28.
7. Roy A, Sahoo J, Narayanan N, Merugu C, Kamalanathan S, Naik D. Dipeptidyl peptidase-4 inhibitor-induced autoimmune diseases: Current evidence. World J Diabetes. 2021;12:1426-41.
8. Yoshiji S, Murakami T, Harashima SI, et al. Bullous pemphigoid associated with dipeptidyl peptidase-4 inhibitors: a report of five cases. J Diabetes Investig. 2018;9:445-7.

9. Randhawa A, Torley D, Kerr A, Wylie G. Dipeptidyl peptidase 4 inhibitors and bullous pemphigoid-more evidence of a link: a report of three cases. Br J Diabetes. 2020;20:147-8.
10. Silverii GA, Dicembrini I, Nreu B, Montereggi C, Mannucci E, Monami M. Bullous pemphigoid and dipeptidyl peptidase-4 inhibitors: a meta-analysis of randomized controlled trials. Endocrine. 2020;69:504-7.
11. Phan K, Charlton O, Smith SD. Dipeptidyl peptidase-4 inhibitors and bullous pemphigoid: A systematic review and adjusted meta-analysis. Australas J Dermatol. 2020;61:15-21.
12. Béné J, Moulis G, Bennani I, Auffret M, et al. Bullous pemphigoid and dipeptidyl peptidase IV inhibitors: a case-noncase study in the French Pharmacovigilance Database. Br J Dermatol. 2016;175:296-301.
13. Kridin K, Bergman R. Association of Bullous Pemphigoid With Dipeptidyl-Peptidase 4 Inhibitors in Patients With Diabetes: Estimating the Risk of the New Agents and Characterizing the Patients. JAMA Dermatol. 2018;154:1152-8.
14. Langan SM, Smeeth L, Hubbard R, Fleming KM, Smith CJ, West J. Bullous pemphigoid and pemphigus vulgaris--incidence and mortality in the UK: population based cohort study. BMJ. 2008;337:a180.
15. Benzaquen M, Borradori L, Berbis P, et al. Dipeptidyl peptidase IV inhibitors, a risk factor for bullous pemphigoid: retrospective multicenter case-control study from France and Switzerland. J Am Acad Dermatol. 2018;78:1090-6.

DOI: 10.4274/MMJ.galenos.2024.05760
Medeni Med J 2024;39:144-145

Letter to the Editor

Correspondence on "Is ChatGPT an Accurate and Reliable Source of Information for Patients with Vaccine and Statin Hesitancy?"

"ChatGPT, Aşı ve Statin Tereddütü Olan Hastalar için Doğru ve Güvenilir Bir Bilgi Kaynağı mıdır?" Konulu Yazışma

Hinpetch DAUNGSUPAWONG[1], Viroj WIWANITKIT[2]

[1]Private Academic Consultant, Phonhong, Laos
[2]Chandigarh University Centre for Research & Development, Department of Pharmaceutical Sciences, Mohali, India

Keywords: ChatGPT information, statin, hesitancy
Anahtar kelimeler: ChatGPT bilgileri, statin, tereddüt

Dear Editor,

We would like to comment on "Is ChatGPT an Accurate and Reliable Source of Information for Patients with Vaccine and Statin Hesitancy?"[1]. This study compared the answers provided by ChatGPT-3.5 with those from doctors for vaccine and statin hesitancy-related queries. Experts in internal medicine, microbiology, and cardiology evaluated the responses. The similarity between the average scores of ChatGPT and physicians suggests that ChatGPT was able to produce comments that were as precise, understandable, and succinct as those from physicians.

The study's methodological flaw is that it only used ChatGPT version 3.5 to generate the questions' answers. Artificial intelligence (AI) language models come in various iterations and versions; thus, relying only on one could restrict how broadly the results can be applied. Furthermore, the study excluded the opinions of patients or those who were dubious about vaccinations and statins, and evaluated replies solely from ChatGPT and doctors. Including various viewpoints could result in a more thorough comprehension of the problem.

The fact that ChatGPT ignored sources of disinformation about statins and vaccines constitutes another flaw in the study. Conspiracy theories and misleading information frequently contribute to vaccine and statin reluctance, therefore it's critical that AI language models can confront and disprove these assertions. Subsequent research endeavors may examine the training of AI models to identify and furnish precise data in response to conspiracy theories and false material around statins and vaccines.

Subsequent research paths may entail contrasting ChatGPT's answers with those of alternative AI language models or with those from people with varying degrees of healthcare experience. Furthermore, gathering information from those who are dubious about

Address for Correspondence: H. Daungsupawong, Private Academic Consultant, Phonhong, Laos
E-mail: hinpetchdaung@gmail.com **ORCID ID:** orcid.org/0009-0002-5881-2709

Received: 22 March 2023
Accepted: 05 April 2024
Online First: 16 May 2024

Cite as: Daungsupawong H, Wiwanitkit V. Correspondence on "Is ChatGPT an Accurate and Reliable Source of Information for Patients with Vaccine and Statin Hesitancy?". Medeni Med J 2024;39:144-145

vaccinations and statins through qualitative interviews or surveys may shed light on their concerns and worldviews. Then, with these data, AI models that are better able to confront and dispel myths about statins and vaccinations might be developed.

Ethics

Author Contributions

Surgical and Medical Practices: H.D., V.W., Concept: H.D., V.W., Design: H.D., V.W., Data Collection or Processing: H.D., V.W., Analysis or Interpretation: H.D., V.W., Literature Search: H.D., V.W., Writing: H.D.

Conflict of Interest: The authors have no conflict of interest to declare.

Financial Disclosure: The authors declared that this study has received no financial support.

REFERENCES

1. Torun C, Sarmis A, Oguz A. Is ChatGPT an Accurate and Reliable Source of Information for Patients with Vaccine and Statin Hesitancy? Medeni Med J. 2024;39:1-7.

DOI: 10.4274/MMJ.galenos.2024.66281
Medeni Med J 2024;39:146-147

Letter to the Editor

Response to Letter to the Editor, "Is ChatGPT an Accurate and Reliable Source of Information for Patients with Vaccine and Statin Hesitancy?"

Editöre Mektuba Yanıt, "ChatGPT, Aşı ve Statin Tereddütü Olan Hastalar için Doğru ve Güvenilir Bir Bilgi Kaynağı mıdır?"

Cundullah TORUN[1], Abdurrahman SARMIS[2], Aytekin OGUZ[1]

[1]Istanbul Goztepe Prof. Dr. Suleyman Yalcin City Hospital, Clinic of Internal Medicine, Istanbul, Türkiye
[2]Istanbul Goztepe Prof. Dr. Suleyman Yalcin City Hospital, Clinic of Microbiology, Istanbul, Türkiye

Keywords: Primary prevention, artificial intelligence, medication hesitancy
Anahtar kelimeler: Primer koruma, yapay zeka, tedavi şüpheciliği

Dear Editor,

We are grateful for the comments provided in the letter by Daungsupawong and Wiwanitkit[1], and we extend our thanks to the editors for giving us the chance to address the criticisms raised and broaden the discussion on our study.

During our study (March 2023), the easy accessibility and high popularity of ChatGPT 3.5 as an artificial intelligence (AI) tool were the reasons for our preference[2]. However, considering the rapid advancement of AI technology, we noted in our study that conducting research with both ChatGPT 4 and various machine learning tools would offer a more comprehensive understanding of the usefulness of AI technologies in addressing vaccine and statin hesitancy.

This study assessed the accuracy and explanatory nature of the responses provided by ChatGPT 3.5 to questions from individuals with vaccine and statin hesitancy. The viewpoints of skeptical individuals could be the subject of another study.

In our study, we demonstrated that when patients' frequently asked questions regarding vaccine and statin hesitancy were directed to ChatGPT, it did not provide responses that supported misleading information. However, as highlighted by Daungsupawong and Wiwanitkit[1], it was also observed that ChatGPT did not confront this misleading information. Nevertheless, our study was not intended to evaluate the capacity of AI technology to combat misinformation related to vaccines and statins. Especially on social media, the variety and quantity of negative content regarding both vaccine and statin use are too vast to respond to each one individually[3,4]. Mentioning these negative contents in AI outputs may further confuse individuals seeking information and spread skepticism among patients. Given this scenario, it should be a separate research topic to determine which approach, providing only accurate information or confronting misinformation, would be more effective in reducing vaccine and statin hesitancy.

Thank you for your consideration.

Sincerely

Address for Correspondence: C. Torun, Istanbul Goztepe Prof. Dr. Suleyman Yalcin City Hospital, Clinic of Internal Medicine, Istanbul, Türkiye
E-mail: cundullaht@gmail.com **ORCID ID:** orcid.org/0000-0003-4933-7635

Received: 03 April 2024
Accepted: 05 April 2024
Online First: 21 May 2024

Cite as: Torun C, Sarmis A, Oguz A. Response to Letter to the Editor, "Is ChatGPT an Accurate and Reliable Source of Information for Patients with Vaccine and Statin Hesitancy?". Medeni Med J Medeni Med J 2024;39:146-147

Ethics

Author Contributions

Concept: C.T., A.O., Design: C.T., A.O., Analysis or Interpretation: C.T., A.S., A.O., Literature Search: C.T., A.S., A.O., Writing: C.T., A.S., A.O.

Conflict of Interest: The authors have no conflict of interest to declare.

Financial Disclosure: The authors declared that this study has received no financial support.

REFERENCES

1. Daungsupawong H, Wiwanitkit V. Correspondence on "Is ChatGPT an Accurate and Reliable Source of Information for Patients with Vaccine and Statin Hesitancy?" Medeni Med J. 2024 May 16. [Epub ahead of print].
2. Torun C, Sarmis A, Oguz A. Is ChatGPT an Accurate and Reliable Source of Information for Patients with Vaccine and Statin Hesitancy? Medeni Med J. 2024;39:1-7.
3. Wilson SL, Wiysonge C. Social media and vaccine hesitancy. BMJ Glob Health. 2020;5:e004206.
4. Slavin SD, Berman AN, Beam AL, Navar AM, Mittleman MA. Statin Twitter: Human and Automated Bot Contributions, 2010 to 2022. J Am Heart Assoc. 2024;13:e032678.

DOI: 10.4274/MMJ.galenos.2024.e001
Medeni Med J 2024;39:148-151

Erratum

DOI: 10.5222/MMJ.2019.08870, Published by Logos Medical Publishing

Ağırcan D., Orhan Varoğlu A. Prognostic Importance of Endocan Level in Patients with Ischemic Cerebrovascular Disease. Med Med J. 2019;34(1):1-6

In the published article 'Prognostic Importance of Endocan Level in Patients with Ischemic Cerebrovascular Disease', we inadvertently misstated the number of enrolled patients. Upon careful review of our data, we confirm that this error does not impact the findings or conclusions of our study. We apologize for any confusion this may have caused and provide the correct patient enrollment number below.

1. On page 1, in the abstract section

Original version

'Method: We compared the serum level of endocan of 80 patients and of 60 healthy controls.'

should be corrected as

'Method: We compared the serum level of endocan of 60 patients and of 40 healthy controls.'

2. On page 1, in the özet section

Original version

'Yöntem: Seksen hastanın endokan serum düzeyi ve 60 sağlıklı kontrol karşılaştırıldı.'

should be corrected as

'Yöntem: Altmış hastanın endokan serum düzeyi ve 40 sağlıklı kontrol karşılaştırıldı.'

3. On page 2, in the MATERIAL AND METHOD section

Original version

'This prospective study was performed at Istanbul Medeniyet University University, Neurology Department, between January and June 2015, and contained 80 patients with a diagnosis of cerebrovascular disease. Moreover, 60 age-, and sex-matched individuals who had no neurologic disorder served as the control group.'

should be corrected as

'This prospective study was performed at Istanbul Medeniyet University University, Neurology Department, between January and June 2015, and contained 60 patients with a diagnosis of cerebrovascular disease. Moreover, 40 age-, and sex-matched individuals who had no neurologic disorder served as the control group.'

4. On page 2, in the MATERİAL AND METHOD section

Original version

'As a control group, we selected 60 age-matched participants who had vascular risk factors without any history of stroke, systemic or central nervous system malignancy, recent heart failure and myocardial infarction, and diagnosis of sepsis at the time of the study.'

should be corrected as

'As a control group, we selected 40 age-matched participants who had vascular risk factors without any history of stroke, systemic or central nervous system malignancy, recent heart failure and myocardial infarction, and diagnosis of sepsis at the time of the study.'

5. On page 3, in the RESULTS section

Original version

'We enrolled 80 patients with acute ischemic cerebrovascular disease with a mean age of 63.85±11.47 years and 60 healthy controls with a mean age of 61.55±12.37 years.'

should be corrected as

'We enrolled 60 patients with acute ischemic cerebrovascular disease with a mean age of 63.85±11.47 years and 40 healthy controls with a mean age of 61.55±12.37 years.'

6. On page 3, in Table 1

Original version

Table 1. The baseline demographic and laboratory data in patients with ICD and controls.

		Controls n:60	ICD n:80	P-value
Age		61.55±12.37	63.85±11.47	0.343
Sex	Female	32 / 55.00%	36 / 43.33%	0.253
	Male	28 / 45.00%	44 / 56.67%	
Glucose (mg/dL)		99.71±16.81	124.87±43.7	0.001
Urea (mg/dL)		33.21±9.41	36.03±11.63	0.220
Creatinine (mg/dL)		0.83±0.15	0.86±0.22	0.539
AST (IU/L)		19.57±4.55	18.27±6.69	0.309
ALT (IU/L)		19.29±7.85	16.48±7.56	0.089
Triglycerides (mg/dL)		155.83±85.86	150.4±65.17	0.731
Total cholesterol (mg/dL)		210.28±40.67	197.8±51.73	0.240
HDL cholesterol (mg/dL)		46.92±13.71	43.72±11.35	0.22
LDL cholesterol (mg/dL)		129.78±36.8	126.35±44.03	0.710
WBC (K/uL)		7.24±1.57	8.77±5.19	0.074
RBC (M/uL)		4,75±0.52	4.59±0.59	0.173
HGB (g/dL)		14,23±4,52	13.32±1.73	0.162
Platelet count (K/uL)		243.85±72.95	244±66.61	0.991
TSH (uIU/mL)		1.43±0.89	1.38±1.09	0.846
fT3 (pg/mL)		2.49±0.92	2.79±0.3	0.034
fT4 (ng/dL)		0.96±0.18	0.95±0.13	0.774
HbA1c (%)		5.87±0.64	6.61±1.77	0.116
Insulin		8.11±5.02	13.94±12.36	0.103

Student's t-test was used to compare groups. Data arepre- sented as mean ± standard deviation, *Median (min-max); AST: Aspartate Transaminase, ALT: Alanineaminotransferase, TSH:Thyrotrophin-Stimulating Hormone, fT3:free T3, fT4:free T4, HbA1c: Glycated hemoglobin.

should be corrected as

Table 1. The baseline demographic and laboratory data in patients with ICD and controls.

		Controls n:40	ICD n:60	P-value
Age		61.55±12.37	63.85±11.47	0.343
Sex	Female	32 / 55.00%	36 / 43.33%	0.253
	Male	28 / 45.00%	44 / 56.67%	
Glucose (mg/dL)		99.71±16.81	124.87±43.7	0.001
Urea (mg/dL)		33.21±9.41	36.03±11.63	0.220
Creatinine (mg/dL)		0.83±0.15	0.86±0.22	0.539
AST (IU/L)		19.57±4.55	18.27±6.69	0.309
ALT (IU/L)		19.29±7.85	16.48±7.56	0.089
Triglycerides (mg/dL)		155.83±85.86	150.4±65.17	0.731
Total cholesterol (mg/dL)		210.28±40.67	197.8±51.73	0.240
HDL cholesterol (mg/dL)		46.92±13.71	43.72±11.35	0.22
LDL cholesterol (mg/dL)		129.78±36.8	126.35±44.03	0.710
WBC (K/uL)		7.24±1.57	8.77±5.19	0.074
RBC (M/uL)		4,75±0.52	4.59±0.59	0.173
HGB (g/dL)		14,23±4,52	13.32±1.73	0.162
Platelet count (K/uL)		243.85±72.95	244±66.61	0.991
TSH (uIU/mL)		1.43±0.89	1.38±1.09	0.846
fT3 (pg/mL)		2.49±0.92	2.79±0.3	0.034
fT4 (ng/dL)		0.96±0.18	0.95±0.13	0.774
HbA1c (%)		5.87±0.64	6.61±1.77	0.116
Insulin		8.11±5.02	13.94±12.36	0.103

Student's t-test was used to compare groups. Data arepre- sented as mean ± standard deviation, *Median (min-max); AST: Aspartate Transaminase, ALT: Alanineaminotransferase, TSH:Thyrotrophin-Stimulating Hormone, fT3:free T3, fT4:free T4, HbA1c: Glycated hemoglobin.

7. On page 3, in Table 2

Original version

Table 2. Comparison of Endocan levels between the patients and the control groups.			
Endocan level (ng/ml)	**Controls n:60**	**ICD n:80**	**P-value**
1st day	1.47±0.48	1.48±0.6	0.092
7th day		1.47±0.43	0.093
3rd month		1.57±0.64	0.361
Student's t-test was used to compare groups.			

should be corrected as

Table 2. Comparison of Endocan levels between the patients and the control groups.			
Endocan level (ng/ml)	**Controls n:40**	**ICD n:60**	**P-value**
1st day	1.47±0.48	1.48±0.6	0.092
7th day		1.47±0.43	0.093
3rd month		1.57±0.64	0.361
Student's t-test was used to compare groups.			

8. On page 5, after Conclusion, before References, we request that the acknowledgments section be added as follows

'Acknowledgements: We would like to thank Dr. Aybala Erek Toprak for her contributions to obtaining biochemical data and Dr. Abdulkadir Koçer for his contributions to patient collection and the thesis writing process.'